國立臺灣大學生物資源暨農學院動物科學技術學系

碩士論文

Department of Animal Science and Technology

College of Bioresources and Agriculture

National Taiwan University

Master Thesis

纖維母細胞生長因子訊息對於斑馬魚始基生殖細胞遷移時期的重要性

Intrinsic Fgf signaling is required for primordial germ cell migration in zebrafish

張家騰

Chia-Tang Chang

指導教授：劉逸軒 博士

Advisor: I-Hsuan Liu, D.V.M., Ph.D.

中華民國 108 年 6 月

June 2019

doi:10.6342/NTU201903081

國立臺灣大學（碩）博士學位論文
口試委員會審定書

纖維母細胞生長因子訊息對於斑馬魚始基生殖細胞遷移時期的重要性

Intrinsic Fgf signaling is required for primordial germ cell migration in zebrafish

本論文係張家騰君（R06626005）在國立臺灣大學動物科學技術學系、所完成之碩士學位論文，於民國 108 年 6 月 26 日承下列考試委員審查通過及口試及格，特此證明

口試委員：　　（簽名）

（指導教授）

系主任、所長　　（簽名）

doi:10.6342/NTU201903081

誌謝

本論文承蒙指導教授　劉逸軒博士以及口試委員　李士傑博士、江運金博士、皇甫維君博士和管永恕博士的悉心審閱及斧正，使內容更加完備與嚴謹。

感謝明斯特大學（Universität Münster）Eraz Ras 博士贈送敝實驗室 *Tg(kop:egfp-F-nanos3-3'UTR)* 轉基因魚，以及國立台灣大學生命科學院 TechComm 科技共同空間　姚婉恕技術員協助操作流式細胞分析儀，使本研究得以順利進行。

感謝指導教授　劉逸軒老師從大五到碩士班兩年的指導，還有大學和碩士班具有啟發性的課程；老師給了我研究方法上很大的自由與信任，同時在策略上給了我許多建議。感謝動科系上所有老師在大學及碩士班的指導，茁壯了我的學術背景。另外，特別感謝昆蟲系　張俊哲老師以及生科系　李士傑老師使我對探索生物奧秘產生興趣，還有中文系　張麗麗老師、電機系　葉丙成老師以及物理系朱士維老師讓學生們相信自己能成為優秀的人。感謝游位育學長和廖奕雯學姊在日常以及公事上的協助，讓我能在系上安心生活以及致力做實驗。

感謝實驗室妍樺學姊引領我開始斑馬魚及分子生物實驗，感謝彥慈、Peiya、雁茹、明剛、銓良、迪旭、佳惠、姵延、喆云和欣儀在實驗室互相協助。感謝同實驗室的吳信志老師及其學生在生活上的陪伴。最後，感謝我的家人給予我最好的資源，讓我能夠適性成長。僅以此論文獻予您們。

doi:10.6342/NTU201903081

中文摘要

始基生殖細胞（primordial germ cell, PGC）是配子的前驅細胞。由於 PGC 與體細胞分歧於發育早期，因此需要橫越胚胎遷移至未來性腺形成的位置。在脊索動物中，體細胞分泌的趨化因子 Cxcl12 能夠激發 PGC 細胞膜上的受器 Cxcr4，引導 PGC 沿著趨化因子的濃度梯度移動。

利用斑馬魚為動物模式，我發現另一種訊息傳遞途徑——纖維母細胞生長因子（fibroblast growth fator, Fgf）訊息傳遞也參與在 PGC 的遷移。首先，為了瞭解 PGC 是否能夠感知 Fgf 訊息，我將 PGC 專一表現綠螢光蛋白之轉基因魚 *Tg(kop:egfp-F-nanos3-3'UTR)* 的 PGC 分選出來，進行 RNA 表現量分析。我們發現斑馬魚 PGC 表現了 Fgf 受器（*fgfr1a*, *fgfr1b*, *fgfr2*, and *fgfr4*），其中 *fgfr4* 表現量最高，暗示斑馬魚 PGC 可以偵測 Fgf 訊息。

接著，為了檢驗 PGC 對於 Fgf 訊息的需求，我們利用了顯性失活形式（dominant negative form）的 Fgf 受器 dn-Fgfr3 來競爭內源性 Fgf 訊息傳遞，為了專一在 PGC 中過量表現 dn-Fgfr3，在其序列中連接了 *nanos3* 基因的 3 端非轉譯區（3'-UTR），並在斑馬魚胚發育一細胞時期顯微注射入細胞中。在對照組中，PGC 在受精後六小時分佈在胚盤的邊緣，並在受精後一日齡時抵達生殖脊；當 Fgf 訊息傳遞受干擾時，有些 PGC 在受精後六小時脫離了胚盤邊緣，往動物極（animal pole）移動，並在受精後一日齡時散落在胚的各處，表示 PGC 仰賴接受 Fgf 訊息完成定向遷移。此失能表現型可以透過同時讓 PGC 表現持續激活形式（constitutively active form）的 Fgf 受器 ca-Fgfr4 拯救之，表示 dn-Fgfr3 導致的 PGC 分佈異常為專一性抑制 Fgf 訊息傳遞的結果。

總結來說，我們發現斑馬魚 PGC 可能具有接收 Fgf 訊息的能力，而 Fgf 訊息參與在 PGC 的遷移中。據我們所知，這是第一個脊索動物 PGC 與 Fgf 訊息在體內直接互動的證據。

關鍵字：始基生殖細胞、纖維母細胞生長因子、斑馬魚、細胞遷移

doi:10.6342/NTU201903081

Abstract

Gametes are derived from primordial germ cells (PGCs). As one of the first cell lineages specified, PGCs migrate across the embryo toward where the gonad forms during development. In vertebrates, somatic cell-secreted chemokine Cxcl12 is known to guide PGCs up the chemokine gradient.

Using zebrafish as the animal model, I report here that fibroblast growth factor (Fgf) signaling is participated in PGC migration. To determine the competence of PGCs to respond to Fgf signals, I isolated PGCs from *Tg(kop:egfp-F-nanos3-3'UTR)* embryos to measure the gene expressions of Fgf receptors. I identified all five Fgf receptors (*fgfr1a*, *fgfr1b*, and *fgfr2-4*) expressed in zebrafish PGCs while the *fgfr4* transcript is the most abundant. It suggests PGCs may be able to perceive Fgf signals.

Next, to assess the necessity of Fgf signaling by PGCs themselves, I performed loss-of-function experiments by introducing mRNA encoding a dominant negative form of Fgf receptor 3 (*dn-Fgfr3*) with the 3'-UTR of *nanos3*, which inhibits its mRNA translation in the soma. In the control embryos, representative PGCs were aligned at the blastoderm margin during early gastrulation (6 hours post-fertilization, hpf) and accumulated at the gonadal ridge at the end of somitogenesis (24 hpf). In those embryos in which the Fgf signaling in PGCs was repressed, however, some of PGCs were centralized toward the animal pole at 6 hpf and mislocalized throughout the embryo at 24 hpf. The loss-of-function phenotypes could be rescued by co-expression of constitutively-active Fgfr4 (ca-Fgfr4), suggesting the specific effects of dn-Fgfr3. Taken together, Fgf signals are required for directional migration of PGCs in zebrafish.

doi:10.6342/NTU201903081

My study illustrates the direct participation of Fgf signaling in PGC migration *in vivo*. To my knowledge, it is the first *in vivo* evidence to show that Fgf signaling plays a direct role in the migration of vertebrate PGCs.

Keywords: Primordial germ cell, fibroblast growth factor, zebrafish, cell migration

doi:10.6342/NTU201903081

Contents

doi:10.6342/NTU201903081

List of tables

doi:10.6342/NTU201903081

List of figures

doi:10.6342/NTU201903081

1. Introduction

1.1. Primordial germ cells (PGCs)

Sexual reproduction is a clever strategy to increase genetic variation in eukaryotes. In such event within the animal kingdom, ova and sperm, collectively termed gametes, fuse into zygotes and generate new individuals. Germline refers to the cell lineage all the way back to the zygote that passes the genetic information of an organism to the next generation. Cells belonging to the germline are called germ cells while the others are collectively termed somatic cells. Throughout the germline, primordial germ cells (PGCs) are described as the first determined gamete progenitors until sex determination —when the germ cells then are alternatively called gametogonia. PGCs are usually set apart from the somatic lineage early during development, usually before gonad formation (Hayashi et al., 2007; Raz, 2003; Strome and Lehmann, 2007); accordingly, PGCs have to migrate across the embryo through chemotaxis (Richardson and Lehmann, 2010), simultaneously eluding somatic induction with unique mechanisms (Strome and Updike, 2015). Understanding the molecular mechanisms of PGCs paves the way for solutions to infertility (Hayashi et al., 2012; Hayashi et al., 2011). Moreover, the mobile property of PGCs is often reminiscent of stem cell homing as well as tumor metastasis, inspiring the research on stem cells (Petit et al., 2002; Sugiyama et al., 2006) and cancers (Burger and Peled, 2009; Li et al., 2014). Therefore, studies on the natures of PGCs have been of not only biological but also therapeutic significance.

doi:10.6342/NTU201903081

1.1.1. Zebrafish, a rising star to study PGCs

In the early days, invertebrates like *Drosophila melanogaster* (Williamson and Lehmann, 1996) and *Caenorhabditis elegans* (Seydoux and Strome, 1999) were preferred models to investigate the molecular mechanisms of PGCs *in vivo* owing to their tractability on gene manipulations. Not until recently have zebrafish popped up as a popular model for PGC research using genetic approaches (Yoon et al., 1997). As a member of vertebrates, zebrafish share 70% orthologous genes with human (Howe et al., 2013) and are also flexible in genetic manipulation (Koprunner et al., 2001; Nasevicius and Ekker, 2000; Westerfield, 2007). They have a short, approximately 3-month, generation time and are capable of weekly reproduction with hundreds of offspring in one spawn (Westerfield, 2007). Furthermore, the advantages of rapid and extrauterine development combined with the property of transparent embryos facilitate the possibilities to visualize the cellular processes throughout the embryonic development in vertebrates. As a result, zebrafish serves as a salient animal model not only bridging the understanding of PGCs in invertebrates (Koprunner et al., 2001; Yoon et al., 1997) but also disclosing novel molecular mechanisms conserved thought vertebrates (Doitsidou et al., 2002; Weidinger et al., 2003). Considering the aforementioned advantages, I selected zebrafish PGCs as the animal model to unveil the interactions between PGCs and extracellular signaling; therefore, in this part of literature review, I am going to discuss the current insights of PGCs—mainly focusing on zebrafish.

doi:10.6342/NTU201903081

1.1.2. Specification of PGCs

Preventing from commitment into somatic fates, PGCs diverge from the somatic lineage early—usually before gastrulation—to preserve their totipotency to the next generation. To approach germline segregation, two distinct strategies are employed by varied vertebrates. One is epigenesis, in which PGCs are induced by somatic signals. This mechanism is generally thought to be ancestral within vertebrates (Johnson and Alberio, 2015) and has been described in urodeles (Chatfield et al., 2014), turtles (Bachvarova et al., 2009), and mice (Lawson et al., 1999). In detail, mouse PGCs are derived from the most proximal epiblast cells upon receiving bone morphogenetic proteins (BMPs) emitted from the extra-embryonic ectoderm (ExE) (Lawson et al., 1999), and axolotl PGCs are induced by fibroblast growth factors (Fgfs) in existence of BMP signals (Chatfield et al., 2014).

Another way to determine PGCs is through germ plasm acquisition, represented by zebrafish (Knaut et al., 2000), *Xenopus* (Tada et al., 2012), and chickens (Lee et al., 2016). In these species applying such mechanisms, the germline determinants—generally termed germ plasm—are inherited from the oocyte and the disproportionate acquisition of the germ plasm segregates PGCs from somatic fates. Specification by germ plasm tolerates morphological innovation and expedites evolution, thus evolved repeatedly by convergence and deriving more species compared to their sister clades (Evans et al., 2014).

In zebrafish, germ plasm mRNAs, such as *ddx4* (Yoon et al., 1997), *nanos3* (Koprunner et al., 2001), and *dnd1* (Weidinger et al., 2003), are synthesized during oogenesis and reunite in the blastomere following fertilization (Kosaka et al., 2007). In the first few divisions of a zygote, the germplasm mRNAs accumulate at the cleavage

doi:10.6342/NTU201903081

furrows (Figure 1A-D) and subsequently move into four blastomeres at the 32-cell stage (1.75 post-hour fertilization, hpf) (Figure 1E) (Theusch et al., 2006; Yoon et al., 1997). Until the 8k-cell stage (sphere stage, 4.33 hpf), four descendant cells are continuously insulated by acquiring the germ plasm through asymmetric divisions (Figure 1F) (Braat et al., 1999; Knaut et al., 2000; Yoon et al., 1997). Since then, the germ plasm starts to be distributed equally in the following mitoses (Figure 1G), and PGCs are now determined apart from the soma (Figure 1H) (Knaut et al., 2000).

doi:10.6342/NTU201903081

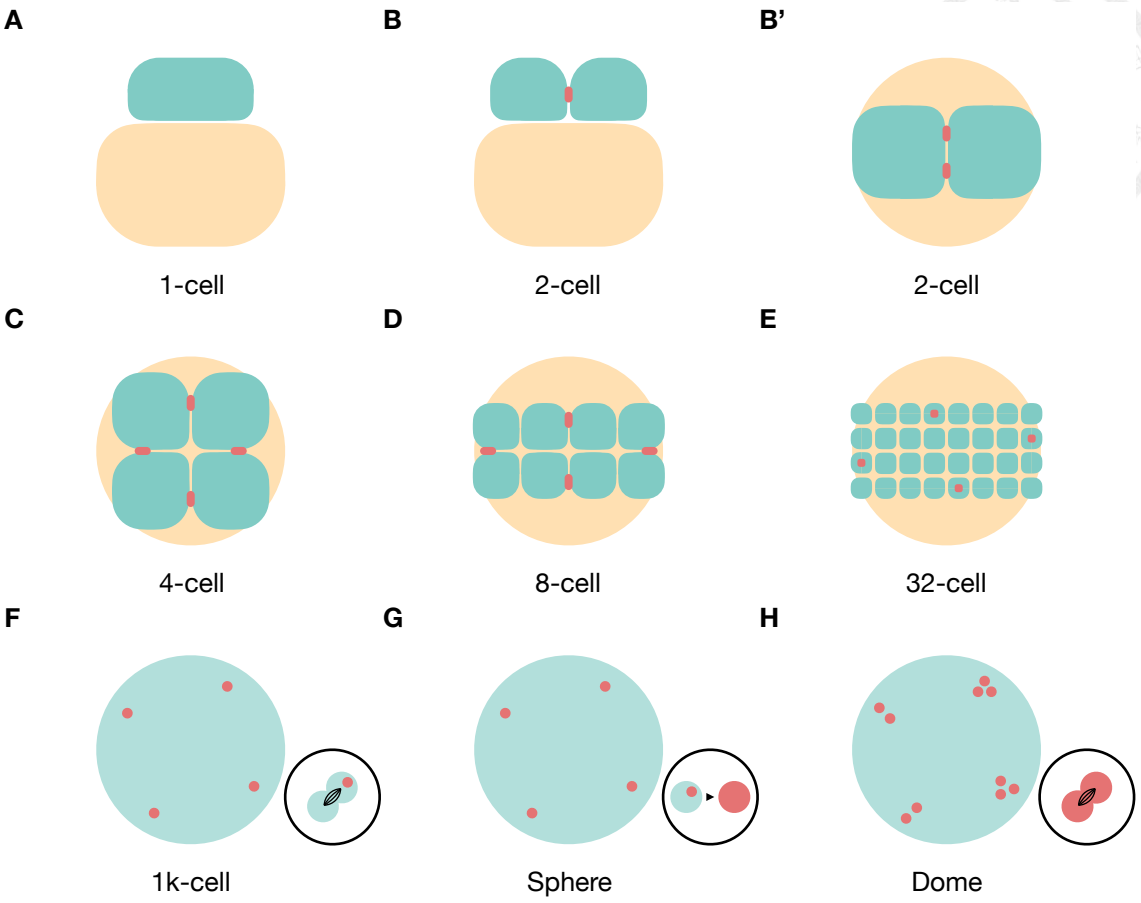

Figure 1. PGC specification in zebrafish (adapted from Yoon et al., 1997).

(A-D) Germ plasm accumulates at the distal ends of furrows during first few divisions. (E) At 32-cell stage, the germ plasm enters four cells. (F) Prior to the sphere stage, the germ plasm recipients divide asymmetrically and only four descendants keep the germ plasm. (G) At the sphere stage (8k-cell stage), the germ plasm diffuses in the cytosol. (H) Since the sphere stage, the germ plasm is distributed equally into the descendant cells and the germline is segregated from the somatic lineage. (A and B) lateral view; (B' and C-H) animal view.

doi:10.6342/NTU201903081

1.1.3. Guiding PGCs toward the gonads

Specified prior to gastrulation, PGCs trek across the embryo from their birthplaces to where the gonad develops. In zebrafish, nascent PGCs are anchored by cadherin 1 (Cdh1, also known as E-cadherin) on the cell membrane and stay immobile at the margin of the blastoderm under control of Rgs14a—a negative regulator of G-protein signaling (Hartwig et al., 2014). Around 30% epiboly (4.66 hpf), Rgs14a dwindles, allowing PGCs to escape from the detention by Cdh1 and perceive the environmental attractants (Blaser et al., 2005; Hartwig et al., 2014). Following the acquisition of motility, PGCs start to respond to chemokine Cxcl12a (also known as Sdf1a) (Doitsidou et al., 2002), which is conserved across vertebrates (Molyneaux et al., 2003; Stebler et al., 2004; Takeuchi et al., 2010). Expressing the cognate receptor Cxcr4b at their cell surface, PGCs snuffle along the way marked by the chemoattractant, migrating from the germ ring at the shield stage (6 hpf) and progressively converging to the gonadal ridge during gastrulation and segmentation (Figure 2) (Doitsidou et al., 2002; Weidinger et al., 1999).

However, since Cxcl12a-Cxcr4b signaling is not a delegated mechanism for PGC migration (David et al., 2002; Mizoguchi et al., 2008), moving in a speed of 2 μm/min (Reichman-Fried et al., 2004), PGCs would potentially reach every point emitting Cxcl12a in an embryo following hours of journey. Therefore, it is not surprising that several molecular mechanisms prune the dynamic chemokine breadcrumbs. In such sensitive chemotactic event, another Cxcl12a receptor, Ackr3b (also known as Cxcr7b), are dispersed globally to shape superfluous Cxcl12a proteins into a more unambiguous itinerary for PGCs (Boldajipour et al., 2008). Besides, though under debate (Goudarzi et al., 2013; Staton et al., 2011, 2013), miRNAs regulating *cxcl12a* and *ackr3b* levels in

doi:10.6342/NTU201903081

the soma may consolidate the robustness of PGC guidance (Staton et al., 2011).

Cxcl12a binds to its receptor Cxcr4b on PGCs with the help of co-receptor heparan sulfates (HS), a sort of glycosaminoglycans (Charnaux et al., 2005; Uchimura et al., 2006; Wei and Liu, 2014). Upon ligand-receptor binding, Cxcr4b becomes phosphorylated and activates scaffold protein Baiap2a (also known as Irsp53), which promotes the formation of dynamic filopodia, polarizing the distribution of Cxcr4b biased toward the cell front by extending the surface for chemokine interaction (Meyen et al., 2015). Furthermore, active Cxcr4b signals through G protein-coupled receptor (GPCR) signaling (Xu et al., 2012), in which Ca15b, existing specifically in PGCs, elevates the pH value at the leading edge (Tarbashevich et al., 2015). The polar pH elevation promotes phosphorylation of the monomeric GTPase Rac1, which triggers actin polymerization at the cell front (Kardash et al., 2010; Tarbashevich et al., 2015). Then, against the Cdh1-mediated traction and retrograde flows generated by active RhoA, PGCs bleb and move up the chemokine gradient (Blaser et al., 2006; Kardash et al., 2010).

doi:10.6342/NTU201903081

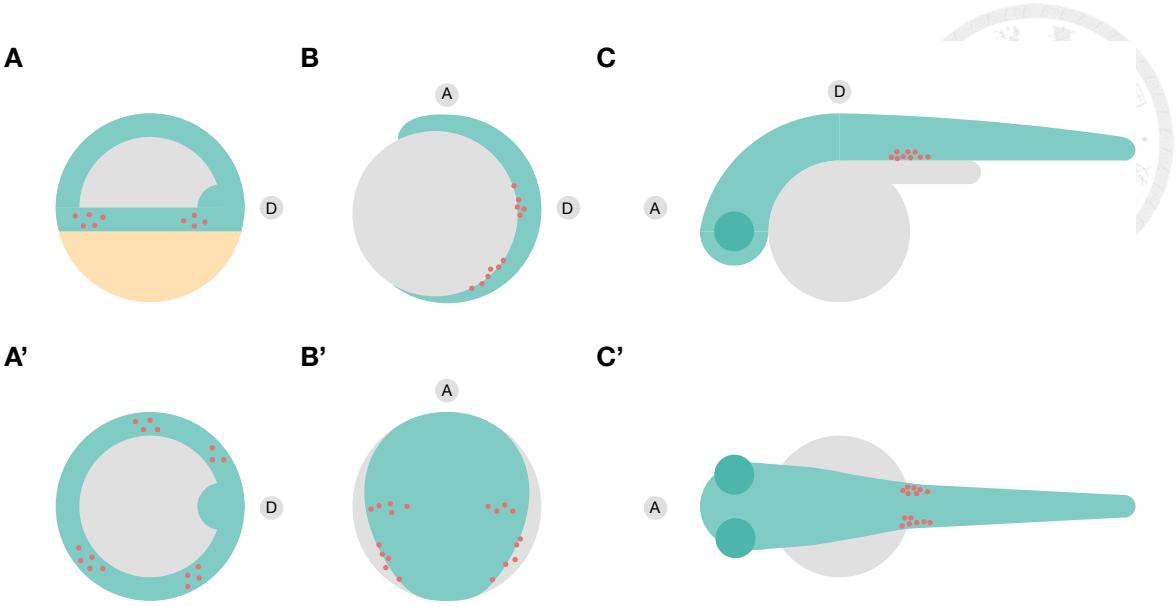

Figure 2. PGC migration in zebrafish (adapted from Weidinger et al., 1999).

(A,A') At the shield stage (6 hpf), PGCs locate at the blastoderm margin and migrate toward the determinative dorsal side where the embryo body forms. (B,B') At the bud stage (10 hpf), PGCs are align at the lateral border of the embryo and two clusters start to converge bilaterally. (C,C') At the prim-5 stage, PGCs arrive at the gonadal ridge, ventrally to the trunk and in the anterior side of the yolk extension. (A-C) side view; (A') top view; (B',C') dorsal view; A: anterior; D: dorsal.

doi:10.6342/NTU201903081

1.1.4. Interactions of PGCs and extracellular signals

For animals determining PGCs through epigenesis, PGCs, as expected, interact with soma through paracrine signaling quite frequently for their specification, proliferation, migration, and survival. Take mouse for example, *in vivo* evidence suggests that BMP signals induce PGC formation (Lawson et al., 1999), while KIT (Runyan et al., 2006) and FGF (Takeuchi et al., 2005) signalings matter to their motility and survival. On the other hand, although specification by germ plasm is deemed a strategy to liberate somatic evolution (Johnson and Alberio, 2015), PGCs seem not to be indifferent to the adjacent environments. For instance, chicken PGCs can be propagated *in vitro* infinitely, but only on a feeder cell layer (van de Lavoir et al., 2006) or substituted by a medium supplied with FGF2, insulin, and activin A (Whyte et al., 2015).

In zebrafish, deficiency of *cxcl12a* or *cxcr4b* disrupts PGC positioning but not their number in the first day of development (Doitsidou et al., 2002; Knaut et al., 2003), yet a few lines of evidence allude to interactions between PGCs and somatic cells beyond guidance mechanisms. For example, when intrinsically introduced with Heparanase (Hpse), an HS degrading enzyme, PGCs culminates in aberrant positioning as early as the shield stage (6 hpf) and apoptosis since late stage of gastrulation (8-10 hpf) (Wei and Liu, 2014). Considering the canonical role of HS as co-factors participating in varied ligand-receptor interactions (DiGabriele et al., 1998; Kuo et al., 2010; Lau et al., 2004; Ori et al., 2011), zebrafish PGCs tend to rely on certain morphogens to remain oriented and alive. In addition, global ablation of insulin-like growth factor (Igf) signaling

doi:10.6342/NTU201903081

discommodes PGC survival during late somitogenesis (18-24 hpf) (Schlueter et al., 2007), but not in the case when Igf signaling is repressed PGC-specifically (Sang et al., 2008). It implies that the fluctuation of PGC number in global repression of Igf signaling is a relay mechanism through somatic tissues. However, as far as I know, no intrinsic signaling, including Kit signaling that is crucial in mice (Mellgren and Johnson, 2005; Parichy et al., 1999), have been found vital to zebrafish PGCs.

doi:10.6342/NTU201903081

1.2. Fibroblast growth factor (FGF) signaling

Cells communicate, especially in multicellular organisms. A strategy for intercellular communication is paracrine signaling, in which the signal molecules (or ligands) are released into the extracellular spaces and act on the neighboring cells. Among the paracrine signal molecules, fibroblast growth factors (FGFs) refer to a family of signal molecules sharing phylogenetic homology. FGFs were first found as a mitogen inducing proliferation of mouse fibroblasts (Abraham et al., 1986; Gospodarowicz, 1974) but later revealed their versatile functions on cell proliferation (Gritti et al., 1996; Lindner and Reidy, 1991), survival (Gospodarowicz et al., 1976; Walicke et al., 1986), and migration (Devore et al., 1995; Sutherland et al., 1996) conserved across vertebrates and invertebrates. FGF signaling drives multiple physiological functions, such as angiogenesis (Schweigerer et al., 1987) and regeneration (Lee et al., 2005), and is particularly substantial to embryonic development (Ciruna and Rossant, 2001; Fletcher and Harland, 2008; Sekine et al., 1999; Streit et al., 2000). With its multifunctional manner as well as omnipresent significance, FGF signaling has been extensively investigated and continues to unveil its fine-tuned orchestration on miscellaneous biological events.

doi:10.6342/NTU201903081

1.2.1. Classification of ligands and receptors

In vertebrates, FGF family comprises at least 22 members, including 12 paracrine factors, four endocrine factors (FGF15/19, FGF21, and FGF23), and four FGF homologous factors that do not act as signal proteins (FGF11-14) (Ornitz and Itoh, 2001). Based on the phylogenetic analyses, the paracrine FGFs can be further classified into five groups, namely FGF1, FGF4, FGF7, FGF8, and FGF9 subfamilies (Itoh and Ornitz, 2004). In zebrafish, additional *fgf24*, belonging to *fgf8* subfamily, is encoded in the genome, and *fgf1/6/8/10-13/18/20* has gene duplicates (Ncbi Resource Coordinators, 2018), so zebrafish has at least 33 *fgf* genes. Since I am more interested in the extrinsic factors and stages prior to the onset of blood circulation (25-26 hpf) (Herbert et al., 2009), I will focus on the mechanisms of paracrine FGF signaling in this part of review.

A cell receives and relays a canonical Fgf signal through FGF receptors (FGFRs) on its cell membrane. FGFRs belong to enzyme-coupled receptors which relay the extracellular signals via their cytosolic domains called receptor tyrosine kinases (RTKs). The extracellular domain of a FGFR comprises three immunoglobulin−like (Ig) domains (Williams and Barclay, 1988). The Ig domain I and the acidic box between Ig domain I and II prevent auto-dimerization of FGFRs (Kalinina et al., 2012; Wang et al., 1995) while Ig domains II and III regulate the ligand binding affinity (Plotnikov et al., 2000; Yeh et al., 2003). In contrast with the copiousness of FGF ligands, only four paralogous FGF receptors (FGFRs) are identified across vertebrates, namely FGFR1-4 (Ornitz and Itoh, 2001). In zebrafish, *fgfr1* has gene duplicates so that five *fgfr* genes—*fgfr1a*, *fgfr1b*, and *fgfr2-4*—have been identified.

doi:10.6342/NTU201903081

1.2.2. Transduction of signaling

FGFs preferably interact with FGFRs and activate them by bringing two FGFR monomers together (Ornitz et al., 1996). Nevertheless, FGFs cannot bind FGFRs directly, instead requiring fortification by HS on the cell membrane to form a 2:2:2 ternary complex (Rapraeger et al., 1991; Schlessinger et al., 2000; Yayon et al., 1991). Notably, HS existing in extracellular matrix (ECM), in addition to involved directly in ligand-receptor binding, arrest FGF ligands in preference, enabling spatial regulation of ligand distribution (Kalinina et al., 2009; Makarenkova et al., 2009).

According to the studies in mammalian cells, at least four intracellular downstream signaling pathways are possible to relay FGF signaling onward depending on the intracellular context, including RAS-MAPK (Kouhara et al., 1997), PI3K-AKT (Hadari et al., 2001), PLCγ (Peters et al., 1992), and JAK-STAT (Hart et al., 2000) pathways. Though Fgf signals drive diverse signaling cascades and cell responses, a cell or tissue appears to respond to Fgf ligands quantitatively (Barak et al., 2012; Sun et al., 2002; Urness et al., 2011). In other words, the transductions through different FGFRs are believed to be redundant to each other (Gattineni et al., 2014; Lavine et al., 2005; Weinstein et al., 1998). Some evidence revealed that FGFRs seem to signal through the same pathways with dissimilar signal amplitudes (Raffioni et al., 1999); however, it remains disputable whether FGFRs preferentially activate one downstream signaling pathway over another.

doi:10.6342/NTU201903081

1.2.3. FGF signaling and PGCs

The interaction between FGFs and PGCs is not an epiphany within the scientific community. FGF signals were disclosed to be vital for PGC maintenance. During *in vitro* cultivation, supplementation of FGF2 promotes proliferation of mouse (Matsui et al., 1992; Resnick et al., 1992) and chicken (Choi et al., 2010) PGCs. In mice, when FGF signaling was inhibited, the number of PGCs on embryo slices or in *FGFR2-IIIb* knockout embryos decreased by apoptosis without affecting proliferation (Takeuchi et al., 2005). In addition, expressing Fgfs into the adjacency of zebrafish PGCs augmented PGC number since the second week of development (Wong and Collodi, 2013). In chickens, on the contrary, *FGF8* promoted self-renewal *in vitro*, and global knockdown of *FGF8* increased the proportion of PGCs *in vivo* (Wang et al., 2018).

FGF signaling has also been shown to play a role in PGC migration. In mouse explants, manipulation of global Fgf signaling illustrated a positive association of PGC motility with the intensity of FGF signaling (Takeuchi et al., 2005). However, until now, no *in vivo* or cell-intrinsic study has depicted the regulation of Fgfs on PGC migration.

In my study, using zebrafish as the animal model, I reveal that PGCs require Fgf signals to complete migration. To my surprise, loss of intrinsic Fgf signaling did not interfere with PGC quantity in zebrafish. As far as I know, it is the first *in vivo* evidence of direct interaction between Fgfs and PGCs and the first *in vivo* description of migratory roles of Fgfs on vertebrate PGCs.

doi:10.6342/NTU201903081

2. Specific aims

According to the roles of Fgf signaling on PGCs suggested in previous studies, I hypothesize that Fgf signaling functions on PGC survival, proliferation or migration *in vivo*. Therefore, I selected zebrafish as the *in vivo* animal model to assess the interactions between PGCs and Fgfs. Three questions were asked to clarify the roles of Fgf signaling in zebrafish PGCs:

1. May zebrafish PGCs receive Fgf signals?

To determine the competence of zebrafish PGCs to receive Fgf signals via Fgfrs, migrating PGCs were isolated and their RNA profiles were identified.

2. Do zebrafish PGCs require Fgf signals intrinsically?

To determine the intrinsic requirement of Fgf signaling for PGCs, a dominant-negative Fgfr (dn-Fgfr) was introduced specifically to PGCs, and the quantity and localization of PGCs were assessed. A constitutive-active Fgfrs (ca-Fgfr) was also introduced to dn-Fgfr overexpressed PGCs to determine the specific effects of the dn-Fgfr.

3. What are the cytosolic signalings evoked by Fgf signals in zebrafish PGCs?

To determine the cytosolic signaling pathways evoked by Fgf signals, I attempted to assess Rac1 and Mapk activities in Fgf signaling manipulated PGCs.

doi:10.6342/NTU201903081

3. Material and methods

3.1. Zebrafish

3.1.1. Zebrafish facility

AB wild-type and *Tg(kop:EGFP-F-nanos3-3'UTR)* zebrafish (Blaser et al., 2005) were kept in a recirculation aquaculture system at 28 °C with the light/dark cycle of 14/10 hr (Wei and Liu, 2014). The single-sex adult fish were housed in a density below 5 fish/L and fed routinely with live brine shrimps, twice a day (10 a.m. and 4 p.m.) on weekdays or once (2 p.m.) on weekends. All animal protocols in this study were approved by Institutional Animal Care and Use Committee (IACUC) of National Taiwan University (NTU-105-EL-00146). The materials used in this study and their sources are listed in Table 5.

3.1.2. Mating and embryo cultivation

One day before mating, male and female fish were transferred into a mating chamber with a separator following the second meal of the day. In the next morning, the separator was removed to allow spontaneous spawning for 10 min. Eggs were then collected and transferred into a 10-cm dish containing E3 medium (100 nM NaCl, 3.4 nM KCl, 6.6 nM $CaCl_2$, 6.6 nM $MgSO_4$, and 2 ppm methylene blue in reverse osmosis water). Embryos were incubated at 28.5 °C and staged depending on hpf and their morphogenic features (Kimmel et al., 1995).

doi:10.6342/NTU201903081

3.2. Identification of transcripts between cell types

3.2.1. Embryo dissociation and cell fixation

Embryo dissociation (Samsa et al., 2016) and the procedures from cell fixation to RNA extraction (Thomsen et al., 2016) were adapted from previous literatures. Embryos reproduced by *Tg(kop:EGFP-nanos3-3'UTR)* (Blaser et al., 2005) or wild-type female fish were staged and dechorionated in 1 mg/mL pronase in E3 medium for 10 min. Dechorionated embryos were then transferred to a 2-mL microcentrifuge tube and deyolked by pipetting in 1 mL of 0.9× PBS. Dissociated cells were pelleted from dissolved yolk (300 ×*g*, 1 min, 4 °C), resuspended with 1 mL of 1% paraformaldehyde (PFA) in 1× PBS, and passed through a 40-μm cell strainer into a new 2-mL microcentrifuge tube. After fixation at room temperature (RT) for 10 min with agitation, fixed cells were pelleted (500 ×*g*, 1 min, 4 °C), washed once with PBSR (1 U/mL RNaseOUT in 1× PBS) and resuspended in PBSR—1/3, 2/3, or 1 μL per 6, 8, or 10 hpf embryos respectively. The samples were preserved at -80 °C until cell sorting.

3.2.2. Fluorescence-activated cell sorting (FACS)

Samples prepared in 3.2.1 were thawed on ice, and the FACS was carried on BD FACSAria III sorter (Instrumentation Center, National Taiwan University). PGCs or somatic cells were sorted out via 2-step sequential gating: The first gate identified cells from debris depending on the size (FSC) and granularity (SSC) while the second one distinguished GFP positive from negative events based on the green fluorescence intensity. The second gate was circumscribed according to the FSC and GFP intensities since PGCs do not generate distinct population on GFP intensity histograms due to their scarce percentage (< 1%) (Goto-Kazeto et al., 2010). Cells were sorted into 1 well of a

doi:10.6342/NTU201903081

96-well plate containing 150 μL of Buffer PKD with 10 μL of proteinase K, supplied in RNeasy FFPE Kit.

3.2.3. RNA extraction of PFA-fixed samples

Total RNA in samples prepared in 3.2.2 were extracted with RNeasy FFPE Kit with a modified protocol (Thomsen et al., 2016). To reverse formaldehyde modification, samples containing proteinase K were sealed with parafilm and incubated at 56 °C for 1 hr and then cooled on ice for 3 min. Samples were then transferred to a 1.5 mL microcentrifuge tube and centrifuged to precipitate debris (20000 ×*g*, 15 min). To remove the remaining genomic DNA, the supernatant was treated with 10 μL of DNase I and 16 μL of DNase Booster Buffer in a new 1.5-mL microcentrifuge tubes at RT for 15 min. Then, 320 μL of RBC buffer and 720 μL of ethanol were then individually added and mixed by vortex to adjust the binding condition. Lastly, samples were bound on MinElute spin column, washed twice with 500 μL of Buffer RPE, and eluted in 14 μL of water.

3.2.4. In vitro reverse transcription (RT) with gene specific primers

To set up the RT reactions for qualitative analysis (3.2.5), 11 μL of RNA samples from 2.2.3 were mixed with 1 μL of dNTP mixture (2.5 mM each) and 1 μL of 50 ng/μL Random Primers, heated to 65 °C for 5 min, and cooled down to 4 °C for 1 min. The mixtures were thereafter added 4 μL of 5× FS buffer, 1 μL of RNase Inhibitor, and 1 μL of SuperScript III Reverse Transcriptase, then incubated at 25 °C for 5 min for primer extension, 50 °C for 1 hr for reverse transcription, and 70 °C for 15 min for heat inactivation.

doi:10.6342/NTU201903081

For quantitative analysis (3.2.6), 12 μL of RNA samples were reverse transcribed with gene-specific primer pool (2 mM/each primer) (reverse primers in Table 1) by EasyScript III RTase system. The RT reaction was incubated at 55 °C instead of 50 °C without primer extension step. Synthesized cDNA samples were stored at -20 °C prior to use.

3.2.5. Nested polymerase chain reaction (PCR)

To identify the expressions of genes of interest in scarce material, 1 μL of cDNA was preamplified in 20 μL reaction of Q5 High-Fidelity DNA Polymerase reaction with pool of outer primers (*actb1, ca15b, dnd1 and fgfrs* in Table 1), 62.5 nM each. The preampfification program was set as 98 °C denaturation for 30 s followed by 15 cycles of denaturation at 98 °C for 10 s, annealing at 60 °C for 30 s, and extension at 72 °C for 20 s with addition final extension 72 °C for 2 min. Then, 1 μL of of PCR products were used in 20 μL reaction of Q5 High-Fidelity DNA Polymerase reaction with nested primers of the independent genes (Table 2), 0.5 mM each. The thermocycling condition was set as 98 °C denaturation for 30 s followed by 25 cycles of 98 °C for 5 s, 60 °C for 1 s, and 72 °C for 10 s with final extension at 72 °C for 2 min. The PCR products were visualized on 2% agarose gel in 1× TBE buffer (89 mM Tris, 89 mM boric acid, 2 mM EDTA) with electrophoresis.

doi:10.6342/NTU201903081

3.2.6. Nested real-time quantitative PCR (qPCR)

To quantify gene expressions starting with sparse RNA material, 2.5 μL of cDNA was pre-amplified in 50 μL of Q5 High-Fidelity DNA Polymerase reaction with the outer primer pool (Table 1, 0.05 μM each). The pre-amplified program was set as follows: denaturation at 98 °C for 30 s and 20 cycles of denaturation at 98 °C for 10 s, annealing at 60 °C for 30 s, and extension at 72 °C for 20 s. One μL of pre-amplified products were then underwent the second round of PCR in 10 μL reaction of iQ SYBR Green Supermix, with the concentration of each inner primer (Table 2) supplied as 0.3 μM. Real-time PCR was performed on QuantStudio 3 System (Applied Biosystems, Foster City, CA) with following protocol: 95 °C for 3 min followed by 30 cycles of 95 °C for 15 s, 60 °C for 15 s, and 72 °C for 30 s.

3.2.7. Data processing

I used $\Delta\Delta C_q$ method to analyze gene expressions (Livak and Schmittgen, 2001). The C_q values (amplification cycles upon detection) of each gene from different samples were first normalized with mean ΔC_q of *actb1* (to generate ΔC_q). Then $\Delta\Delta C_q$ were calculated by further subtraction of the averages of all ΔC_q of a gene; that is, the expression of a specific gene within a specific cell-type and stage would be normalized to the average of RNA expressions in every sample. Relative expressions were calculated as the negative $\Delta\Delta C_q$ power of 2. The stepwise mathematic equations are listed below:

i. $\Delta C_q = C_{q\ gene} - C_{q\ actb1}$

ii. $\Delta\Delta C_q = \Delta C_{q\ celltype,stage} - \Delta C_{q\ average}$

iii. Relative gene expression $= 2^{-\Delta\Delta Cq}$

doi:10.6342/NTU201903081

3.3. Introduction of extrinsic mRNA into embryos

3.3.1. Plasmid construction

To specifically express mRNA within zebrafish PGCs, *pT7-nanos3-3'UTR*—in abbreviation, *pT7-nos*—was used as the backbone as previously described (Wei and Liu, 2014). The caR4 sequence was a gift from Dr. Yamasu, Saitama University (Ota et al., 2009). To subclone specific genes to the backbone, the coding regions of desired genes were amplified with primers with additional restriction enzyme cutting sites at their 5'-end (Table 3). For efficient translation of the introduced mRNAs, the zebrafish Kozak sequence (AAAC before ATG) (Grzegorski et al., 2014) and preferred stop codon (TAA with additional A) (Horstick et al., 2015) were generated by modifying sequences on the aforementioned primers.

3.3.2. mRNA *in vitro* transcription (IVT)

To obtain complete linearized templates for errorless IVT, 2 μg of plasmids was digested with NotI-HF and NdeI (NheI instead if desire sequences contain *NdeI* cutting sites) at 37 °C overnight followed by electrophoresis and gel extraction using GenepHlow Gel Extraction Kit. The linearized DNA templates were eluted with 20 μL of DEPC water and 6 μL of the products were taken for IVT with mMESSAGE mMACHINE T7 Transcription Kit in 20 μL reaction. I incubated the reaction at 37 °C for 2 hr, digested the DNA templates with TURBO DNase at 37 °C for 15 min, and purified the products by lithium chloride (LiCl) precipitation, in which 30 μL of Nuclease-free Water and 30 μL LiCl Precipitation Solution were added before chilled at -20 °C for 30 min, and RNA were pelleted (20000 ×*g*, 15 min, 4 °C) and washed once with 70% ethanol. Synthesized RNA was eluted in 20-50 μL of nuclease-free water,

doi:10.6342/NTU201903081

quantified with NanoDrop 1000 Spectrophotometer (Thermo Fisher Scientific, Waltham, MA), and stored at -80 °C.

3.3.3. Microinjection

For microinjection needles, glass capillaries (1.0 mm outer diameter, 0.75 mm inner diameter) were pulled using a P-97 Flaming/Brown type micropipette puller (Sutter Instrument) (PULL = 300, HEAT = 80, PULL = 60, VEL = 60, TIME = 150). After broken back the tip to make a ~10 μm opening, the microinjection needles were backloaded with the injection material containing 0.05% of phenol red for visualization within the cytoplasm. The microinjection needles were then connected to an IM-31 Electric Controlled Pneumatic Microinjector (Narishige Co., Tokyo, Japan) and calibrated in a drop of mineral oil on a micrometer (bal = 1.0-1.2 kPa, inj = 50-100 kPa, on-timer = 20 ms). Afterward, freshly laid eggs were aligned on a tray and injected with 1 nL (1.3 μm diameter) of solution directly into the cytoplasm prior to the first division of the zygotes (before 45 min-post-fertilization). Injected embryos were incubated at 28.5 °C and staged according to developing time and morphogenic features. The embryos with delayed development or defects were discarded according to the assumption that *nos* conjugated mRNAs should act exclusively on PGCs.

doi:10.6342/NTU201903081

3.4. Quantification of gene expressions in zebrafish embryos

3.4.1. RNA extraction

Thirty to fifty staged embryos were transferred into a 2-mL microcentrifuge tube and homologized in 700 μL TRIzol or GENEzol Reagent with TissueLyser LT (Qiagen). The lysate was incubated for 5min and the debris in lysates was removed by centrifugation (16000 ×*g*, 1 min, RT). Then the total RNA was purified with TriRNA Pure Kit following the manual. In brief, the lysates were passed through the column to bind the RNA and underwent on-column DNase I treatment. After 3 washes, the total RNA was eluted with 20 μL of nuclease free water and quantified with NanoDrop 1000 Spectrophotometer.

3.4.2. Primer design for qPCR

All primer used in qPCR (3.4.3) were designed on Primer-BLAST (Ye et al., 2012). The melting temperatures (TM) of primers were set around 60 °C, and Thermodynamic Template Alignment was used to predict primer amplification quality. The sequences of primers did not contain known SNP to interfere with their efficiency. The targets should include all validated and predicted isoforms and at least one intron in the genome referring to RefSeq database (NCBI Resource Coordinators, 2018). No off-target predictions were allowed for any primer pair, and the PCR products were validated with proper melting curves as well as single band on electrophoresis gel. All primers used in qPCR are listed in Table 2.

doi:10.6342/NTU201903081

3.4.3. RT-qPCR

I synthesized cDNA from 2 μg of total RNA in 20-μL reaction of SuperScript III Reverse Transcriptase system supplied with 200 ng of Random Primers. To quantify gene expressions at 10 hpf, I mixed 0.1 μL of cDNA and 0.3 μL of each 10 nM forward or reverse primers in 10 μL of iQ SYBR Green Supermix reaction. For 24-hpf cDNA, 1 μL of cDNA were used considering lower expressed PGC markers, and Power SYBR Green Master Mix were used to quantify gene expressions using the same protocol. Real-time PCR was performed on QuantStudio 3 System with following protocol: 50°C for 2 min, 95 °C for 10 min, and 40 cycles of 95 °C for 15 s and 60 °C for 1 min. Gene expressions were analyzed by $\Delta\Delta C_q$ method, first normalizing to *actb1* and then the wild-type siblings.

doi:10.6342/NTU201903081

3.5. Visualization of RNA spatial distribution within zebrafish embryos

3.5.1. RNA probe synthesis

A T7 promoter were added on the 5'-end of the anti-sense strand of a gene by amplifying zebrafish cDNA with designed reverse primers (Table 4) (Wei and Liu, 2014). After gel extraction, the DNA templates were *in vitro* transcribed in T7 RNA Polymerase reaction supplied with digoxigenin (DIG) or fluorescein RNA Labeling Mix at 37 °C for 2 hr. Then, the DNA templates were removed and the synthesized RNA probes were purified with lithium chloride precipitation using mMESSAGE mMACHINE T7 Transcription Kit, detailed in 3.3.2.

3.5.2. Embryo preparation

I performed whole-mount *in situ* hybridization (WISH) as described previously (Thisse and Thisse, 2008; Wei and Liu, 2014). In detail, embryos were collected and fixed in 4% PFA in 1× PBST (1× PBS with 0.1% Tween 20) overnight at 4 °C. Dechorionation was done before fixation for 24 hpf embryos and following fixation for earlier ones. On the next day, the fixed embryos were dehydrated in methanol for 20 min and kept in methanol at -20 °C at least overnight.

3.5.3. *In situ* hybridization

For more amiable probe penetration, the embryos prepared in 3.5.1 were permeabilized in 2% H_2O_2 in methanol for 20 min at RT, then progressively rehydrated to 1× PBST (25% increase in each wash). Then, the embryos were pre-hybridized in Hybridization Mix (HM: 50% formamide, 5× SSC, 0.1 % Tween 20, 5% dextran

doi:10.6342/NTU201903081

sulfate, 50 μg/mL heparin, 500 μg/mL tRNA, 9.2 mM citric acid) in a 70 °C water bath for 2 hr, and incubated in 250 ng/mL probe in HM overnight.

3.5.4. Antibody detection

The embryos from 3.5.3 were successively transferred into 2× SSCT (2× SSC with 0.1% tween 20) (25% increase in each replacement) and incubated twice in 0.2× SSCT for 30 min to remove unhybridized probes. All steps mentioned above took place in a 70 °C water bath. Thereafter, the embryos were wash once with 1× PBST, blocked in Blocking Buffer (2% BSA and 2% sheep serum in 1× PBST) at RT for 1 hr, and incubated in 1:4000 alkaline phosphatase DIG or FLU antibody in Blocking Buffer at 4 °C overnight.

On the next day, the excessive antibodies were washed 6 times in 1× PBST within 2 hr. For chromatic staining, the embryos were incubated in AP Buffer (100 mM Tris-HCl pH 9.5, 50 mM $MgCl_2$, 100 mM NaCl, 0.1 % Tween 20) for 15 min and then in Staining Buffer (0.01× NBT/BCIP Stock Solution in AP Buffer) at 28.5 °C until desired coloring.

3.5.5. Mounting and imaging

Stained embryos in 3.5.4 were briefly wash once in 1× PBST and dehydrated in MeOH. Dehydrated embryos were then transferred into a 35mm petri dish with minimal MeOH. About 2 mL of clearing reagent (benzyl benzoate:benzyl alcohol, 2:1) was added to cover the embryos. Following entire clearance of embryos (~5 min), embryos were observed under a microscope (Z16 APO, Leica, Wetzlar, Germany).

doi:10.6342/NTU201903081

3.6. Evaluation of cytosolic signaling activation in PGCs

3.6.1. Introduction of biosensors into PGCs

The *cytoplasmic EKAR (EGFP-mRFP)* and *pTriEx4-Rac1-2G* were gifts from Karel Svoboda (Harvey et al., 2008) and Olivier Pertz (Fritz et al., 2015). The coding sequences of EKAR (Harvey et al., 2008) and Rac1-2G (Fritz et al., 2015) were cloned to *pT7-nos*, *in vitro* transcribed, and microinjected into the embryos as described in 3.3. Because of the laser-filter sets available for the flow cytometry I used, the mTFP-Venus fluorescence pair in Rac1-2G biosensor was substituted by EGFP-mRFP1 (Harvey et al., 2008; Peter et al., 2005), and the 177-192 amino acid sequence of Rac1 was truncated to reduce the accumulation of the biosensor in the nucleus (Kardash et al., 2010). All primers used for plasmid construction are listed in Table 3.

3.6.2. Evaluation of signaling intensity in PGCs with flow cytometry

Microinjected embryos were dechorionated just before collection at 8 hpf. The embryos were dissociated and fixed as stated in 3.2.1. Cell cytometries were performed on BD FACSAria III sorter at Instrumentation Center, National Taiwan University. I excited the biosensors in PGCs with a 488 nm laser and received the green (530/30) and red (616/23) emission simultaneously. PGCs were identified as the GFP positive particles with proper FSC/SSC, and the activity of desired signaling were calculated by dividing the green fluorescent intensity to the red one.

doi:10.6342/NTU201903081

3.7. **Statistics**

3.7.1. Comparisons among more than 2 groups

For gene expression analysis, the distributions of variables were assume to be Gaussian distribution, and analysis of variance (ANOVA) was performed—One way for Figure 10 and two-way for factorial designs (Figure 6 and 11). As parametric tests (such as *t*-test and ANOVA) assume data sampled from Gaussian distributions, for non-Gaussian populations with continuous variables (Figure 15AC and 16), I instead used Kruskal-Wallis tests followed by Dunn's tests. Statistical analysis was performed on GraphPad Prism 8 (San Diego, California USA, www.graphpad.com).

3.7.2. Comparisons among zero-inflated populations

Kruskal-Wallis test treats non-Gaussian data as ranks. As a result, they are limited when processing count data and zero-inflated ones (distributions with lots of zeros), which will not be transformed in to a flat Gaussian distribution by ranking. For zero-inflated populations (Figures 13 and 15B), I compared them with negative binomial generalized linear model (GLM) using R (version 3.6.0, R Core Team, 2019). Distributions with continuous variable were first binned within width of 0.1 (10%) before fitted into negative binomial GLM. To correct increased type-one errors by multiple comparisons within more than two groups, two-stage step-up method of Benjamini, Krieger and Yekutieli was used to adjust *P* values (Benjamini et al., 2006).Here's an example R code used for two sample comparison using negative binomial GLM:

```
>  Control <- c(37,5,4,1,0,0,1,0,0,0,0,0,0,0,0)
>  Treatment <- c(43,8,8,8,2,2,1,1,2,1,1,0,0,0,1)
>  # enter the count data starting from the minimal number
```


doi:10.6342/NTU201903081

```
>  resp <- c(rep(0:14,times= Control), rep(0:14,times= Treatment))
>  # enter minimal and maximum observed values as data input
>  injRNA <- factor(c(rep("Control", sum(Control)), rep("Treatment",
   sum(Treatment))), levels = c("Control","Treatment"))
>  data <- data.frame(resp, injRNA)
>  library(MASS)
>  nbGLM <- glm.nb(resp ~ injRNA, data=data)
>  summary(nbGLM)

Coefficients:
             Estimate Std. Error z value Pr(>|z|)
(Intercept)    -0.7802     0.3260  -2.393  0.01670 *
injRNATreatment   1.2755     0.3892   3.277  0.00105 **

             Theta:  0.3426
         Std. Err.:  0.0823
```

When the difference of two distributions fit into a negative binomial regression model, the variable "injRNA" was significant (P = 0.001), meaning that the difference between "Control" and "Treatment" differs from zero. The estimate 1.28 indicates the rate of "Treatment" is $e^{1.28}$ (positive) fold of that of "Control", which equals to $e^{-0.78}$. To visualize the fit of a count regression model by rootogram (Kleiber and Zeileis, 2016) (Figure 3):

```
>  install.packages("countreg", repos="http://R-Forge.R-
   project.org")
>  library(countreg)

>  SixHours <- rep(0:6, c(85,25,13,15,6,0,1))
>  rootogram(SixHours, fitted = "negative binomial", style =
   c("hanging"), xlim = c(-0.5,6.4), ylim = c(-1, 10), main = "",
   xlab = "Ectopic PGC (10%)", fill = "#D9D9D9", col = "#239788")

>  OneDay <- rep(0:22, c(776,84,63,34,17,18,9,4,6,1,2,2,1,1,2,0,0,0,
   0,1,0,0,1))
>  rootogram(OneDay, fitted = "negative binomial", style =
   c("hanging"), xlim = c(-0.5,10.4), ylim = c(-1, 30), main = "",
   xlab = "Ectopic PGC #", fill = "#D9D9D9", col = "#239788")
```


doi:10.6342/NTU201903081

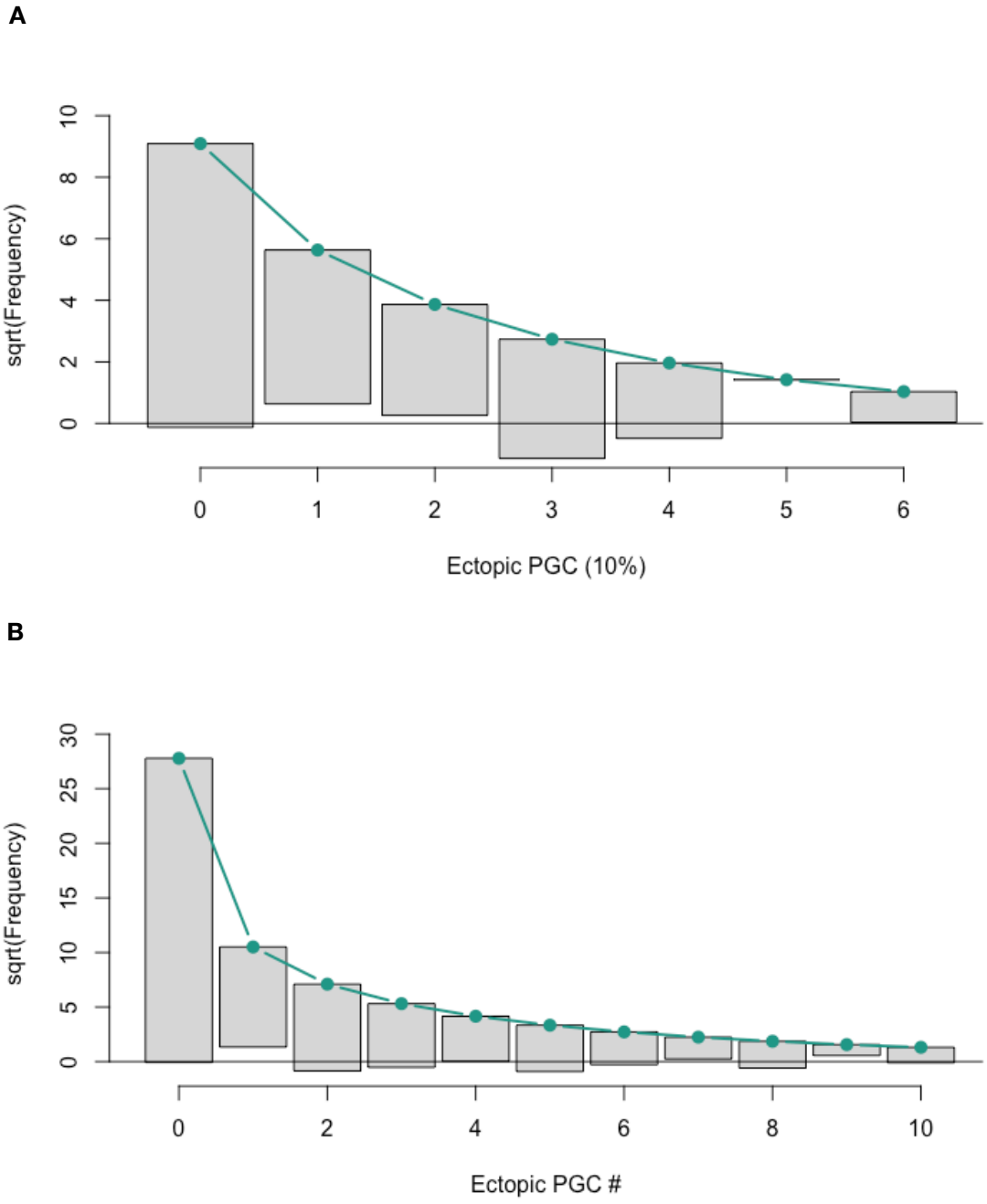

Figure 3. Fitting data into negative binomial GLM.

Rootograms of pools of all groups from ectopic PGC percentages at 6 hpf (A) or ectopic PGCs numbers at 24 hpf (B). Green dots indicate the fitted frequencies from a probability model and the gray hanging bars present the empirical frequencies.

doi:10.6342/NTU201903081

Table 1. Outer primers for pre-amplification and reverse transcription.

Gene		Sequence (5' → 3')	Product size
actb1	F	CCTTCCTGGGTATGGAATCT	368
	R	TGCATGGCCATTTTAAGGTG	
ca15b	F	TCCTTGACCACACCAAACTG	334
	R	CATTTCGTGGAGCAGAGTGG	
dnd1	F	TGAATCGAAGCTGCTGATGG	311
	R	CTGGGACGTCATAATGCAGG	
a2ml	F	CCTTAAAGAGTGTGGGGCTG	444
	R	AGTTGAAGACAGTGGCCTTG	
hkdc1	F	ATGTTGAGTTGGAACGAGGC	358
	R	ATACCTGTCTGATTGCACGG	
fgfr1a	F	GGTTCCTGCCAGTAAAACCG	383
	R	CCTCGATGTGTTTCAGCCAC	
fgfr1b	F	CCTGTTAAATGGATGGCGCC	396
	R	GTCTTGCTCGGACGAACATG	
fgfr2	F	CCTAAACCCAAAATGCGCTG	334
	R	TCGTATAGTGCTGCAACCAC	
fgfr3	F	AAGACTCGGGTGTTTACTCC	461
	R	CAGTCCTGCCTGTAAGATGG	
fgfr4	F	GTGCCTTATTGAACCCGTAC	374
	R	GGCGATTACTGTCCTTCTTG	

doi:10.6342/NTU201903081

Table 2. Inner (nested) primers for gene expression quantification.

Target		Sequence (5' → 3')	Product size
actb1	F	TTGCTCCTTCCACCATGAAG	123
	R	CCTGCTTGCTGATCCACATC	
hatn10	F	TGAAGACAGCAGAAGTCAATG	N/A
	R	CAGTAAACATGTCAGGCTAAATAA	
ca15b	F	TCCTTGACCACACCAAACTG	142
	R	GAGGAGAGTTGCTGGAGTTG	
dnd1	F	CGCATCCATGGCTAAGAAAG	146
	R	TCAGAACAAGTGGGGTTACG	
a2ml	F	GATCTGGGAGCTTGCTGAAG	94
	R	GAAGGCCTCTGTTTCCCAAG	
hkdc1	F	GAACCAATTTCCGCGTGTTG	127
	R	TGGTCAAACAGCTCCTCTCC	
fgfr1a	F	GAAATCCTACACCGACGCTC	97
	R	GTCCACATGTGCTCTCGTAC	
fgfr1b	F	TGCGGTTCCAACACAGAGAC	101
	R	GCACCGACAGCTCCAGATAC	
fgfr2	F	ATACACGCTGGATGTCGTTG	95
	R	TCGCATCTTGTCCAACTTGC	
fgfr3	F	CAAGGGAGAGCAGAGAATGG	98
	R	ATGTGTAATTTCCCCGGTCG	
fgfr4	F	AAGCATAACATCCGGGGAAC	100
	R	TCCTCCGACCAACACAGTAG	
cxcl12a	F	GCCATTCATGCACCGATTTC	89
	R	CTCTGTGGGACTGTGTTGAC	
ddx4	F	GGACGGGATCTAATGGCTTG	116
	R	ATCTCACTGAACTTGCTGGC	
ackr3b	F	TTTCTCCAGGCATCGGAATC	113
	R	CACACTCATCTTGGTCCGTC	
cxcr4b	F	CGCCTTTTTGAGCACACTTA	118
	R	CTGAGAGGTCGCAAAGTTCT	

doi:10.6342/NTU201903081

Table 3. Primers for plasmid construction.

Target		Sequence (5' → 3')	Enzyme
EGFP	**F**	TA GTCGAC AAACATG GTGAGCAAGGG	*SalI*
	R	ATA GGATCC TTTA CTTGTACAGCTCGTC	*BamHI*
dnR3	**F**	TA GTCGAC AAACATG TCTGAGTCTGCTCTC	*SalI*
	R	ATA GGATCC TTTA TTCAAGTTCAGACACGTTAG	*BamHI*
caR4	**F**	ATA AAGCTT AAACATG CTTATTTTCTATGCGAAG	*HindIII*
	R	ATA GGATCC TTTA TCGCATTGTCGTCTTTAGG	*BamHI*
Map2k	**F**	TATA CTCGAG AAACATGCAGAAAAGGAGGAAGC	*XhoI*
	R	ATA GGATCC TTTA CATTCCCACACTGTGAGTC	*BamHI*
Map2k **(K98M)**	**F**	ATGGCCAGGAtGTTGATCCACC	-
	R	GATGAAGCCTGACGGCCT	-
Map2k **(S219D)**	**F**	ACTCATTGACgaCATGGCCAATTCC	-
	R	TGTCCACTCACACCAAAG	-
EKAR	**F**	TATA CTCGAG AAACATG GCCTCCTCCGAGGA	*XhoI*
	R	TA AGATCT TTATTCGTCAAGTTCAAGTTCTTC	*BglII*
Rac1-2G	**F**	TATA CTCGAG CTCGAGAAACATG GCGTCCACCGACGGCATGGAC	*XhoI*
	R	ATA GGATCC TTTA TGACGAAGCGATCCGAGCAGT	*BamHI*
ΔNotI+HindIII **(*pT7-nos*** **for *Rac1-2G*)**	**F**	TT AAGGCGTAAATTGTAAG	-
	R	GCTT TATTAAGTCTAGAGAAAATG	-
EGFP **(Rac1-2G)**	**F**	TA GTCGAC AAACATG GTGAGCAAGGG	*SalI*
	R	ATATA TCCGGA CTTGTACAGCTCGTCCAT	*BspEI*
mRFP **(Rac1-2G)**	**F**	A GCGGCCGC CGCCTCCTCCGAGGACGTC	*NotI*
	R	TA GGTACC GGCGCCGGTGGAGTGGCG	*BamHI*

SalI and *XhoI* were ligated to *XhoI* on the vector; *BamHI* and *BglII* were ligated to *BamHI*.

doi:10.6342/NTU201903081

Table 4. Primers for WISH probes.

Target		Sequence (5' → 3')
T7 promoter	**R**	TAATACGACTCACTATAGG-
ddx4*	**F**	AAGGGCTGCAATGTTCTGTG
	R	CACTGGGAGAAGAGGCTTTG
fgfr1a†	**F**	AAAGCGACTTCAACAGCCAG
	R	GTCAAACAGAGCTTCGGGAG
fgfr2†	**F**	CGAAAGAGGCTGTGACTGTG
	R	GGGCACACAGGTCCAGATAT
fgfr3†	**F**	GCATGTACTCAAGACGGTCC
	R	CGTTGCTGTGGTGGTGTTTA
fgfr4†	**F**	GCGCAGACAGTATTCAGTGG
	R	AACCCCGAAAGACCATACGT
cxcl12a	**F**	GATGTCTGCCAGATGACAAG
	R	TTATCATACCTACAATGCTTTAG
ca15b‡	**F**	ATTTGGTGTGATCGTTAAAAACTGAAAGGGT
	R	AATACCAAAACCATCACCCCACACA

* (Wei and Liu, 2014), † (De Smet et al., 2014), ‡ (Tarbashevich et al., 2015)

doi:10.6342/NTU201903081

Table 5. Reagents and kits used in the study.

Name	Source	City	Identifier	Usage
Artemis	TANG	WuDi, China	2011001	3.1.1
NaCl	Sigma-Aldrich	St. Louis, MO	S5886	3.1.2 3.5.4
KCl	VWR	Solon, OH	0395	3.1.2
$CaCl_2 \cdot 2H_2O$	Sigma-Aldrich	St. Louis, MO	C7902	3.1.2
$MgSO_4$	Sigma-Aldrich	St. Louis, MO	M7506	3.1.2
Methylene blue	Sigma-Aldrich	St. Louis, MO	M9140	3.1.2
Pronase	Roche	Mannheim, Germany	10165921001	3.2.1 3.6.2
PBS - Phosphate-Buffered Saline (10X) pH 7.4, RNase-free	Invitrogen	Carlsbad,CA	AM9625	3.2.1 3.5.2 3.5.3 3.5.4 3.6.2
DEPC (Diethyl pyrocarbonate)	Bio Basic	Markham, Canada	DB0154	3.2.1 3.3.2
Paraformaldehyde	Sigma-Aldrich	St. Louis, MO	P6148	3.2.1 3.5.2 3.6.2
Tween 20	Sigma-Aldrich	St. Louis, MO	P1379 P9416	3.5.2 3.5.3 3.5.4
RNaseOUT Recombinant Ribonuclease Inhibitor	Invitrogen	Carlsbad,CA	10777019	3.2.1
RNeasy FFPE Kit	Qiagen	Hilden,Germany	73504	3.2.2 3.2.3
Ethanol	Honeywell	Morristown, NJ	32221	3.2.3 3.3.2 3.5.1 3.6.1
dNTP mixture	Takara	Kusatsu, Japan	4030	3.2.4
SuperScript III Reverse Transcriptase	Invitrogen	Carlsbad,CA	18080044	3.2.4 3.4.2
Random Primers	Invitrogen	Carlsbad,CA	48190011	3.2.4 3.4.2
EasyScript III RTase	Bioman	New Taipei City, Taiwan	RTM103	3.2.4

doi:10.6342/NTU201903081

Name	Source	City	Identifier	Usage
RNase Inhibitor	Bioman	New Taipei City, Taiwan	RTM201	3.2.4
iQ SYBR Green Supermix	Bio-Rad	Hercules, CA	1708880	3.2.5 3.2.6 3.4.2
Tris	VWR	Solon, OH	0826	3.2.5
Boric acid	J.T.Baker	Center Valley, PA	0084	3.2.5
EDTA	Sigma-Aldrich	St. Louis, MO	E6134	3.2.5
SeaKem® LE Agarose	Lonza	Basel, Switzerland	50004	3.2.5 3.3.2 3.6.1
Q5 High-Fidelity DNA Polymerase	New England Biolabs	Ipswich, MA	M0491S	3.2.6 3.3.1
QuantStudio 3 System	Applied Biosystems	Foster City, CA	A28136	3.2.6 3.4.2
T4 Polynucleotide Kinase	New England Biolabs	Ipswich, MA	M0201S	3.3.1
T4 DNA Ligase	New England Biolabs	Ipswich, MA	M0202S	3.3.1
ECOS 101 Competent Cells [DH5a]	Yeastern	Taipei, Taiwan	FYE607-80VL	3.3.1
Presto Mini Plasmid Kit	Geneaid	New Taipei City, Taiwan	PDH100	3.3.1 3.6.1
pIRES2-EGFP	BD Biosciences Clontech	Franklin Lakes, NJ	6029-1	3.3.1
Dpn1	New England Biolabs	Ipswich, MA	R0176S	3.3.1
SalI-HF	New England Biolabs	Ipswich, MA	R3138S	3.3.1
XhoI	New England Biolabs	Ipswich, MA	R0416S	3.3.1
HindIII-HF	New England Biolabs	Ipswich, MA	R3104S	3.3.1
BamHI-HF	New England Biolabs	Ipswich, MA	R3136S	3.3.1
NotI-HF	New England Biolabs	Ipswich, MA	R3189S	3.3.2
NdeI	New England Biolabs	Ipswich, MA	R0111S	3.3.2
NheI-HF	New England Biolabs	Ipswich, MA	R3131S	3.3.2

doi:10.6342/NTU201903081

Name	Source	City	Identifier	Usage
TAE 50X Buffer	Bioman	New Taipei City, Taiwan	TAE50100	3.3.2 3.6.1
GenepHlow Gel Extraction Kit	Geneaid	New Taipei City, Taiwan	DFG100	3.3.2 3.6.1
mMESSAGE mMACHINE T7 Transcription Kit	Invitrogen	Carlsbad,CA	AM1344	3.3.2 3.5.1 3.6.1
Borosilicate capillary glass	Sutter Instrument	Novato, CA	B100-75-10	3.3.3 3.6.1
Phenol red solution	Sigma-Aldrich	St. Louis, MO	P0290	3.3.3 3.6.1
Mineral oil	Sigma-Aldrich	St. Louis, MO	M8410	3.3.3 3.6.1
TRIzol Reagent	Invitrogen	Carlsbad,CA	15596026	3.4.1
GENEzol Reagent	Geneaid	New Taipei City, Taiwan	GZR050	3.4.1
TissueLyser LT	Qiagen	Hilden,Germany	85600	3.4.1
TriRNA Pure Kit	Geneaid	New Taipei City, Taiwan	TRP050	3.4.1
RNase-Free DNase I Set	Geneaid	New Taipei City, Taiwan	DNS050	3.4.1
Power SYBR Green Master Mix	Applied Biosystems	Foster City, CA	4367659	3.4.5
T7 RNA Polymerase	New England Biolabs	Ipswich, MA	M0251S	3.5.1
Digoxigenin RNA Labeling Mix	Roche	Mannheim, Germany	11277073910	3.5.1
Fluorescein	Roche	Mannheim, Germany	11685619910	3.5.1
Methanol	Honeywell	Morristown, NJ	32213	3.5.2 3.5.3
Methanol	Sigma-Aldrich	St. Louis, MO	32213	3.5.2 3.5.3
H_2O_2	Nacalai Tesque	Kyoto, Japan	18411-25	3.5.3
Formamide	BioShop	Burlington, Canada	FOR001	3.5.3
SSC (20X), RNase-free	Invitrogen	Carlsbad,CA	AM9763	3.5.3 3.5.4
Dextran sulfate	VWR	Solon, OH	0198	3.5.3

doi:10.6342/NTU201903081

Name	Source	City	Identifier	Usage
Heparin sodium salt from porcine intestinal mucosa	Sigma-Aldrich	St. Louis, MO	H3393	3.5.3
Ribonucleic acid, transfer from wheat germ	Sigma-Aldrich	St. Louis, MO	R7876	3.5.3
Citric acid trisodium salt	Sigma-Aldrich	St. Louis, MO	C3674	3.5.3
Tris-HCl	VWR	Solon, OH	0234	3.5.4
$MgCl_2$	MERCK	Darmstadt, Germany	105833	3.5.4
NBT/BCIP Stock Solution	Sigma-Aldrich	St. Louis, MO	11681451001	3.5.4
Bovine serum albumin	Sigma-Aldrich	St. Louis, MO	A2153	3.5.4
Sheep Serum	Millipore	St. Louis, MO	S3772	3.5.4
Anti-Digoxigenin-AP, Fab fragments	Roche	Mannheim, Germany	11093274910	3.5.4
Anti-Fluorescein-AP, Fab fragments	Roche	Mannheim, Germany	11426338910	3.5.4
Benzyl benzoate	Sigma-Aldrich	St. Louis, MO	6630	3.5.5
Benzyl alcohol	Sigma-Aldrich	St. Louis, MO	24122	3.5.5
Cytoplasmic EKAR (EGFP-mRFP)	Addgene	Watertown, MA	18680	3.6.1
pTriEx4-Rac1-2G	Addgene	Watertown, MA	66110	3.6.1
BspEI	New England Biolabs	Ipswich, MA	R0540S	3.6.1

doi:10.6342/NTU201903081

doi:10.6342/NTU201903081

4. Results

4.1. Fgf receptors are expressed in migrating PGCs

Canonically, cells perceive FGF signals via FGFRs at the cell surface; therefore, expressions of FGFR proteins or alternatively their transcripts allude to the competence of a cell to respond to Fgf signals. Previous studies showed that mouse PGCs express *Fgfr1-IIIc* and *Fgfr2-IIIb* transcripts (Takeuchi et al., 2005), and that chicken PGCs contain all *FGFR* mRNAs while *FGFR1*, *FGFR2-IIIc*, and *FGFR4* are more abundant (Whyte et al., 2015). In zebrafish, the transcriptome analysis by next-generation sequencing (RNA-seq) suggests the expressions of *fgfrs* in 7 hpf and 13 hpf PGCs (Gross-Thebing et al., 2017; Paksa et al., 2016) (Table 6). However, it is difficult to tell between existence and absence of a transcript in sheer quantification data. In addition, since RNA-seq quantifies RNA expressions by mapping nucleotide fractions, the counts of a transcript might potentially be the results of the unspecific alignments in the case when the sequences share high similarity. To confirm the *in silico* prediction, the PGCs in *Tg(kop:EGFP-F-nanos3)* fish, a transgenic line with green-fluorescent PGCs (Blaser et al., 2005), were isolated using fluorescence-activated cell sorting (FACS) to identify *fgfr* transcripts (Figure 4A). I segregated the PGCs from somatic cells according to the green fluorescence (Figure 4BC) and collected approximately 2.8/6.0/6.4 cells per 6/8/10 hpf embryo, which contribute ~0.3% of cell population regardless of stages (Table 7). For quality control, wild-type embryos also underwent the same processes and analyses. Less than 0.004% of cells (or events) from wild-type embryos were detected as GFP positive (Figure 4B and Table 7), indicating the distinct segregation of PGCs from the somatic cells.

doi:10.6342/NTU201903081

The total RNA of the collected putative PGCs or somatic cells from 6, 8, or 10 hpf embryos were extracted and reversely transcribed to cDNA. To identify gene expressions starting from scarce material, samples were preamplified with pooled of outer primers for 15 cycles and identified by 25 cycles of PCR. The remaining RNA samples were pooled and underwent RT reaction without RT enzymes to serve as negative control while 24-hpf zebrafish cDNA were sequentially diluted to serve as positive control. In accordance with previous studies, four *fgfrs* (*fgfr1a*, *fgfr1b*, *fgfr2*, and *fgfr4*) were detectable (Figure 5) as shown previously in RNA-seq data (Paksa et al., 2016) while the signals of *fgfr3* were faint. Accordant to previous results, *fgfr4* seemed to be the most abundant (Figure 5) (Paksa et al., 2016). To estimate the abundance of each *fgfr*, I pre-amplified cDNA for 20 cycles and analyzed them by qPCR. *actb1* was selected as the internal control as it, besides its common role as a reference gene, showed no fluctuation between somatic cells and PGCs in transcriptomic data (Paksa et al., 2016). In my case, the C_q values of *actb1* seemed to be equal between cell types ($P = 0.2072$) but not across the stages ($P = 0.0004$) according to repeated measures (RM) two-way ANOVA (Figure 6A); consequently, only comparisons between cell types are valid. Two PGC markers, *dnd1* and *ca15b*, were also quantified as quality controls for sample collections (Figure 6B). The expressions of PGC markers in the presumptive PGC populations were 10^2 to 10^4 higher than somatic ones ($P < 0.0001$) without apparent fluctuations (pooled $\Delta\Delta C_q$ SE = 0.81 for *dnd1* and 0.61 for *ca15b*), suggesting the acceptable quality of sorted PGCs (Figure 6B). Since there were no known somatic markers during gastrulation in zebrafish to my knowledge, I fished for two somatic markers, *a2ml* and *hkdc*, from the transcriptomic data at 7 hpf (Paksa et al., 2016) to detect their gene expressions. However, none of

doi:10.6342/NTU201903081

them showed a trend to express more in putative somatic cells (Figure 6C). Then, I quantified the expressions of *fgfrs*. The abundances of *fgfr* transcripts in PGCs were estimated by multiplying the global expressions of *fgfrs* with the PGC/soma ratios obtained in qPCR (Figure 6D). Regarding global expressions of *fgfrs* as somatic expressions does not introduce biases as PGCs comprise only 0.3% of the cell population (Table 7), and none of *fgfrs* are expressed significantly higher in PGCs (Figure 6C). The global expressions of *fgfrs* were obtained from qPCR on *Tg(kop:EGFP-F-nanos3)* embryos assuming equal efficiencies of different sets of primers (Figure 7A) or EMBL Expression Atlas (Petryszak et al., 2016) (Figure 7B). According to the estimation, I concluded that *fgfr4* has the highest expression followed by *fgfr1b* (Figure 7). My data showed consistency with the transcriptomic data released by other group previously (Gross-Thebing et al., 2017; Paksa et al., 2016). In sum, PGCs express *fgfrs* transcriptionally and thereby may be competent to receive Fgf signals.

doi:10.6342/NTU201903081

4.2. Manipulation of Fgf signaling in zebrafish PGCs

To test the hypothesis that Fgf signaling plays a role in PGC migration, I performed a loss-of-function assay by introducing a dominant negative form of Fgfr (dn-Fgfr) to PGCs. Dn-Fgfrs are truncated Fgfrs lack of the intracellular domain, thus able to receive ligands and dimerize with endogenous Fgfrs without relaying signals (Amaya et al., 1991). As dn-Fgfrs compete promiscuously with all endogenous Fgfrs (Ueno et al., 1992), dn-Fgfr3 (dnR3) instead of dnR4 was chosen because it is the most potent zebrafish dn-Fgfr that is able to rescue dorsalized embryos overexpressing varied Fgf subfamilies (Ota et al., 2009). To promote translation in PGCs and avoid somatic noise, the 3'-UTR of *nanos3* (*nos*) was linked at the 3'-end of the introduced mRNA to make them targeted by microRNA miR-430 in the soma (Giraldez et al., 2006; Koprunner et al., 2001; Mishima et al., 2006). I first assessed the specific translation of introduced mRNA in PGC. Injection of *EGFP-nos* mRNA, as expected, induced green fluorescence in PGC specifically at 6 and 24 hpf (Figure 8A), suggesting the approach to PGC-specific translation worked in my hand. Next, I constructed a dnR3-EGFP fusion protein with a $(GSSS)_3$ linker (Figure 8B). In *dnR3-EGFP-nos* mRNA injected embryos, GFP positive cells were found within the gonadal ridge. Some located outside the gonadal ridge as distinct cells, but I tend to deem them to be mislocalized PGCs. The version of dnR3 without the EGFP domain was utilized in the following experiments to simplify the variables.

Next, I performed injections with varied doses of *dnR3-nos* mRNA from 50 (33 pg) to 400 amol. Embryos injected less than 100 amol of *dnR3-nos* mRNA did not revealed somatic defects on epiboly or trunk formation as in dnR3 globally-overexpressed embryos (Ota et al., 2009) (Figure 9CD). About 10% embryos injected with 200 amol

doi:10.6342/NTU201903081

dnR3-nos mRNA presented tail truncation phenotypes (Figure 9E), and most embryos injected with 400 amol *dnR3-nos* mRNA revealed somatic defects (Figure 9F). These observations suggested that 100 amol of *dnR3-nos* mRNA be used for PGC-specific expression without excessive somatic leakage that interfered with Fgf signaling in the soma. Equal amount of *EGFP-nos* mRNA (100 amol, 44 pg) was performed in parallel as the control group to rule out the possibilities of phenotypes caused by excessive exogenous *nos* sequences in PGCs.

Previous studies revealed that vertebrate PGCs may require Fgfs to maintain the cell number *in vitro* (Choi et al., 2010; Resnick et al., 1992) and *in vivo* (Takeuchi et al., 2005). So I attempted to quantify PGCs by determining the amount of PGC representative transcripts, namely *ddx4*, *dnd1*, and *ca15b*, at the end of gastrulation (10 hpf) as well as 24 hpf with qPCR. As a result, I did not detect statistical fluctuations between treatments in any PGC marker (Figure 10A and 11). I also visualized PGCs by *ca15b* at 6 hpf or *ddx4* at 24 hpf. No PGC depletion phenotype was recorded in those embryos injected with *dnR3-nos* mRNA (Figure 12). Therefore, proliferation and survival of zebrafish PGCs may not depend on Fgf signals. Surprisingly, contradictory to previous study (Wei and Liu, 2014), *hpse-nos* mRNA could not reduce the amount of PGCs (Figure 10A and 11). In addition, chicken PGCs require Fgf signaling to maintain MAPK signaling, which promote proliferation *in vitro* (Choi et al., 2010). However, introducing dn-Map2k1, which dominantly suppresses Mapk signaling, to zebrafish PGCs did not disturb the amount of PGCs (Figure 11). Therefore, whether PGCs require HS-dependent signaling or Mapk signaling need further investigation.

doi:10.6342/NTU201903081

4.3. Fgf signaling is required for PGC migration

Next I aimed to trace the localization of PGCs losing Fgf signaling. I first observed the PGC distribution by the presence of *ddx4* transcripts at 24 hpf—the end point of PGC migration. The representative PGCs, as those in wild-type and *EGFP-nos* treated embryos, clustered ventrally and bilaterally at the anterior end of the yolk extension (Paksa et al., 2016; Weidinger et al., 1999), while some occasionally trailed posteriorly along the trunk (Figure 12A). However, in embryos treated with 100 amol of *dnR3-nos* mRNA, some of PGCs detached from the yolk, or even distributed in the head or on the yolk (Figure 12B). I then defined ectopic PGCs as those neither clustering nor trailing on the yolk extension and counted the number of ectopic PGCs in each embryo (Figure 12B). The *dnR3-nos* treated embryos, as a result, contained more ectopic PGCs compared to the control group with a dose-dependent manner (Figure 13). Note that embryos treated with 400 amol of *dnR3-nos* mRNA reveal severe somatic phenotypes and I only picked those without truncated tail for *ddx4* staining.

I also made use of a constitutively-active form of *fgfr* (*ca-fgfr4, caR4*) corresponding to the most abundant *fgfr* in PGCs (Ota et al., 2009). A dose titration experiment was also performed. In consequence, even when introduced with the least dose of *caR4-nos* mRNA able to cause somatic defects (80 amol, Figure 9G-J), *caR4-nos* mRNA did not induce ectopic PGCs (Figure 13). Intriguingly, simultaneously coinjected with 100 amol of *dnR3-nos* mRNA, 10 amol of *caR4-nos* mRNA was able to partially alleviate the mislocalization defects of PGCs to the level of the control group (Figure 13). Taken together, the sufficient intensity of Fgf signaling is crucial to guarantee the arrival of PGCs. Note that injection of 100 amol of *dnR3-nos* mRNA did not disturb the *cxcl12a* and *ackr3b* (*cxcr7b*) expression levels in the somatic cells at the

doi:10.6342/NTU201903081

bud stage (10 hpf) (Figure 10); therefore, *dnR3-nos* mRNA might not regulate the chemokine level transcriptionally in the soma to disrupt PGC positioning.

I was then inquisitive about the initial stage for PGCs to respond to Fgf signals, so I observed the PGC distribution at the shield stage (6 hpf), when PGCs start to migrate dorsally. To visualize 6-hpf PGCs, I detected *ca15b* rather than *ddx4* because of the remaining *ddx4* transcripts in the soma before mid-gastrulation (Wolke et al., 2002). In the wild-type and control embryos, 6-hpf PGCs were distributed close to the margin of the blastoderm (Figure 14A). In the *dnR3-nos* treated embryos, not all of their PGCs were restricted marginally, instead dispersed toward the animal pole (Figure 14A). To quantify the demargination of PGCs, I captured the images of blastoderms from the view of their animal pole and measured the PGC distances to the centroid of the embryos. The edges of the blastoderms were defined by fitting it to a hexadecagon, and the centroid coordinate as well as the mean radius was calculated. The relative distance of a PGC to the centroid were obtained by dividing the distance to the centroid with the mean radius of its own blastoderm (Figure 14B). As a result, I found a proportion of PGCs in the *dnR3-nos* group had shorter relative distances (Figure 15A). However, the statistics based on cell data overestimated the n number as it is the embryos rather than the PGCs that served as the experimental unit (the unit I performed microinjection). Therefore, I defined the threshold of relative distances between ectopic and normal PGCs by the 95% most marginal PGCs in wild-type embryos to estimate the percentage of ectopic PGCs in each embryo (Figure 15A). The ectopic PGCs were observed more frequently in the *dnR3-nos* group than in the control group (Figure 15B). I also averaged the relative distances of all PGCs in one embryo to reflect the distribution of PGCs in each individual. Root square means (RSM) rather than arithmetic ones were used

doi:10.6342/NTU201903081

considering the occurrence of a stochastic cell distribution on a flat disc should act in a quadratic manner, according to the relative area within a certain radius, despite that the statistical results did not differ from the way to average. Injection of *dnR3-nos* mRNA, as a result, significantly centralized PGC distribution compared to the control mRNA (Figure 15C). Furthermore, co-injected with *caR4-nos* mRNA could partially rescue the mislocalized PGCs (Figure 15). My observations strongly indicated the participation of Fgf signaling in PGC migration at least since the shield stage.

doi:10.6342/NTU201903081

4.4. Manipulation of Fgf signaling did not cause detectable changes in Mapk or Rac1 signaling

Having demonstrated the importance of Fgf signaling on PGC migration, I attempted to identify the cytosolic signaling relaying the Fgf signals. Two potential signaling pathways are considered. One is Mapk (or Erk) signaling, which is the most common signaling cascades evoked by Fgf signaling. The other is Rac1 signaling, which is regulated by chemokine signaling and promote actin polymerization at the lead edge of PGCs (Kardash et al., 2010; Tarbashevich et al., 2015). To assess the Mapk activity, a fluorescence resonance energy transfer (FRET) biosensor, EKAR, was used to assess the Mapk signaling (Harvey et al., 2008). When phosphorylated by active Mapk, the structure of EKAR changes, bringing EGFP and mRFP together, and accordingly, mRFP can be excited by emission light of EGFP. To evaluate the Mapk signaling in PGCs, *EKAR-nos* mRNA was injected and the green and red fluorescences were evaluated under a green fluorescence excitation laser (488 nm) with cell cytometry. The Mapk activity was defined as red:green emission ratio, and the constitutively-active (ca) and dominant-negative (dn) (Kelleher et al., 2004; Liu and Zhong, 2017) forms of Map2k1, an Mapk kinase, were introduced to serve as positive and negative controls respectively (Kelleher et al., 2004; Liu and Zhong, 2017).

As the results, introduction of *ca-map2k1-nos* mRNA statistically increased the FRET ratio. However, *dn-map2k1-nos* mRNA unexpectedly increased the FRET ratio. Though no matter *dnR3-nos* or *caR4-nos* mRNA statistically raised the FRET ratio compared to *EKAR-nos* only group, manipulation on Fgf signaling did not differ from *dn-map2k1-nos* group (Figure 16A). In addition, n numbers were overestimated and the

doi:10.6342/NTU201903081

valid statistics should consider experimental unit as each flow cytometry sample. Therefore, conservatively speaking, dnR3 seemingly did not significantly drop the Mapk activities in PGCs. Furthermore, injection of *dn-map2k1-nos* mRNA did not induce ectopic PGCs at 24 hpf (Figure 13), indicating Fgfs do not affect PGC positioning through Mapk signaling.

For Rac1 signaling, I made use of a Rac1 FRET biosensor to determine the Rac1 activation in PGCs (Fritz et al., 2015). The C-terminal (CT) domain containing the nuclear localization signal (NLS) was truncated as to resemble the endogenous Rac1 distribution within PGCs (Kardash et al., 2010), and the EGFP/mRFP1 fluorophore pair was substituted for mTFP1/Venus pair duo to the available excitation and emission wavelengths for flow cytometry. Analyzed with cell cytometry, I did not detect a significant change when Fgf signaling in PGCs were manipulate (Figure 16B). The results, if reliable, suggest alternative pathways for PGC migration evolved by Fgf signaling.

doi:10.6342/NTU201903081

Table 6. Expressions of *fgfrs* in PGCs in transcriptomic data.

	7 hpf	13 hpf	36 hpf
fgfr1a	16.0	6.3	7.6
fgfr1b	20.9	13.0	13.2
fgfr2	5.0	17.7	6.3
fgfr3	0.5	4.9	0.9
fgfr4	34.8	18.9	31.4

Data were extracted in Sequence Read Archive (SRA, NCBI)—7 and 36 hpf (SRX1539606 & SRX1539608) (Paksa et al., 2016); 13 hpf (SRX3274591 & SRX3274593) (Gross-Thebing et al., 2017). Unit, fragments per kilobase of transcript per million mapped reads (FPKM).

doi:10.6342/NTU201903081

Table 7. Sorting quality assessment.

		6 hpf	8 hpf	10 hpf
Wild-type	**GFP+ %**	0.0033	0.0056	0.0032
Tg(kop:EGFP-F-nanos3)	**GFP+ %**	0.306 ± 0.049	0.296 ± 0.016	0.319 ± 0.136
	PGC/embryo	2.8	6	6.4

Tg(kop:EGFP-F-nanos3) has three biological replicates and the GFP+ % are presented as Mean ± SD.

doi:10.6342/NTU201903081

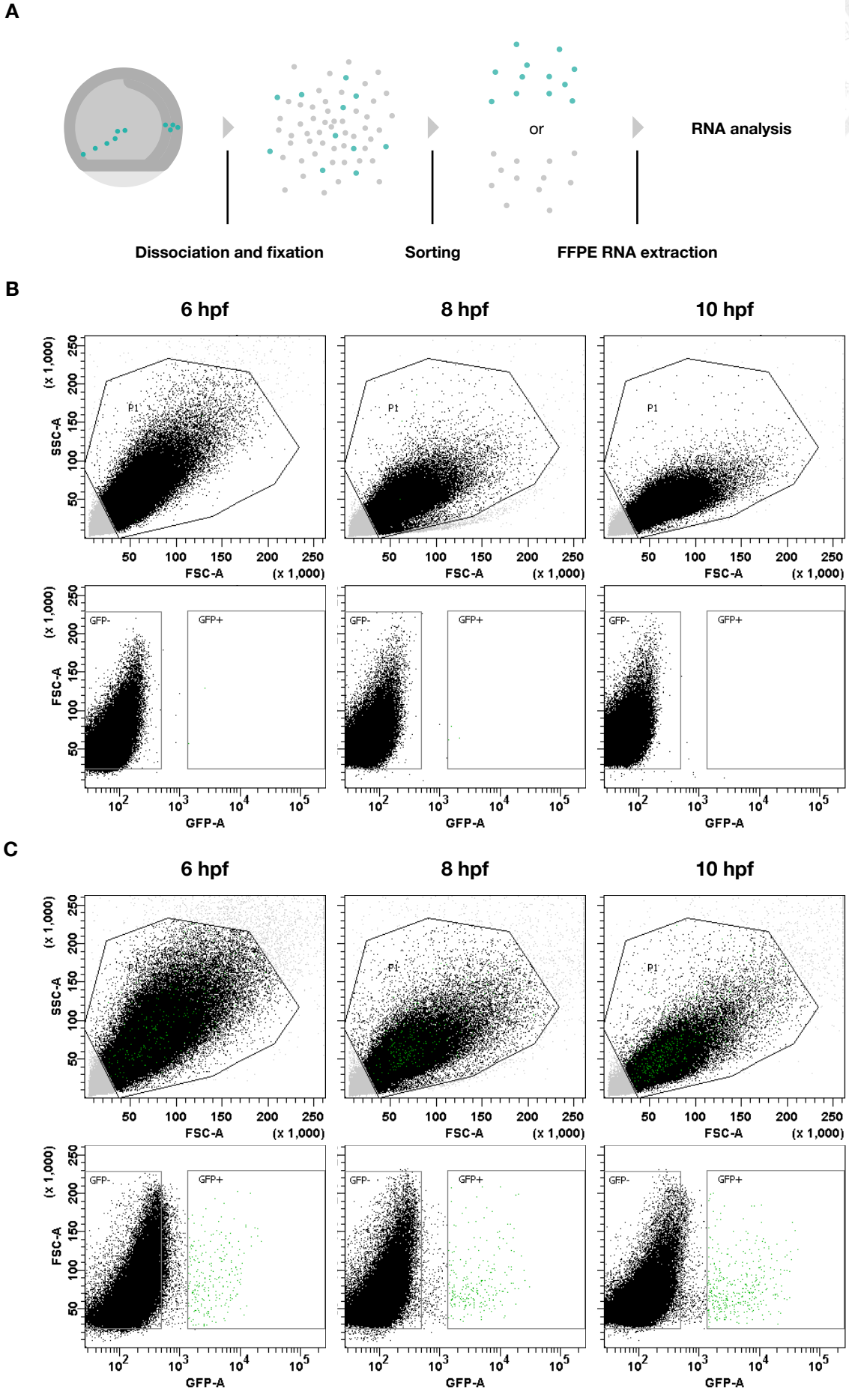

doi:10.6342/NTU201903081

Figure 4. Sorting out PGCs and somatic cells.

(A) Schematic experimental design to sort out PGCs and somatic cell for RNA analysis. (B and C) Two-gate determination of cells and GFP positive/negative events for wild-type (B) and *Tg(kop:EGFP-F-nanos3)* (C) embryos. The first gate (upper panels) discarded the debris according to FSC (forward scatter) and SSC (side scatter), and the second gate (lower panels) distinguished between PGCs and somatic cells referring to the GFP intensity.

doi:10.6342/NTU201903081

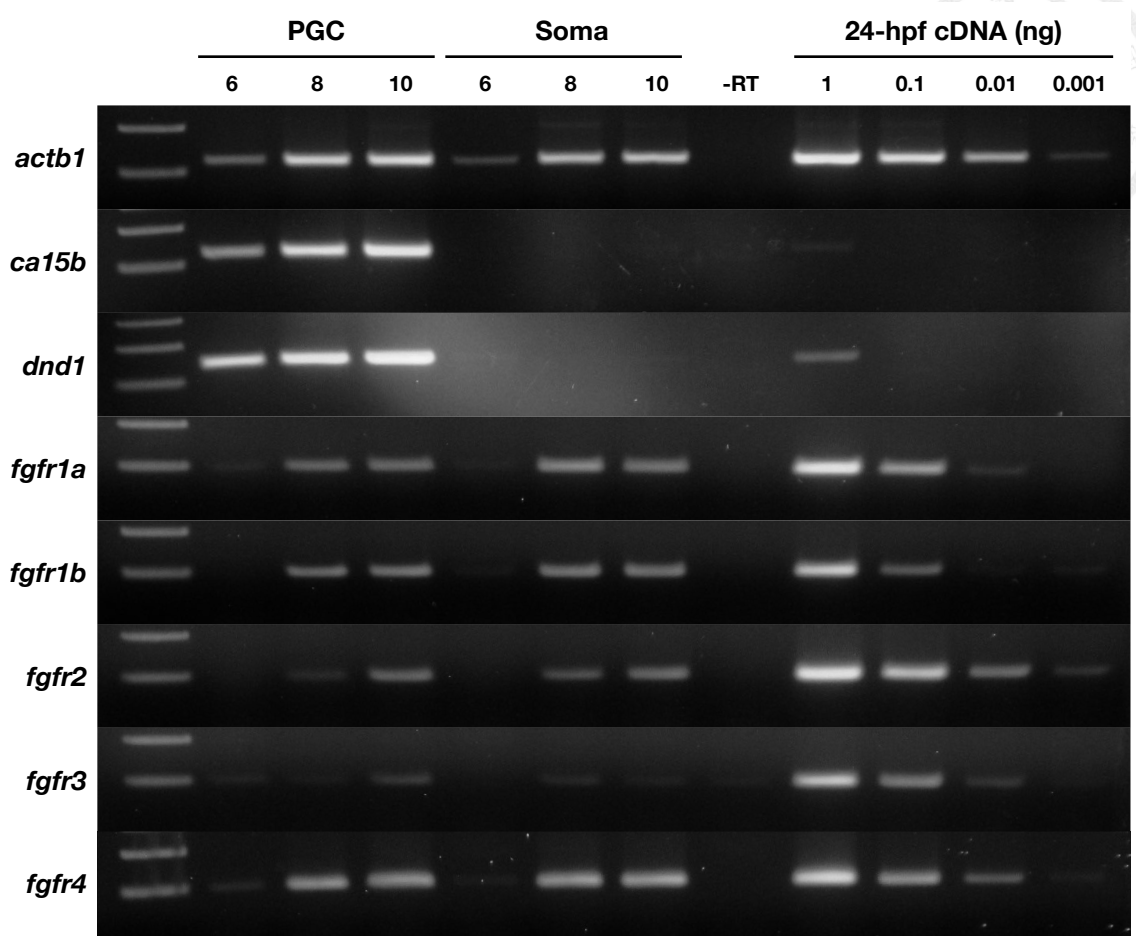

Figure 5. Expressions of *fgfrs* in zebrafish PGCs.

One μL of cDNA starting from 200 (6 hpf), 310 (8 hpf), 350 (10 hpf) PGCs or somatic cells underwent 15 preampfification cycles and then 25 cycles of nested PCR. The remaining RNA samples were pooled and underwent the same processes without adding RT enzymes to serve as negative control (-RT). The pool of cDNA from 24-hpf embryos were analyzed in gradient as positive controls. *actb1*, house keeping gene; *ca15b* and *dnd1*, PGC markers.

doi:10.6342/NTU201903081

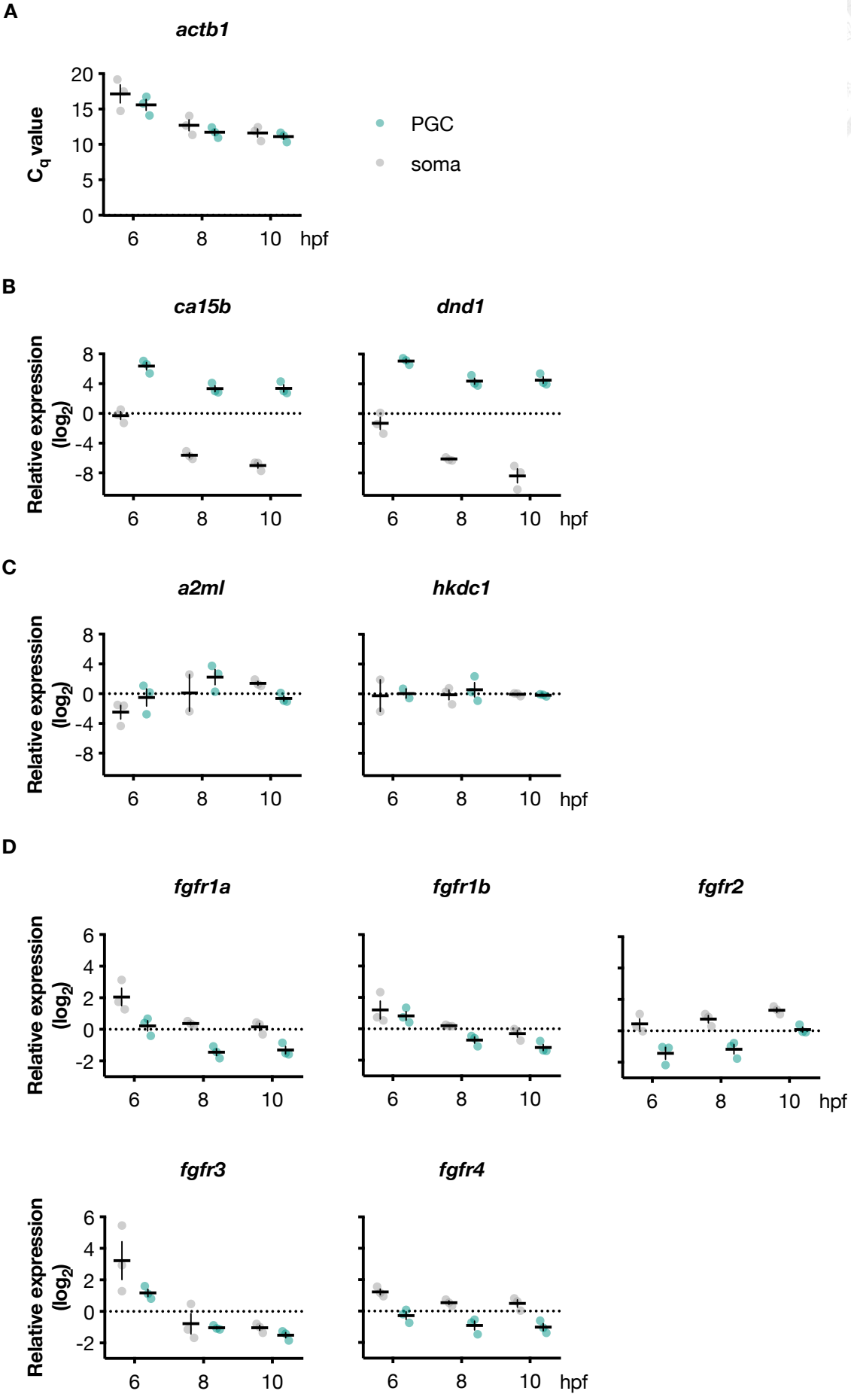

doi:10.6342/NTU201903081

Figure 6. Relative gene expressions in PGCs or somatic cells.

(A) C_q values (the amplification cycles upon detection by qPCR) of *actb1*, the reference gene. Note the lower expression of the reference gene in both cell types at 6 hpf. (B) Relative RNA expressions of PGC markers in PGCs and somatic cells. (C) Relative RNA expressions of putative somatic markers in PGC and somatic cells. (D) Relative RNA expression of *fgfrs* in PGC and somatic cells. Line at mean ± SEM.

doi:10.6342/NTU201903081

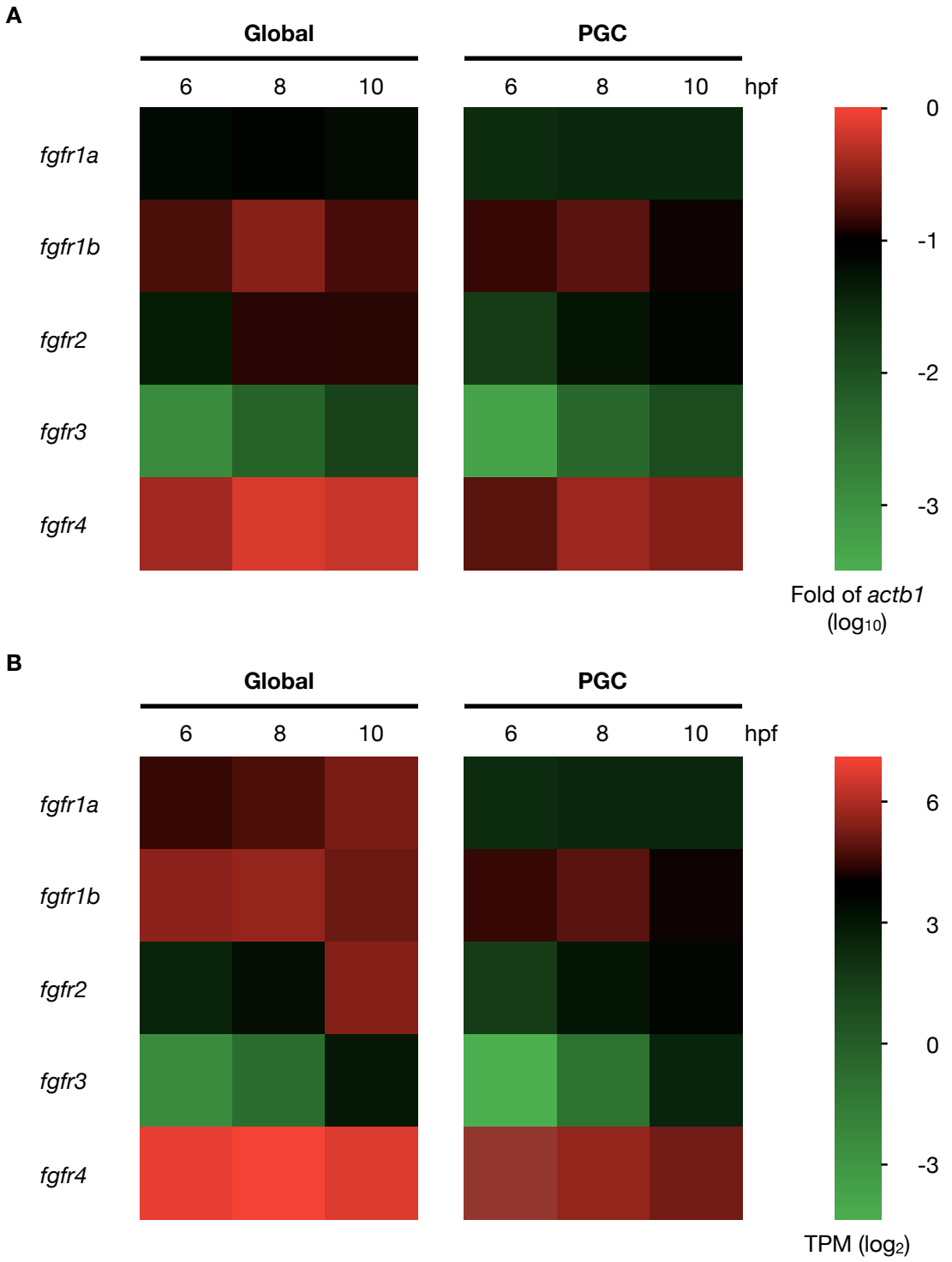

doi:10.6342/NTU201903081

Figure 7. Predicted *fgfr* transcript abundances in zebrafish PGCs.

The predictive *fgfr* abundances were calculated by multiplying global expressions of fgfrs by PGC/soma ratios generated from Figure 6. (A) Normalization on qPCR results generated from *Tg(kop:EGFP-F-nanos3)* fish. The expressions of *actb1* were adjusted to 1 (10^0). The thresholds on the amplification plots were set equal and all primer efficiencies were tested between 90-110%. (B) Normalization on the transcriptomic data from Wellcome Trust Sanger Institute on EMBL Expression Atlas (Petryszak et al., 2016).

doi:10.6342/NTU201903081

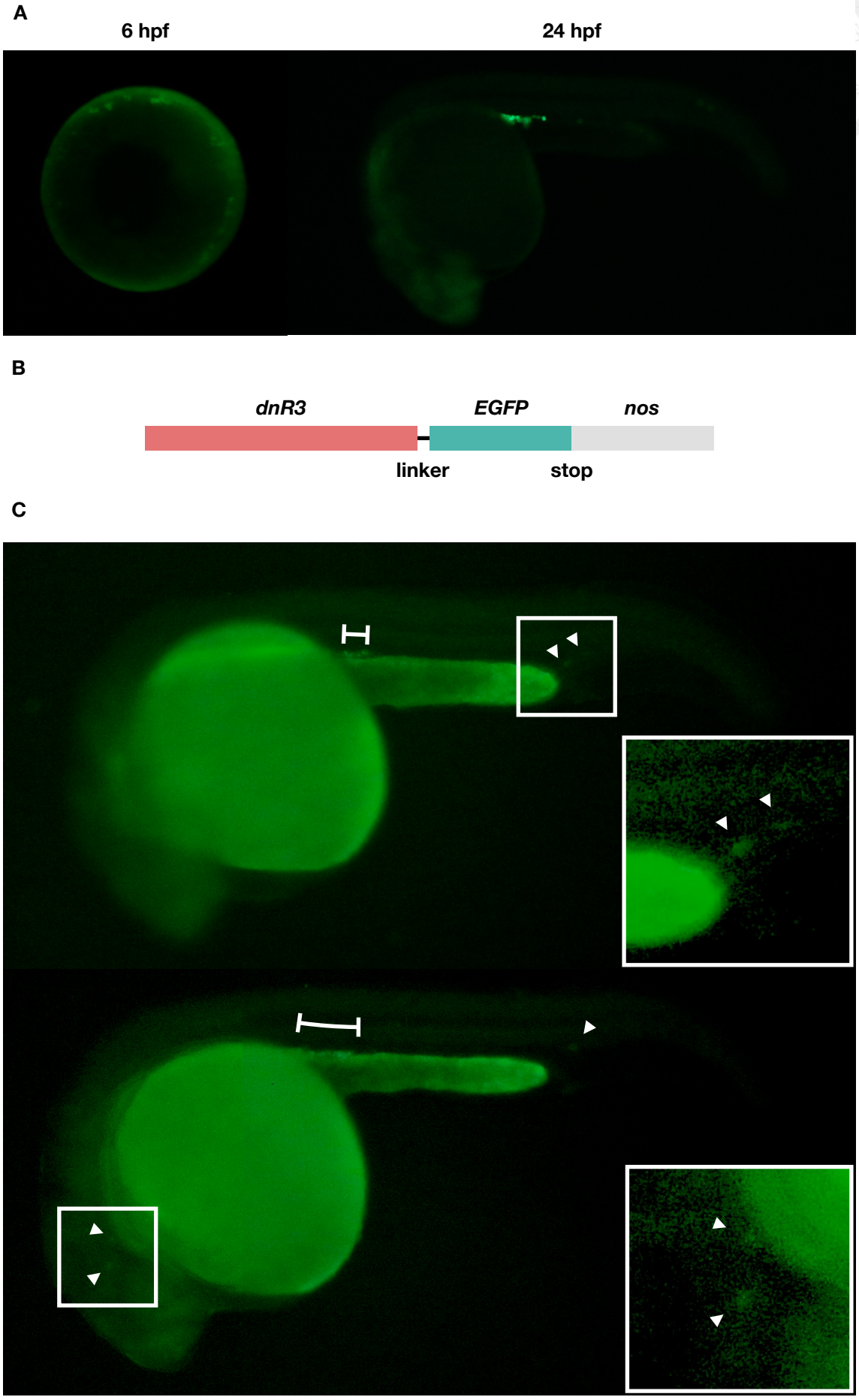

doi:10.6342/NTU201903081

Figure 8. Specific introduction of gene products to PGCs.

(A) Specific expression of *EGFP-nos* mRNA in PGCs at 6 hpf (top view) and 24 hpf (side view). (B) Design of *nos*-conjugated mRNA encoding dnR3 fused to EGFP. (C) Introduction of *dnR3-EGFP-nos* mRNA induced green fluorescence in PGCs. Note that some PGCs were ectopic as marked by arrows.

doi:10.6342/NTU201903081

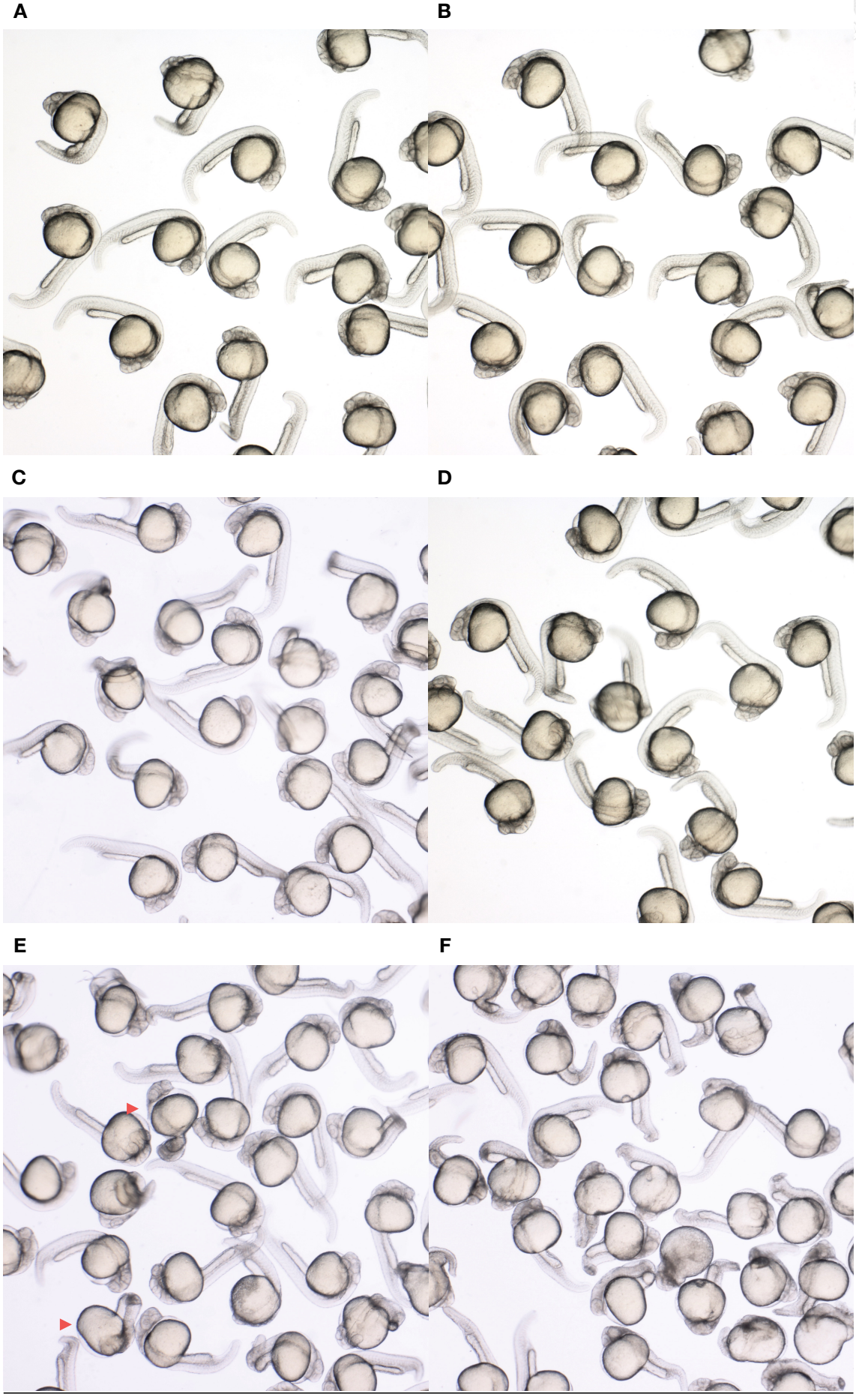

doi:10.6342/NTU201903081

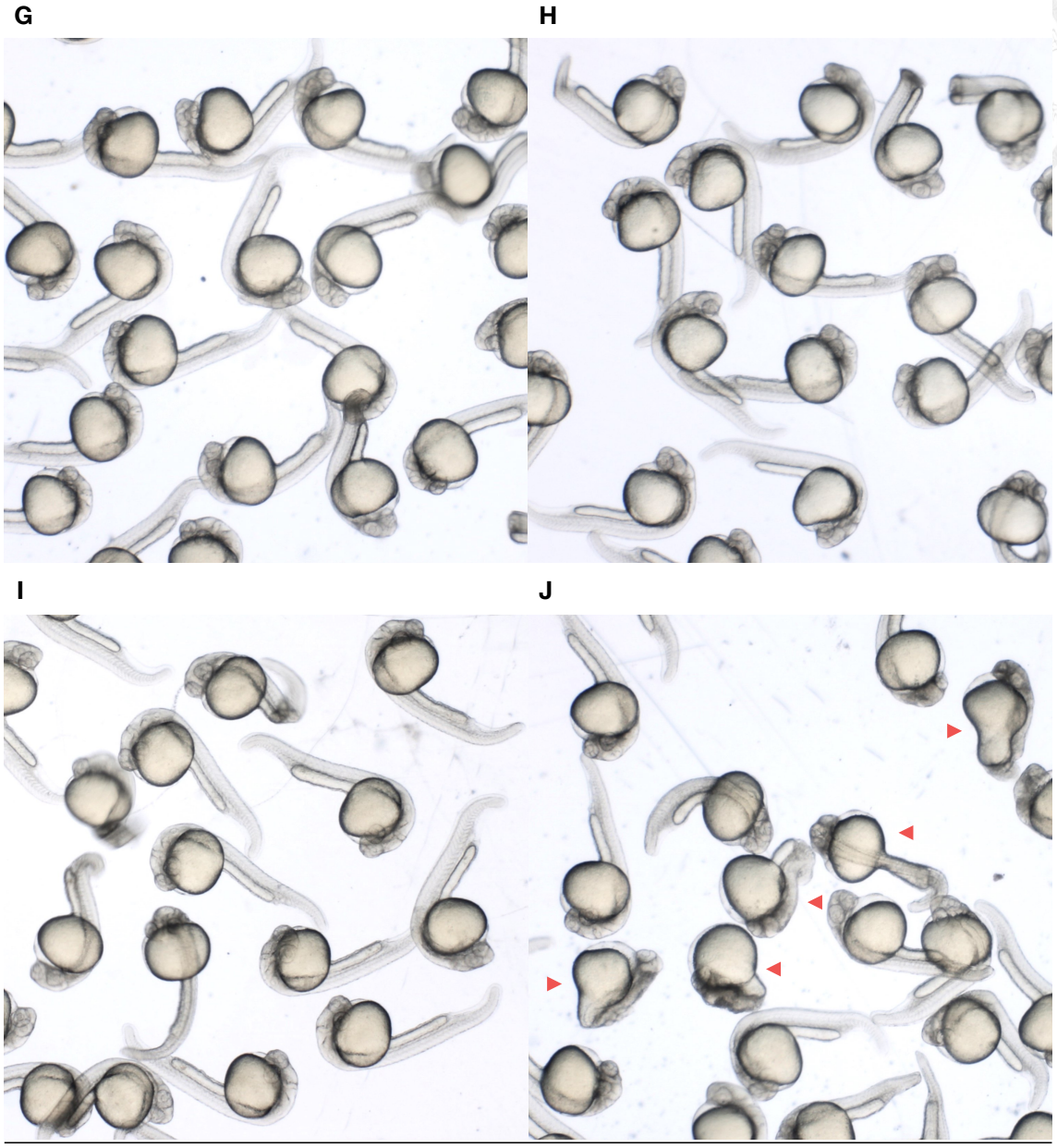

Figure 9. Appearances of live embryos at 24 hpf.

(A) Wild-type embryos (B) Embryos injected with 1 nL of solution with 100 amol of *EGFP-nos* mRNA (44 ng/μL). (C-F) Embryos injected with 50 (C), 100 (D), 200 (E), or 400 (F) amol of *dnR3-nos* mRNA. (G-H) Embryos injected with 10 (G), 20 (H), 40 (I), or 80 (J) amol of *caR4-nos* mRNA. Some embryos with somatic defects were marked by red arrows in (E) and (J).

doi:10.6342/NTU201903081

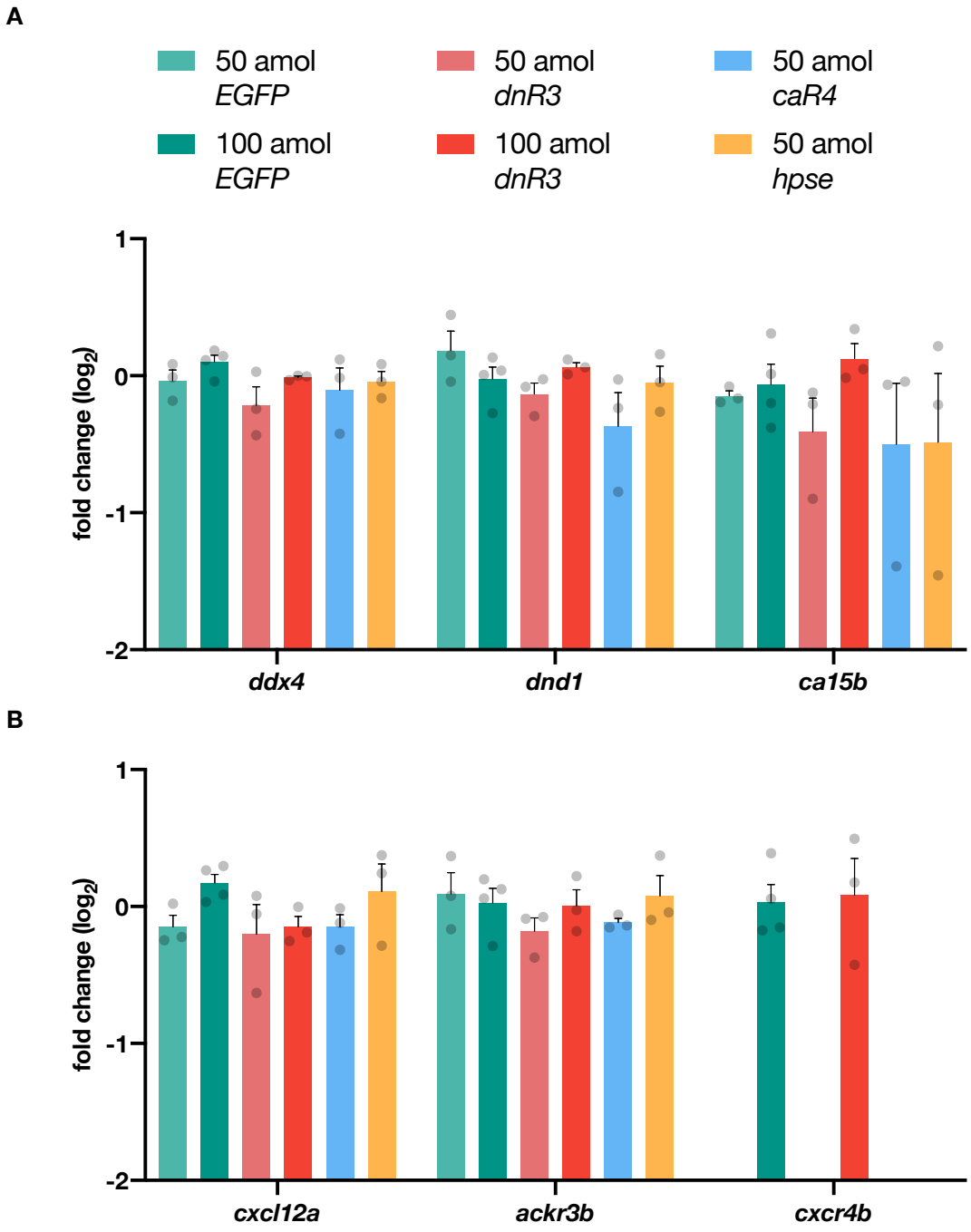

Figure 10. Global RNA expressions in 10-hpf embryos.

PGC markers (*ddx4*, *dnd1*, and *ca15b*) and PGC migration related markers (*cxcl12a* and *ackr3b*) were detected by qPCR. The relative expression levels were first normalized to *actb1* and then their WT siblings. The means and SEM were plotted as bars and error bars.

doi:10.6342/NTU201903081

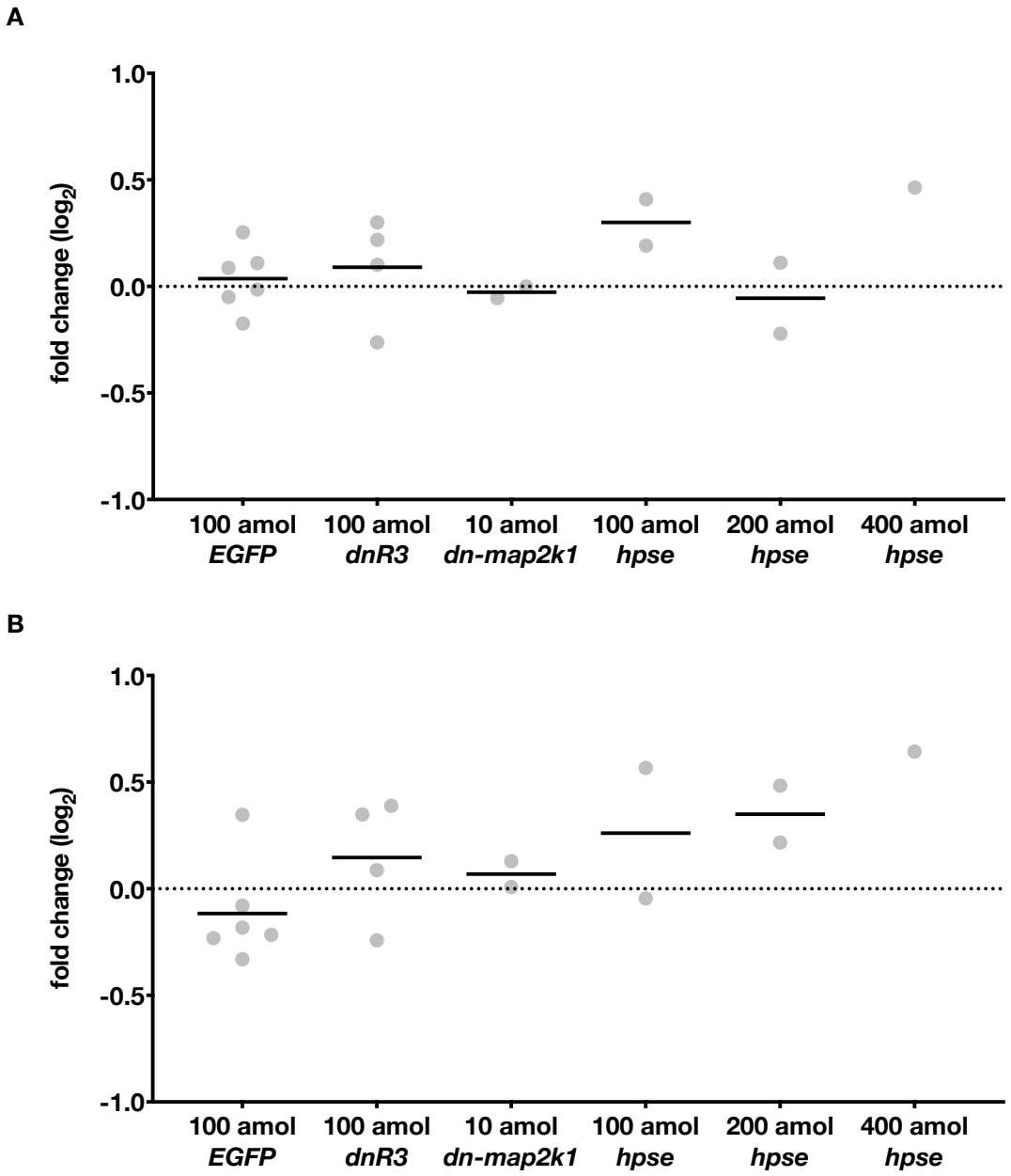

Figure 11. Fold changes of PGC marker expressions in 24-hpf treated embryos.

Two PGC markers—*ddx4* (A) and *dnd1* (B)—were quantified at 24 hpf. The relative expression levels were first normalized to *actb1* and then their WT siblings, lined at mean. The differences of fold changes were analyzed with RM 2-way ANOVA (variables: genes and treatments). No significant differences were found among treatments (P = 0.1112), markers detected (P = 0.2503), or their interaction (P = 0.2673).

doi:10.6342/NTU201903081

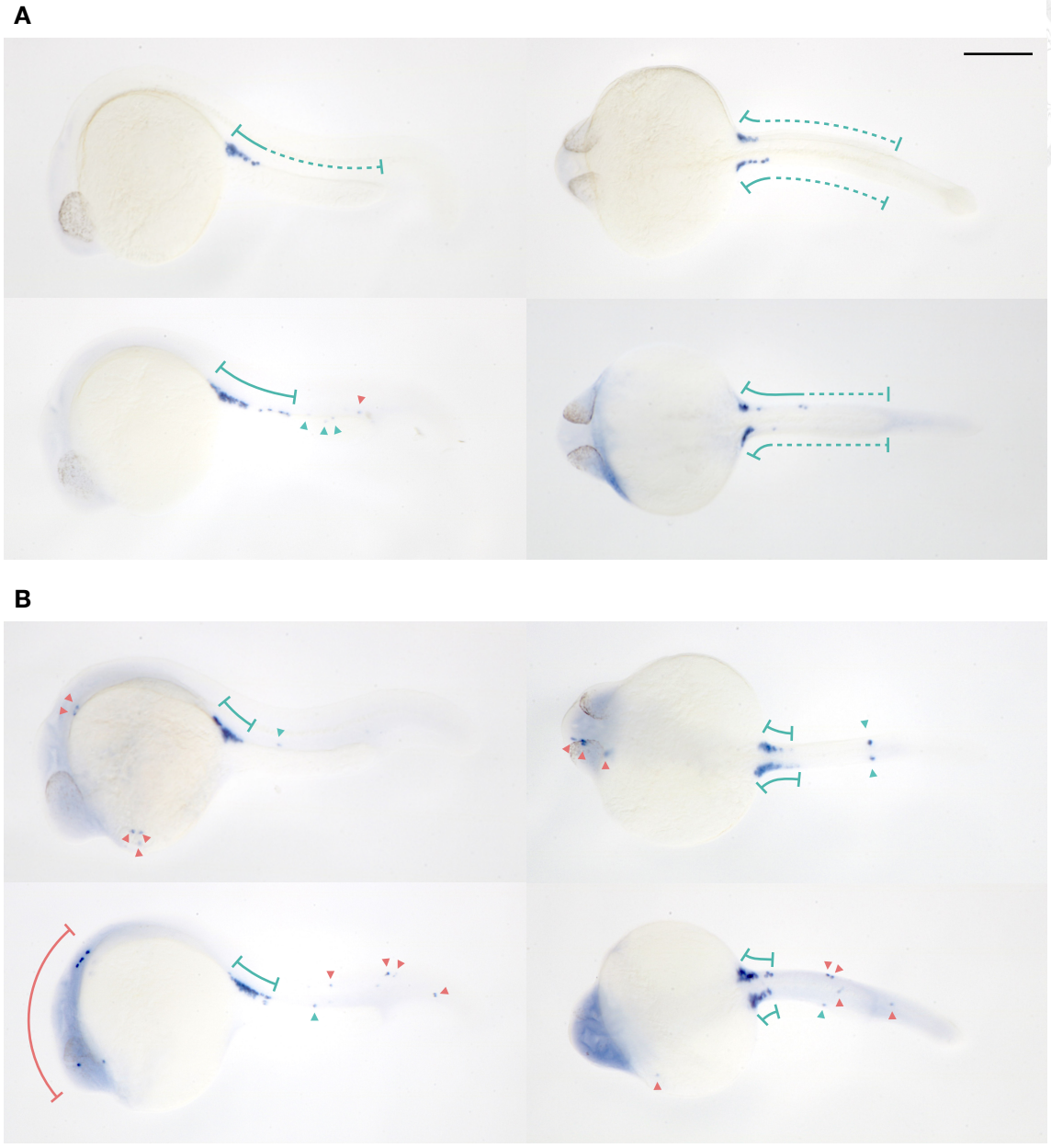

Figure 12. Definition of normal and ectopic PGCs at 24 hpf.

(A) Representative distributions of normal PGCs (marked within green solid lines) in *EGFP-nos* treated embryos. Normal PGCs were defined as those attached on the yolk extension as regions marked as green lines and arrows. (B) Some PGCs in *dnR3-nos* treated embryos (100 amol) contained ectopic PGCs located in the brain, the somites, or on the yolk (marked as red). Left panels, side view; right view, dorsal view; scale bar, 0.2 mm.

doi:10.6342/NTU201903081

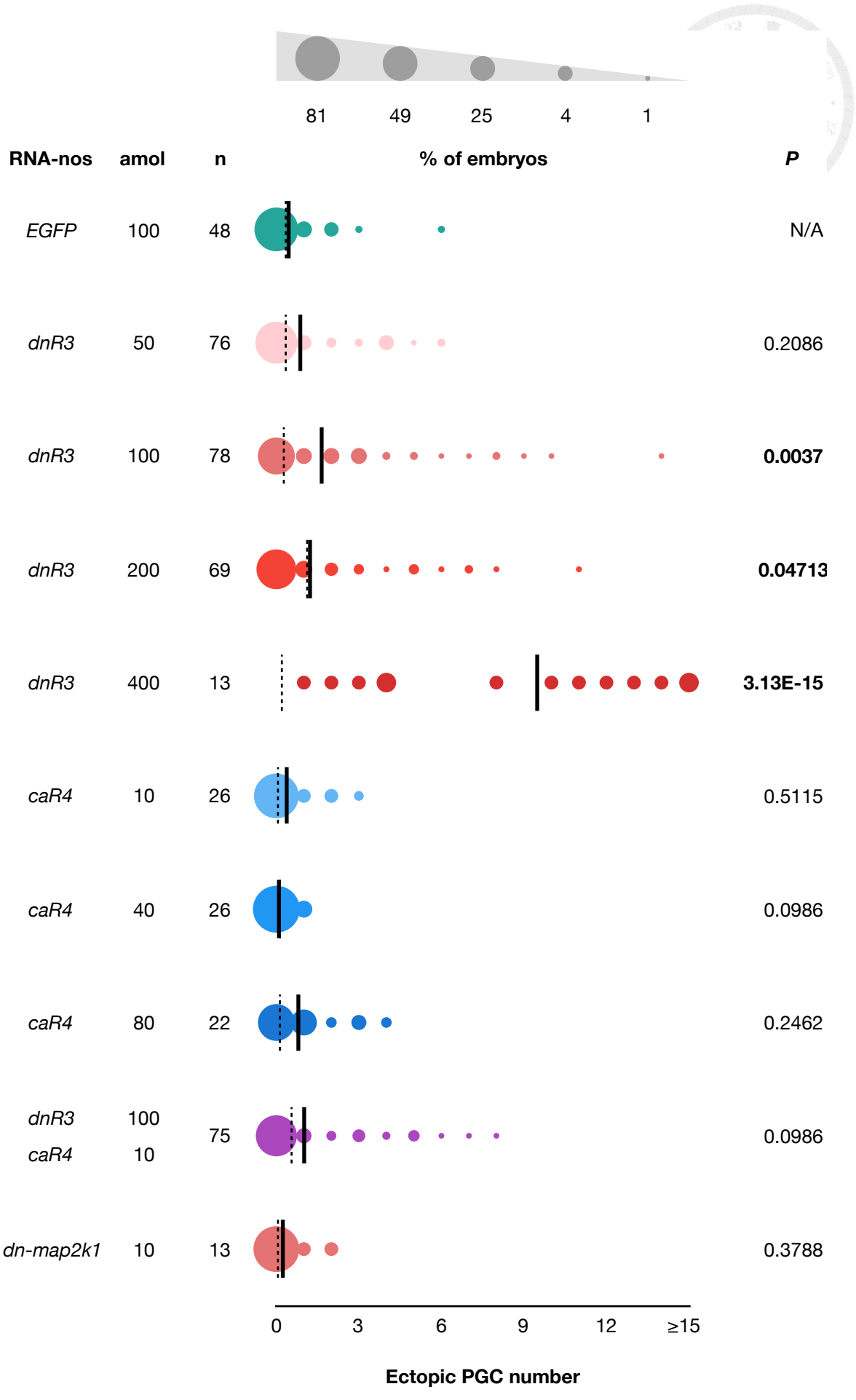

doi:10.6342/NTU201903081

Figure 13. Ectopic PGC numbers in 24-hpf microinjected embryos.

The zygotes were microinjected with combinations of *nos*-conjugated mRNA (unit, amol), and the ectopic PGCs were counted in each embryo at 24 hpf according to *ddx4* distribution. The percentages of embryos with certain number of ectopic PGCs were plotted as bubbles, and the rates (mean) of ectopic PGCs of treatment group as well as their WT siblings were shown as solid and dashed lines respectively. Samples were compared to the control (100-amol *EGFP-nos*) group using negative binomial GLM and the *P* values were corrected during multiple comparisons (Benjamini et al., 2006). n referred to the numbers of embryos observed.

doi:10.6342/NTU201903081

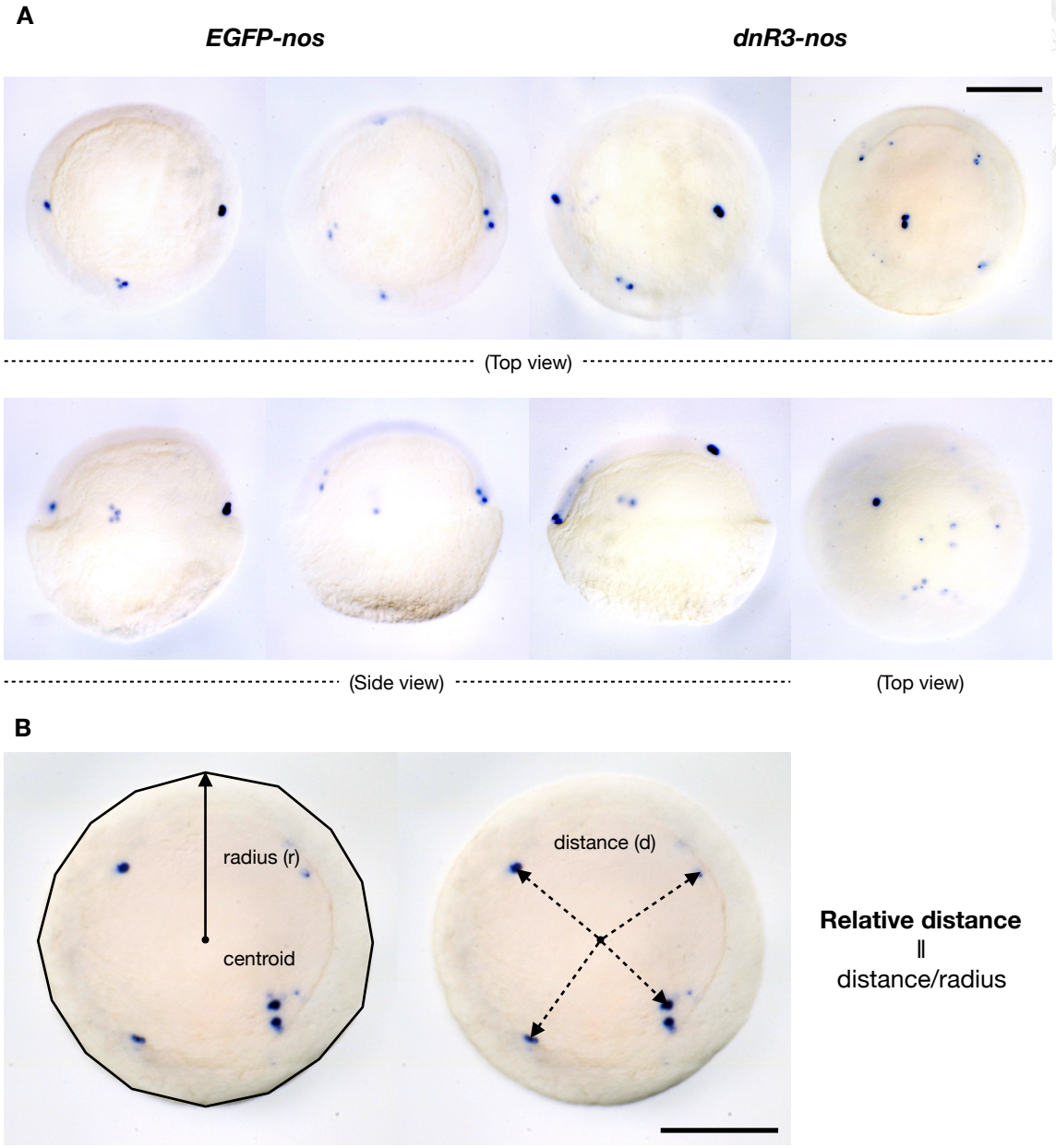

Figure 14. PGC distribution at 6 hpf and quantification of PGC marginality.

(A) Observed by *ca15b* RNA distribution, PGCs in *EGFP-nos* treated embryos (100 amol) existed near the blastoderm margin while some PGCs in *dnR3-nos* treated embryos migrated toward the animal pole. (B) To quantify the marginality of PGCs. The edge of a blastoderm was defined by 16 points to obtain the centroid and mean radius (r). Then the distances (d) between PGCs and the centroid were measured. Relative distances were calculated by dividing d by r. Scale bar, 0.2 mm.

doi:10.6342/NTU201903081

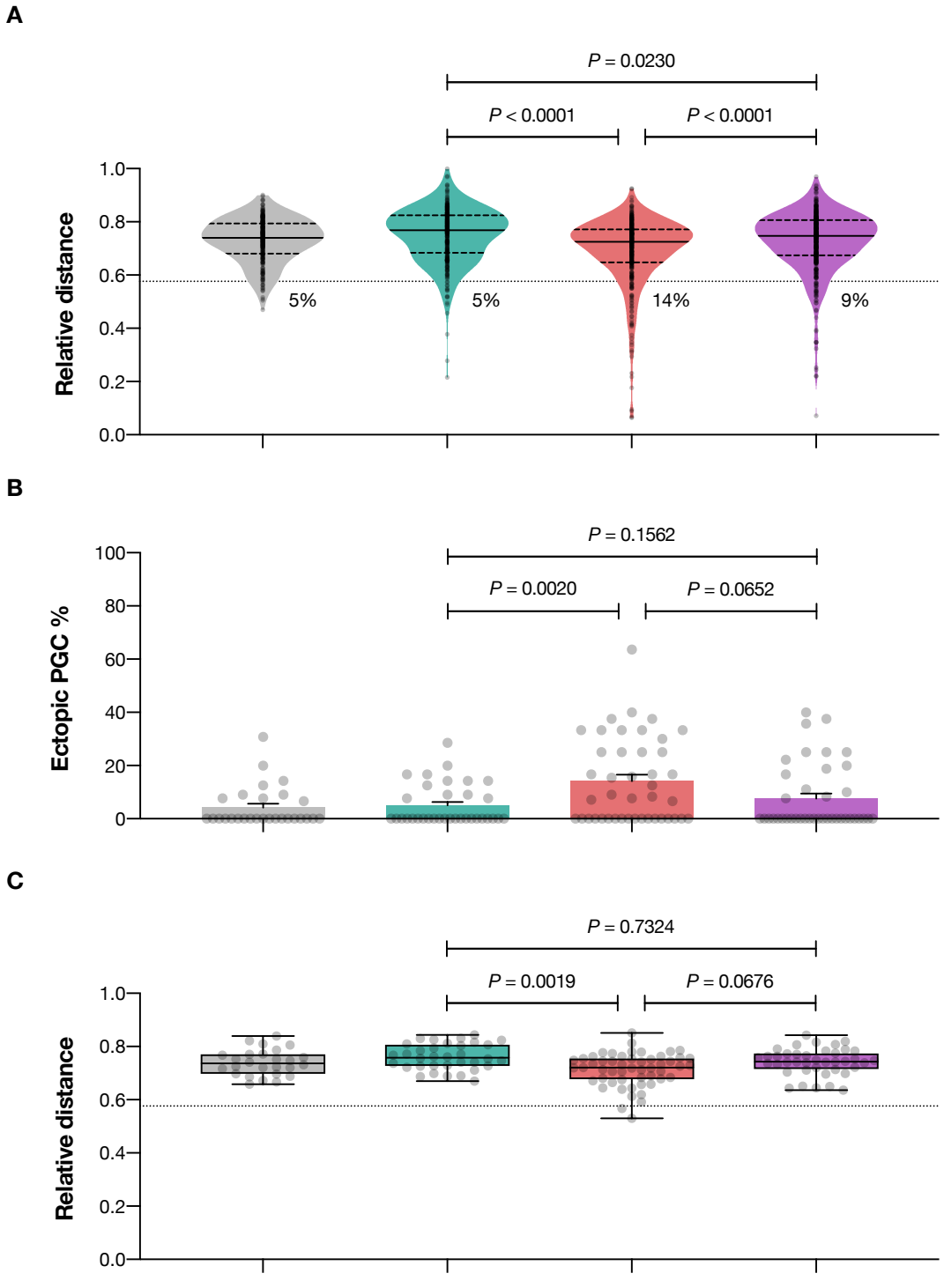

EGFP-nos	-	100	-	-
dnR3-nos	-	-	100	100
caR4-nos	-	-	-	10
N =	28	34	43	40
n =	256	289	339	413

doi:10.6342/NTU201903081

Figure 15. Marginality of PGCs at 6 hpf.

(A) Relative distances (radius/distance, r/d) of observed PGCs at 6 hpf. The threshold distinguishing normal and ectopic PGCs was defined by 95% most marginal wild-type PGCs and shown as the dot line. Percentages of ectopic cells were marked below the threshold line. Dots, data points (each cell); solid line, median; dash lines, quartiles; statistics, Kruskal-Wallis test followed by Dunn's test. (B) The proportions of ectopic PGCs in each embryo. Dots, data points (each embryo); bars, mean; error bar, SEM; statistics, negative binomial GLM, *P* value adjusted (Benjamini et al., 2006). (C) Root square means (RSM) of PGC relative distances in each embryo. Dots, data points (each embryo); statistics, Kruskal-Wallis test followed by Dunn's test. Each group represents embryos pooled from 2-4 microinjection experiments. N, observed embryo numbers; n, observed cell numbers.

doi:10.6342/NTU201903081

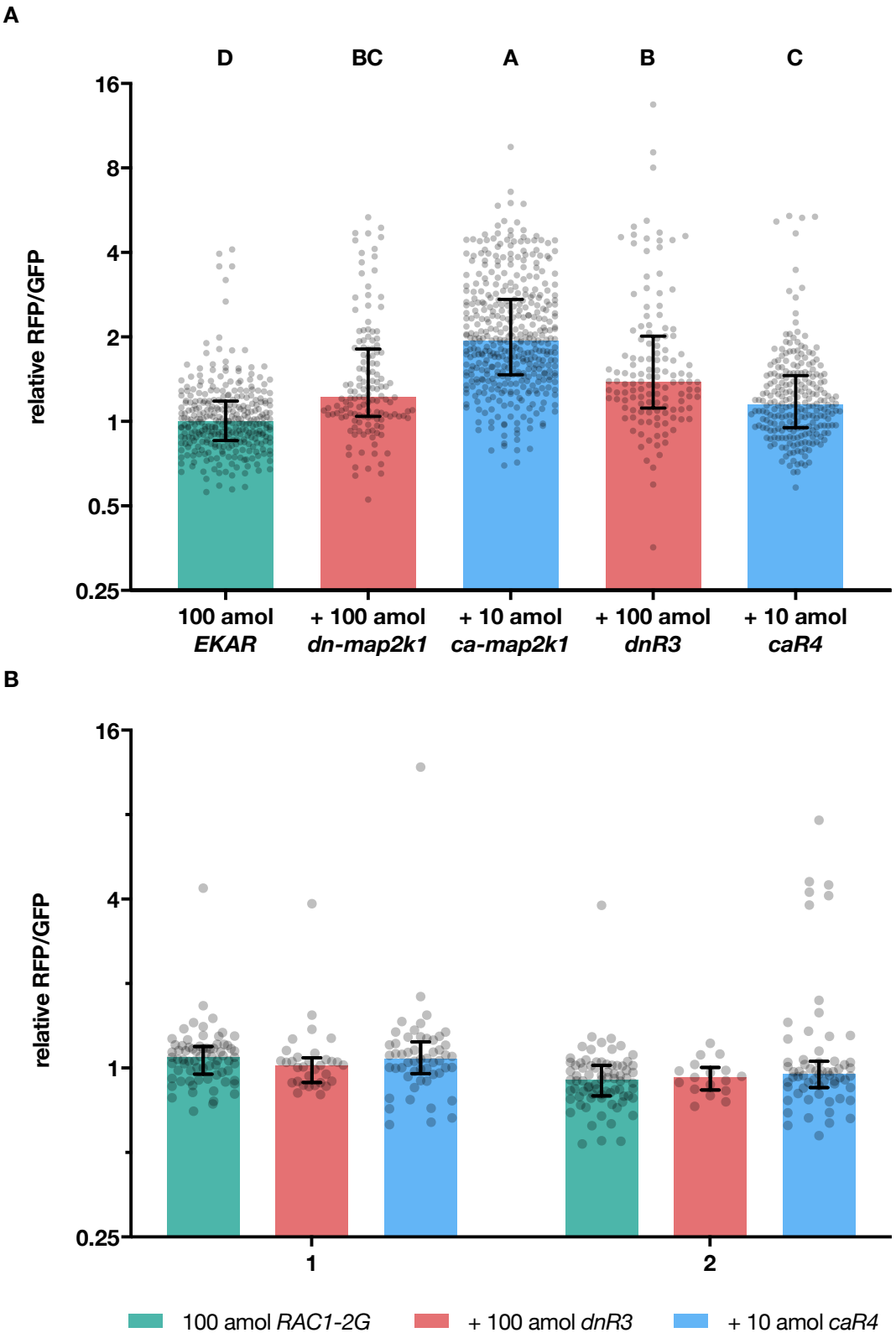

doi:10.6342/NTU201903081

Figure 16. Mapk and Rac1 signaling intensities in PGCs.

The zygotes were injected with 100 amol of *RAC1-2G-nos* (A) or *EKAR-nos* (B) mRNA with or without treatment *nos*-conjugated mRNAs. The embryos were dissociated and fixed at 8 hpf, and the green and red fluorescences were quantified under a 488-nm laser via flow cytometry. The signaling intensity was defined as the red and green fluorescences ratio. The data were proportionally transformed to make the median of control (biosensor-only) groups to 1 and plotted as median with interquartile range. (A) Mapk signaling results were generated in 3 independent days. *EKAR* only, *ca-map2k1*, and *dnR3* groups were pooled from 2 biological replicates while *dn-map2k1* and *caR4* groups were generated from one experiment. Statistics, Kruskal-Wallis test followed by Dunn's test. (B) For Rac1 signaling results, the microinjection procedures were performed twice in independent days, and their results were presented separately on the x axis. Analyzed with 2-way ANOVA with aligned rank transform data, differences between technical repeats were significant ($P < 0.0001$) while differences among treatments and their interaction were not ($P = 0.6650$ and 0.9726 respectively).

doi:10.6342/NTU201903081

5. Discussion

5.1. Competence of PGCs to receive Fgf signals

Previous studies suggested that vertebrate PGCs express FGF receptors transcriptionally (Takeuchi et al., 2005; Whyte et al., 2015). The preferred use of *FGFRs* in PGCs does not seem conserved across species. Mouse PGCs express *FGFR1-IIIc* and *FGFR2-IIIb* (Resnick et al., 1998), while chicken PGCs preferentially express *FGFR1*, *FGFR2-IIIc*, and *FGFR4* (Whyte et al., 2015). In zebrafish, I identified *fgfr* genes expressed in PGCs (Figure 5). The expression of *fgfr4* is the most dominant followed by *fgfr1b* (Figure 7), and the abundances of *fgfrs* seemed relevant to the overall *fgfr* expression in the soma (Figure 7). It appears that PGCs from different species use varied FGFRs. Considering the redundancy among FGFRs (Gattineni et al., 2014; Lavine et al., 2005; Weinstein et al., 1998), switches in using different FGFRs in PGCs, moving as single cells, may not bear fatal penalties during evolution, thus potentially leading to varied orthologous FGFRs used in vertebrate PGCs.

I optimized the procedures to detect more faithful RNA profiles in PGCs. As gene expressions fluctuate responsively under environmental changes, different from previous study, I fixed the cells just following the cell dissociation procedure, which was done within 5 min. Therefore, the RNA profiles might not change during cultivation and sorting, excluding the alternative explanation that *fgfrs* were expressed to accommodate PGCs to *in vitro* environments. Moreover, The PCR results could not be due to the genomic DNA contamination, for in addition to DNase treatment on all RNA samples, all primer pairs I used flanked at least one intron, which is sufficient to distinguish on an agarose gel. I also minimized the possibilities of reagent

doi:10.6342/NTU201903081

contamination. I perform the same process with remaining RNA only without RT enzymes, and no positive results were detected.

Some may concern about somatic contamination, which is more considerable especially when none of *fgfrs* in presumptive PGCs were expressed higher. I did fish for somatic markers, *a2mL* and *hkdc1* as the result, at 7 hpf from a published transcriptomic dataset (Paksa et al., 2016), but none of them showed even a trend in qPCR to exist more in the soma (Figure 6C). According to the numeric results generated from cell cytometry, only ~1% of wild-type events, which might not even be cells but yolk or debris contaminants, would be deemed as positive relative to the *Tg(kop:EGFP-F-nanos3)* ones with identical sorting conditions (Figure 4B and Table 7), insinuating a distinct separation between GFP positive and negative cells (~99%). Additionally, the expressions of *fgfrs* in PGC were 0-4 folds less according to the qPCR results (Figure 6D). I do not consider the contamination of somatic cells comprising a quarter of the assumptive PGC population. Furthermore, before identifying *fgfrs* in PGC via nested PCR, I first tried to perform general PCR for 30 and 35 cycles; the PCR products of *actb1* and *fgfrs* from PGC sample were always brighter than somatic ones on gel. It is reasonable that the presumptive PGC groups might contain more actual cells than somatic groups as they were sorted out according to green fluorescence, which did not appear frequently in dissociated wild-type embryos. Accordingly, the more sorted cells in the PGC groups were more likely to be PGCs, and they contributed to brighter signals of *fgfrs*. All together, I believe the positive expressions of *fgfrs* in PGCs during gastrulation.

doi:10.6342/NTU201903081

Although I did not determine whether or not these transcripts are translated into protein and function on the cell membrane, in the functional assays, competing endogenous Fgfrs on PGCs induced migration phenotypes. Hence, it is reasonable to assume that zebrafish PGCs can respond to signals, though no evidence to be Fgfs, through FGFRs.

doi:10.6342/NTU201903081

5.2. FGF signaling and PGC maintenance

As PGCs are those cells composing every cell of the next generation, *in vitro* cultivation of PGCs expedite generation of transgenic animals through germline transmission. In cell culture, supplementation of FGFs is indispensable to PGC proliferation (Choi et al., 2010; Matsui et al., 1992; Resnick et al., 1992). Nevertheless, FGFs dedifferentiate the cultured mammalian PGCs into embryonic germ (EG) stem cells, which (Durcova-Hills et al., 2006; Matsui et al., 1992; Shamblott et al., 1998), albeit making *in vitro* propagation applicable, does not meet the current comprehension on native physiology. Though I did not find intrinsic evidence *in vivo*, FGF signaling seems to regulate PGC survival as *FGFR2-IIIb* knockout mice contained less PGCs and more dying PGCs (Takeuchi et al., 2005). Unexpectedly, either in *FGFR2-IIIb*$^{-/-}$ mice or transverse slices treated with SU5402 (FGF signaling inhibitor), proliferation of PGCs was not disturbed referring to BrdU assays (Takeuchi et al., 2005). In chickens, opposite phenomenons were observed in *FGF8* knockdown and overexpressed chicken embryos (Wang et al., 2018). No matter up- or down-regulating *FGF8* increased the PGC number and expression of PGC marker (*DDX4*) while effects of *FGF8* repression by shRNAs were more significant (Wang et al., 2018). The *in vitro* experiments in the same study reasoned that autocrine FGF8 promotes PGC self-renewal and prevented PGCs from differentiation into spermatogonial stem cells (Wang et al., 2018).

This project originated from searching for the survival signals for zebrafish PGCs. In our previous study, when *hpse-nos* mRNA was overexpressed in zebrafish PGCs to degrade the adjacent HS, the *ddx4* RNA level significantly decreased at 8 and 10 hpf, and more apoptotic PGCs could be found at 10 hpf according to terminal deoxynucleotidyl transferase dUTP nick end labeling (TUNEL) assays (Wei and Liu,

doi:10.6342/NTU201903081

2014). Considering the common roles of HS as co-receptors in many signalings, I tried to investigate the survival signals involving HS and hypothesized the survival factors to be Fgfs. Unexpectedly, I did not observe a decreasing trend of *ddx4* or other PGC markers in 10-hpf or 24-hpf *hpse-nos* treated embryos (Figure 10A and 11). I also visualized PGCs by staining *ddx4* using WISH. In my hand, *hpse-nos* mRNA induced ectopic phenotypes of PGCs at 6 hpf and 24 hpf but the PGCs did not become less at 24 hpf (Figure 10A and 11). In consequence, I did not obtain expected results when trying to rescue the *hpse-nos* treated PGCs with *caR4-nos* mRNA.

Seeing that no PGC-intrinsic evidence validated the roles of Fgf signaling *in vivo*, I alternatively focused on the roles of Fgf signals in PGC survival or proliferation. Surprisingly, I did not detect an increase or decrease in PGC markers at 10 hpf or 24 hpf when the intrinsic Fgf signaling was manipulated (Figure 10A and 11). There are several possibilities accounted for the results I obtained. Firstly, zebrafish PGCs may apply other mechanisms to maintain cell number, or PGCs may not require Fgfs intrinsically in vertebrates. In other words, PGCs was, as observed, not affected by cell-intrinsic manipulation on Fgf signaling. A related concurrence is that the single homozygous knockout of any *fgfr* did not compromise fertility, though the compensation by redundant *fgfrs* were more likely to occur in mutant lines (Leerberg et al., 2018; Rohner et al., 2009). Secondly, PGCs might change but I did not observe the difference. The observation numbers I obtained might not be large enough to detected the scarce fluctuation, albeit previous studies showed dramatic changes when FGF signaling was manipulated—about half decrease in *FGFR2-IIIb*$^{-/-}$ mice and 0.6 folds increase in shRNA-FGF8 induced chicken embryos. The third explanation is that the cell numbers changed but the RNA levels did not oscillate. PGCs, for instance, might divide more

doi:10.6342/NTU201903081

times but the PGC marker mRNAs were accordingly diluted or asymmetrically distributed, resulting in unchanged cell numbers or overall PGC marker levels. A reminiscent example was that knockdown of *hsp90aa1.2* reduced division rate of PGCs during migration but did not decrease cell number in the first day of development (Pfeiffer et al., 2018). The last possibility I propose is that Fgf signaling may be redundant to other signaling pathways. Fgf signaling probably plays a role in maintenance, but other signaling pathways may compensate by activating/repressing the same downstream signaling participants. It may explain why the fluctuation in *in vitro* studies is usually more dramatic.

Given that Fgf signals are not required for PGC maintenance, what else extracellular signals may be accounted for the proliferation and survival of PGCs? According to chicken PGC study *in vitro*, FGF2, insulin or IGF1, and activin or BMP4 are sufficient to maintain PGC renewal in a defined medium, and they can be replaced by constitutively-active MAP2K1 (MEK1), AKT, and SMAD3 individually (Whyte et al., 2015). Some of these factors, FGF (Yayon et al., 1991) and BMP (Takada et al., 2003), require HS for ligand-receptor binding, potentially accounted for the apoptotic phenotypes seen in *hpse-nos* treated PGCs (Wei and Liu, 2014). IGF (Arai et al., 1994) and activin A (de Winter et al., 1996) signalings are also regulated by HS, but negatively. According to my results, Fgf signaling or Mapk signaling is not required for PGC maintenance. It implies that other signalings may provide proliferative or survival signals *in vivo*. As for insulin/IGF signaling, previous study has revealed that globally expressing dn-IGFR1 or *igfr1b* morpholino compromised the survival of zebrafish PGCs (Schlueter et al., 2007), but it was later confirmed as relay mechanisms (Sang et al., 2008). In mouse, KIT signaling activates AKT signaling (De Miguel et al., 2002) as

doi:10.6342/NTU201903081

IGFRs do and plays pivotal roles in PGC migration and survival (Parichy et al., 1999), yet not the case in zebrafish PGCs (Mellgren and Johnson, 2005). It is thereby intriguing to know whether AKT signaling facilitates the maintenance of zebrafish PGCs *in vivo*, and if so, what factors trigger the AKT pathway. On the other hand, BMP signaling is regulated by HS (Kuo et al., 2010) and crucial for mammalian PGC specification (Lawson et al., 1999) and *in vitro* maintenance of PGCs (Whyte et al., 2015). In chicken, pSMAD2 and pSMAD1/5/8 were nuclear localized in migratory (6 HH) and arrival (19 HH) PGCs, suggesting both activin/nodal and BMP signalings are active in migrating PGCs (Whyte et al., 2015). However, whether BMP signals continue to maintain PGC population ensuing specification *in vivo* has not been disclosed. Although a previous study implemented a gain-of-function approach by expressing Bmp4 specifically in zebrafish PGCs, the project culminated in severe ventralization defects of the embryos (Wong and Collodi, 2013). As Bmp4 emitted by PGCs might affect the somatic development, the experimental design can be improved by alternatively introducing dominant-negative or constitutively-active forms of receptors or cytosolic signaling molecules. It seems to me that BMP signaling is worth investigation of the survival or proliferative mechanisms of PGCs *in vivo*.

doi:10.6342/NTU201903081

5.3. FGF signaling and PGC migration

Few papers discussed the migratory behaviors of PGCs *in vitro* (Donovan et al., 1986; Godin et al., 1990; Godin and Wylie, 1991) since *in vitro* study focused more on the self-renewal and proliferative properties in cell culture (Matsui et al., 1992; van de Lavoir et al., 2006). To my knowledge, only two publications described a role of FGFs in PGC migration (Pares and Ricardo, 2016; Takeuchi et al., 2005) whereas none of them suggested an autonomous effect. In E9.5 mouse explants, when PGCs move dorsolaterally from the hindgut to the mesenchyme, addition of bFGF facilitated the PGC exit from the hindgut and treatment of SU5402 quenched their velocity, yet the directionality of PGCs was not affected by manipulation of overall FGF signaling (Takeuchi et al., 2005). In *Drosophila*, FGF signaling does not interact directly with PGCs but, instead, regulates the cell-cell adhesion of the endodermal epithelia (Pares and Ricardo, 2016). In *fgf* mutants, the midgut epithelia collapsed and trapped PGCs, leading to exodus failure (Pares and Ricardo, 2016; Seifert and Lehmann, 2012). The phenomenon observed in *Drosophila* was reminiscent of roles of FGF signaling in mice. Despite the fact that manipulations of FGF signaling in mice accordingly adjusted the MAPK activity in PGCs (Takeuchi et al., 2005), it is reasonable to assume that FGF signaling be a conserved somatic mechanism involved in transepithelial migration of PGCs (Barton et al., 2016). Accordingly, cell-intrinsic manipulations of signaling are necessary to clear up the direct interaction between the extrinsic signals and PGCs.

In my study, I introduced dnR3 into PGCs to repress Fgf signaling. Although I did not observed reduction in PGCs, interestingly, PGC migration was impaired since 6 hpf, and the mislocalization lasted through 24 hpf. Oddly, only close to half of the treated embryos contained at least one ectopic PGCs during the first day development when

doi:10.6342/NTU201903081

introduced with 100 amol of *dnR3-nos* mRNA (Figure 13). Though the rate of ectopic PGCs rose statistically, the penetrance seems low compared to *cxcl12a*/*cxcr4b*/*ackr3b* knockdown phenotypes (Boldajipour et al., 2008; Doitsidou et al., 2002), but similar to another intrinsic guidance signaling, Igf signaling, and to phenotypes caused by eradicating miRNA processing (Goudarzi et al., 2013; Staton et al., 2011, 2013). In detail, disruption of Igf signaling induced average ~2 (Schlueter et al., 2007) or 5-8 (Sang et al., 2008) ectopic PGCs. Note that Sang et al. might use a looser criterium as the control embryos in their study contained close to 2 ectopic PGCs (Sang et al., 2008). Besides, when the miRNA-mediated repressions of *cxcl12a* or *cxcr7b* were protected, about 50-70% of embryos with at least one ectopic PGCs (Staton et al., 2011, 2013).

There are several possibilities leading to low penetrance of ectopic PGCs. First, loss of FGF signaling may, as observed, only results in mild aftereffects. Fgf signaling may not be the only signaling pathways involved in the same cellular events, or the chemokine signaling, along with other endogenous signaling, is enough to shepherd most but not all PGCs to the gonadal ridge. Another possibility is that loss of Fgf signaling should result in severe positioning defects but did not manifest. As discussed previously, I chose a timid dose for microinjection (100 amol, or 66 pg of *dnR3-nos*), about one fourth used in the original paper (Ota et al., 2009), and most previous studies applied higher dose for dominant negative repression—350 pg for Rock2a (Blaser et al., 2006), 450 pf for mDAPK1 (Blaser et al., 2006), 1200 pg for Mlck (Blaser et al., 2006), 450 pg for Rac1 and RhoA (Kardash et al., 2010), 300 pg for Ctnnb1 (β-catenin), 250-400 pg for Rgs14a (Hartwig et al., 2014), and 600 pg for Baiap2a (Irsp53) (Meyen et al., 2015). Accordingly, the remaining FGF signaling in PGCs to some degree maintained the proper migration of the cells. To confirm the assumption, I increased the

doi:10.6342/NTU201903081

dose of *dnR3-nos* mRNA to 400 amol (623 pg) per embryo. The ectopic phenotypes became significant as all embryos observed contained at least one ectopic PGC (Figure 13) but also revealed apparent somatic defects (Figure 9F). Therefore, microinjection of mRNA into one cell of the blastodisc may be a potential solution to overcome somatic leakage. Furthermore, I applied a very stringent criterium determining ectopic PGCs. Since introducing excessive *nanos3* 3'-UTR into the embryo induces slight migration defects of PGCs (Goudarzi et al., 2013; Pfeiffer et al., 2018), and even in wild-type embryos, PGCs occasionally fall posteriorly to the clusters, it is arbitrary and technically problematic to define the normal range of PGCs aligned on the yolk, especially visually under a microscope. Therefore, to avoid imprudent judgement, I did not count the trailing PGCs in, so those embryos with no ectopic PGCs did not literally revealed the precise arrival of all PGCs, and I did notice a trend of arising trailing PGCs in those embryos introduced with *dnR3-nos* mRNA.

My study features the first approach on the direct interaction between Fgf signaling and PGCs *in vivo*. However, one can still challenge that the phenotypes were potentially cause by the somatic effects as *nos*-conjugated RNA would be more or less left in the soma and translated into proteins, yet I reason that the observed phenotypes are PGC-intrinsic. I, again, used a modest amount of RNAs introduced into the embryos, and rarely observed somatic phenotypes in the clusters treated with *dnR3-nos* mRNA (Figure 9D). Occasionally, some defects did transpire in injected and even wild-type embryos. Those unsound embryos were discarded on sampling as they did not accord with the assumption of PGC-exclusive effects, and they occurred in a low penetrance without apparent difference between treatment and control mRNAs. Moreover, *dnR3-nos* mRNA did not alter the transcript levels of *cxcl12a* or *ackr3b* (Figure 10B). I also

doi:10.6342/NTU201903081

stained *cxcl12a* at 10 hpf and did not notice a different pattern. Additionally, providing Cxcl12a were somehow up- or down-regulated by leakage of *dnR3-nos* mRNA, it is unlikely that *caR4-nos* mRNA would be able to rescue the phenotypes as it should even flatten the distinction of chemokine distribution. Therefore, I conclude that Fgf signaling is involved in PGC migration in a PGC-intrinsic manner.

doi:10.6342/NTU201903081

5.4. Intracellular signaling in PGCs evoked by Fgfs

Based on current knowledge, FGFs can signal through MAPK signaling in PGCs. In chicken, PGCs require FGFs to maintain proliferation via MAPK signaling *in vitro* (Choi et al., 2010); the requirement of FGFs could be substituted by ca-MAP2K (Whyte et al., 2015). In mouse, supplementation of FGFs or their inhibitors could accordingly adjust the MAPK activities, yet the functional correlation has not been disclosed (Takeuchi et al., 2005). In my study, using FRET biosensor to detect Mapk activities, I could not disturb the Mapk signaling in PGC by manipulating Fgf signaling (Figure 16A). Additionally, *dn-map2k1* did not induce ectopic PGCs, suggesting PGC migration did not require Mapk signaling (Figure 13). However, since the batch effects were significant using flow cytometry strategies, the fluctuations of signaling could not be assessed properly; therefore, more sensitive quantification methods, such as confocal microscopy, western blotting and immunostaining, should also be included to determine the intracellular signaling. Besides, it is worth trying to rescue dnR3-treated PGCs with ca-Map2k1 if Mapk in PGCs is activated by alternative pathways than the Map3k-Map2k-Mapk cascade.

I also consider Rac1 signaling to be a candidate responsive to Fgf signals. Rac1 signaling is evoked by Cxcl12a via Cxcr4b and then Ca15b and required for polarity of PGCs (Kardash et al., 2010; Tarbashevich et al., 2015). Therefore, it is possible that Fgf signaling alters the cytoskeletons through Rac1 signaling. Using FRET biosensors and flow cytometry for analysis, I could not detect a significant change by *dnR3-nos* or *caR4-nos* mRNA (Figure 16B). However, again, considering the shifts of Rac1 FRET ratio in *cxcr4b* or *ca15b* knockdown PGCs were only within ~10% (Kardash et al., 2010; Tarbashevich et al., 2015), the variances within the samples and between the

doi:10.6342/NTU201903081

batch might not able to detect the fluctuations in FRET ratio. As concluded previously in Mapk study, it is suggested to reanalyze the intracellular signaling pathways using more sensitive approaches.

doi:10.6342/NTU201903081

6. Conclusion

Germ cell migration is a conserved behavior across animals. In vertebrate, PGCs are guided by chemotaxis, in which CXCL12 navigates CXCR4-expressing PGCs to where the gonad develops. As preservation of germ cells matter to the survival of a species, several mechanisms orchestrate the migration for the accuracy of the PGC arrival. Here, using zebrafish as an animal model, I depict an intrinsic involvement of Fgf signaling—formerly deemed as a mitogen to PGCs—in germ cell migration. Competing with endogenous Fgfrs, truncated Fgfrs disrupted the positioning of PGCs since early gastrulation when expressed specifically in PGCs. The migration defects could be ameliorated by constitutively activating the Fgf signaling in PGCs, excluding the possibility of unspecific effects of dnR3 on other signaling. In sum, Fgf signaling participates directly in zebrafish PGC migration. More signaling pathways other than chemokine signaling are integrated into the scrupulosity of the cell movement.

doi:10.6342/NTU201903081

7. References

Abraham, J.A., Mergia, A., Whang, J.L., Tumolo, A., Friedman, J., Hjerrild, K.A., Gospodarowicz, D., and Fiddes, J.C. (1986). Nucleotide-sequence of a bovine clone encoding the angiogenic protein, basic fibroblast growth-factor. Science *233*, 545-548.

Amaya, E., Musci, T.J., and Kirschner, M.W. (1991). Expression of a dominant negative mutant of the Fgf receptor disrupts mesoderm formation in *Xenopus* embryos. Cell *66*, 257-270.

Arai, T., Parker, A., Busby, W., Jr., and Clemmons, D.R. (1994). Heparin, heparan sulfate, and dermatan sulfate regulate formation of the insulin-like growth factor-I and insulin-like growth factor-binding protein complexes. J. Biol. Chem. *269*, 20388-20393.

Bachvarova, R.F., Crother, B.I., Manova, K., Chatfield, J., Shoemaker, C.M., Crews, D.P., and Johnson, A.D. (2009). Expression of Dazl and Vasa in turtle embryos and ovaries: evidence for inductive specification of germ cells. Evol. Dev. *11*, 525-534.

Barak, H., Huh, S.H., Chen, S., Jeanpierre, C., Martinovic, J., Parisot, M., Bole-Feysot, C., Nitschke, P., Salomon, R., Antignac, C.*, et al.* (2012). FGF9 and FGF20 maintain the stemness of nephron progenitors in mice and man. Dev. Cell *22*, 1191-1207.

Barton, L.J., LeBlanc, M.G., and Lehmann, R. (2016). Finding their way: themes in germ cell migration. Curr. Opin. Cell. Biol. *42*, 128-137.

Benjamini, Y., Krieger, A.M., and Yekutieli, D. (2006). Adaptive linear step-up procedures that control the false discovery rate. Biometrika *93*, 491-507.

Blaser, H., Eisenbeiss, S., Neumann, M., Reichman-Fried, M., Thisse, B., Thisse, C., and Raz, E. (2005). Transition from non-motile behaviour to directed migration during early PGC development in zebrafish. J. Cell Sci. *118*, 4027-4038.

Blaser, H., Reichman-Fried, M., Castanon, I., Dumstrei, K., Marlow, F.L., Kawakami, K., Solnica-Krezel, L., Heisenberg, C.P., and Raz, E. (2006). Migration of zebrafish primordial germ cells: a role for myosin contraction and cytoplasmic flow. Dev. Cell *11*, 613-627.

Boldajipour, B., Mahabaleshwar, H., Kardash, E., Reichman-Fried, M., Blaser, H., Minina, S., Wilson, D., Xu, Q., and Raz, E. (2008). Control of chemokine-guided cell migration by ligand sequestration. Cell *132*, 463-473.

doi:10.6342/NTU201903081

Braat, A.K., Zandbergen, T., van de Water, S., Goos, H.J., and Zivkovic, D. (1999). Characterization of zebrafish primordial germ cells: morphology and early distribution of vasa RNA. Dev. Dyn. *216*, 153-167.

Burger, J.A., and Peled, A. (2009). CXCR4 antagonists: targeting the microenvironment in leukemia and other cancers. Leukemia *23*, 43-52.

Charnaux, N., Brule, S., Hamon, M., Chaigneau, T., Saffar, L., Prost, C., Lievre, N., and Gattegno, L. (2005). Syndecan-4 is a signaling molecule for stromal cell-derived factor-1 (SDF-1)/CXCL12. FEBS J. *272*, 1937-1951.

Chatfield, J., O'Reilly, M.A., Bachvarova, R.F., Ferjentsik, Z., Redwood, C., Walmsley, M., Patient, R., Loose, M., and Johnson, A.D. (2014). Stochastic specification of primordial germ cells from mesoderm precursors in axolotl embryos. Development *141*, 2429-2440.

Choi, J.W., Kim, S., Kim, T.M., Kim, Y.M., Seo, H.W., Park, T.S., Jeong, J.W., Song, G., and Han, J.Y. (2010). Basic fibroblast growth factor activates MEK/ERK cell signaling pathway and stimulates the proliferation of chicken primordial germ cells. PLoS One *5*, e12968.

Ciruna, B., and Rossant, J. (2001). FGF signaling regulates mesoderm cell fate specification and morphogenetic movement at the primitive streak. Dev. Cell *1*, 37-49.

Coordinators, N.R. (2018). Database resources of the National Center for Biotechnology Information. Nucleic Acids Res. *46*, D8-D13.

Dai, X., Jin, X., Chen, X., He, J., and Yin, Z. (2015). Sufficient numbers of early germ cells are essential for female sex development in zebrafish. PLoS One *10*, e0117824.

David, N.B., Sapede, D., Saint-Etienne, L., Thisse, C., Thisse, B., Dambly-Chaudiere, C., Rosa, F.M., and Ghysen, A. (2002). Molecular basis of cell migration in the fish lateral line: role of the chemokine receptor CXCR4 and of its ligand, SDF1. Proc. Natl. Acad. Sci. USA *99*, 16297-16302.

De Miguel, M.P., Cheng, L., Holland, E.C., Federspiel, M.J., and Donovan, P.J. (2002). Dissection of the c-Kit signaling pathway in mouse primordial germ cells by retroviral-mediated gene transfer. Proc. Natl. Acad. Sci. USA *99*, 10458-10463.

doi:10.6342/NTU201903081

De Smet, F., Tembuyser, B., Lenard, A., Claes, F., Zhang, J., Michielsen, C., Van Schepdael, A., Herbert, J.M., Bono, F., Affolter, M.*, et al.* (2014). Fibroblast growth factor signaling affects vascular outgrowth and is required for the maintenance of blood vessel integrity. Chem. Biol. *21*, 1310-1317.

de Winter, J.P., ten Dijke, P., de Vries, C.J., van Achterberg, T.A., Sugino, H., de Waele, P., Huylebroeck, D., Verschueren, K., and van den Eijnden-van Raaij, A.J. (1996). Follistatins neutralize activin bioactivity by inhibition of activin binding to its type II receptors. Mol. Cell Endocrinol. *116*, 105-114.

Devore, D.L., Horvitz, H.R., and Stern, M.J. (1995). An Fgf receptor signaling pathway is required for the normal-cell migrations of the sex myoblasts in *C. elegans* hermaphrodites. Cell *83*, 611-620.

DiGabriele, A.D., Lax, I., Chen, D.I., Svahn, C.M., Jaye, M., Schlessinger, J., and Hendrickson, W.A. (1998). Structure of a heparin-linked biologically active dimer of fibroblast growth factor. Nature *393*, 812-817.

Doitsidou, M., Reichman-Fried, M., Stebler, J., Koprunner, M., Dorries, J., Meyer, D., Esguerra, C.V., Leung, T., and Raz, E. (2002). Guidance of primordial germ cell migration by the chemokine SDF-1. Cell *111*, 647-659.

Donovan, P.J., Stott, D., Cairns, L.A., Heasman, J., and Wylie, C.C. (1986). Migratory and postmigratory mouse primordial germ cells behave differently in culture. Cell *44*, 831-838.

Durcova-Hills, G., Adams, I.R., Barton, S.C., Surani, M.A., and McLaren, A. (2006). The role of exogenous fibroblast growth factor-2 on the reprogramming of primordial germ cells into pluripotent stem cells. Stem Cells *24*, 1441-1449.

Evans, T., Wade, C.M., Chapman, F.A., Johnson, A.D., and Loose, M. (2014). Acquisition of germ plasm accelerates vertebrate evolution. Science *344*, 200-203.

Fletcher, R.B., and Harland, R.M. (2008). The role of FGF signaling in the establishment and maintenance of mesodermal gene expression in *Xenopus*. Dev. Dyn. *237*, 1243-1254.

Fritz, R.D., Menshykau, D., Martin, K., Reimann, A., Pontelli, V., and Pertz, O. (2015). SrGAP2-Dependent Integration of Membrane Geometry and Slit-Robo-Repulsive Cues Regulates Fibroblast Contact Inhibition of Locomotion. Dev. Cell *35*, 78-92.

doi:10.6342/NTU201903081

Gattineni, J., Alphonse, P., Zhang, Q., Mathews, N., Bates, C.M., and Baum, M. (2014). Regulation of renal phosphate transport by FGF23 is mediated by FGFR1 and FGFR4. Am. J. Physiol. Renal. Physiol. *306*, F351-358.

Giraldez, A.J., Mishima, Y., Rihel, J., Grocock, R.J., Van Dongen, S., Inoue, K., Enright, A.J., and Schier, A.F. (2006). Zebrafish MiR-430 promotes deadenylation and clearance of maternal mRNAs. Science *312*, 75-79.

Godin, I., Wylie, C., and Heasman, J. (1990). Genital ridges exert long-range effects on mouse primordial germ cell numbers and direction of migration in culture. Development *108*, 357-363.

Godin, I., and Wylie, C.C. (1991). TGF beta 1 inhibits proliferation and has a chemotropic effect on mouse primordial germ cells in culture. Development *113*, 1451-1457.

Gospodarowicz, D. (1974). Localisation of a fibroblast growth factor and its effect alone and with hydrocortisone on 3T3 cell growth. Nature *249*, 123-127.

Gospodarowicz, D., Moran, J., Braun, D., and Birdwell, C. (1976). Clonal Growth of Bovine Vascular Endothelial Cells - Fibroblast Growth-Factor as a Survival Agent. P. Natl. Acad. Sci. USA *73*, 4120-4124.

Goto-Kazeto, R., Saito, T., Takagi, M., Arai, K., and Yamaha, E. (2010). Isolation of teleost primordial germ cells using flow cytometry. Int. J. Dev. Biol. *54*, 1487-1492.

Goudarzi, M., Strate, I., Paksa, A., Lagendijk, A.K., Bakkers, J., and Raz, E. (2013). On the robustness of germ cell migration and microRNA-mediated regulation of chemokine signaling. Nat. Genet. *45*, 1264-1265.

Gritti, A., Parati, E.A., Cova, L., Frolichsthal, P., Galii, R., Wanke, E., Faravelli, L., Morassutti, D.J., Roisen, F., Nickel, D.D.*, et al.* (1996). Multipotential stem cells from the adult mouse brain proliferate and self-renew in response to basic fibroblast growth factor. J. Neurosci. *16*, 1091-1100.

Gross-Thebing, T., Yigit, S., Pfeiffer, J., Reichman-Fried, M., Bandemer, J., Ruckert, C., Rathmer, C., Goudarzi, M., Stehling, M., Tarbashevich, K.*, et al.* (2017). The vertebrate protein Dead end maintains primordial germ cell fate by inhibiting somatic differentiation. Dev. Cell *43*, 704-715.

doi:10.6342/NTU201903081

Grzegorski, S.J., Chiari, E.F., Robbins, A., Kish, P.E., and Kahana, A. (2014). Natural variability of Kozak sequences correlates with function in a zebrafish model. PLoS One *9*, e108475.

Hadari, Y.R., Gotoh, N., Kouhara, H., Lax, I., and Schlessinger, J. (2001). Critical role for the docking-protein FRS2 alpha in FGF receptor-mediated signal transduction pathways. Proc. Natl. Acad. Sci. USA *98*, 8578-8583.

Hart, K.C., Robertson, S.C., Kanemitsu, M.Y., Meyer, A.N., Tynan, J.A., and Donoghue, D.J. (2000). Transformation and Stat activation by derivatives of FGFR1, FGFR3, and FGFR4. Oncogene *19*, 3309-3320.

Hartwig, J., Tarbashevich, K., Seggewiss, J., Stehling, M., Bandemer, J., Grimaldi, C., Paksa, A., Gross-Thebing, T., Meyen, D., and Raz, E. (2014). Temporal control over the initiation of cell motility by a regulator of G-protein signaling. Proc. Natl. Acad. Sci. USA *111*, 11389-11394.

Harvey, C.D., Ehrhardt, A.G., Cellurale, C., Zhong, H., Yasuda, R., Davis, R.J., and Svoboda, K. (2008). A genetically encoded fluorescent sensor of ERK activity. Proc. Natl. Acad. Sci. USA *105*, 19264-19269.

Hayashi, K., Lopes, S.M.C.D., and Surani, M.A. (2007). Germ cell specification in mice. Science *316*, 394-396.

Hayashi, K., Ogushi, S., Kurimoto, K., Shimamoto, S., Ohta, H., and Saitou, M. (2012). Offspring from oocytes derived from in vitro primordial germ cell-like cells in mice. Science *338*, 971-975.

Hayashi, K., Ohta, H., Kurimoto, K., Aramaki, S., and Saitou, M. (2011). Reconstitution of the mouse germ cell specification pathway in culture by pluripotent stem cells. Cell *146*, 519-532.

Herbert, S.P., Huisken, J., Kim, T.N., Feldman, M.E., Houseman, B.T., Wang, R.A., Shokat, K.M., and Stainier, D.Y.R. (2009). Arterial-venous segregation by selective cell sprouting: an alternative mode of blood vessel formation. Science *326*, 294-298.

Horstick, E.J., Jordan, D.C., Bergeron, S.A., Tabor, K.M., Serpe, M., Feldman, B., and Burgess, H.A. (2015). Increased functional protein expression using nucleotide sequence features enriched in highly expressed genes in zebrafish. Nucleic Acids Res. *43*, e48.

doi:10.6342/NTU201903081

Howe, K., Clark, M.D., Torroja, C.F., Torrance, J., Berthelot, C., Muffato, M., Collins, J.E., Humphray, S., McLaren, K., Matthews, L.*, et al.* (2013). The zebrafish reference genome sequence and its relationship to the human genome. Nature *496*, 498-503.

Itoh, N., and Ornitz, D.M. (2004). Evolution of the Fgf and Fgfr gene families. Trends Genet. *20*, 563-569.

Johnson, A.D., and Alberio, R. (2015). Primordial germ cells: the first cell lineage or the last cells standing? Development *142*, 2730-2739.

Kalinina, J., Byron, S.A., Makarenkova, H.P., Olsen, S.K., Eliseenkova, A.V., Larochelle, W.J., Dhanabal, M., Blais, S., Ornitz, D.M., Day, L.A.*, et al.* (2009). Homodimerization Controls the fibroblast growth factor 9 subfamily's receptor binding and heparan sulfate-dependent diffusion in the extracellular matrix. Mol. Cell Biol. *29*, 4663-4678.

Kalinina, J., Dutta, K., Ilghari, D., Beenken, A., Goetz, R., Eliseenkova, A.V., Cowburn, D., and Mohammadi, M. (2012). The alternatively spliced acid box region plays a key role in FGF receptor autoinhibition. Structure *20*, 77-88.

Kardash, E., Reichman-Fried, M., Maitre, J.L., Boldajipour, B., Papusheva, E., Messerschmidt, E.M., Heisenberg, C.P., and Raz, E. (2010). A role for Rho GTPases and cell-cell adhesion in single-cell motility in vivo. Nat. Cell Biol. *12*, 47-53.

Kelleher, R.J., 3rd, Govindarajan, A., Jung, H.Y., Kang, H., and Tonegawa, S. (2004). Translational control by MAPK signaling in long-term synaptic plasticity and memory. Cell *116*, 467-479.

Kimmel, C.B., Ballard, W.W., Kimmel, S.R., Ullmann, B., and Schilling, T.F. (1995). Stages of Embryonic-Development of the Zebrafish. Dev. Dyn. *203*, 253-310.

Kleiber, C., and Zeileis, A. (2016). Visualizing Count Data Regressions Using Rootograms. Am. Stat. *70*, 296-303.

Knaut, H., Pelegri, F., Bohmann, K., Schwarz, H., and Nusslein-Volhard, C. (2000). Zebrafish vasa RNA but not its protein is a component of the germ plasm and segregates asymmetrically before germline specification. J. Cell Biol. *149*, 875-888.

Knaut, H., Werz, C., Geisler, R., Nusslein-Volhard, C., and Consortium, T.S. (2003). A zebrafish homologue of the chemokine receptor Cxcr4 is a germ-cell guidance receptor. Nature *421*, 279-282.

 doi:10.6342/NTU201903081

Koprunner, M., Thisse, C., Thisse, B., and Raz, E. (2001). A zebrafish nanos-related gene is essential for the development of primordial germ cells. Genes Dev. *15*, 2877-2885.

Kosaka, K., Kawakami, K., Sakamoto, H., and Inoue, K. (2007). Spatiotemporal localization of germ plasm RNAs during zebrafish oogenesis. Mech. Dev. *124*, 279-289.

Kouhara, H., Hadari, Y.R., Spivak-Kroizman, T., Schilling, J., Bar-Sagi, D., Lax, I., and Schlessinger, J. (1997). A lipid-anchored Grb2-binding protein that links FGF-receptor activation to the Ras/MAPK signaling pathway. Cell *89*, 693-702.

Kuo, W.J., Digman, M.A., and Lander, A.D. (2010). Heparan sulfate acts as a bone morphogenetic protein coreceptor by facilitating ligand-induced receptor hetero-oligomerization. Mol. Biol. Cell *21*, 4028-4041.

Lau, E.K., Paavola, C.D., Johnson, Z., Gaudry, J.P., Geretti, E., Borlat, F., Kungl, A.J., Proudfoot, A.E., and Handel, T.M. (2004). Identification of the glycosaminoglycan binding site of the CC chemokine, MCP-1 - Implications for structure and function in vivo. J. Biol. Chem. *279*, 22294-22305.

Lavine, K.J., Yu, K., White, A.C., Zhang, X., Smith, C., Partanen, J., and Ornitz, D.M. (2005). Endocardial and epicardial derived FGF signals regulate myocardial proliferation and differentiation in vivo. Dev. Cell *8*, 85-95.

Lawson, K.A., Dunn, N.R., Roelen, B.A., Zeinstra, L.M., Davis, A.M., Wright, C.V., Korving, J.P., and Hogan, B.L. (1999). Bmp4 is required for the generation of primordial germ cells in the mouse embryo. Genes Dev. *13*, 424-436.

Lee, H.C., Choi, H.J., Lee, H.G., Lim, J.M., Ono, T., and Han, J.Y. (2016). DAZL Expression Explains Origin and Central Formation of Primordial Germ Cells in Chickens. Stem Cells Dev. *25*, 68-79.

Lee, Y., Grill, S., Sanchez, A., Murphy-Ryan, M., and Poss, K.D. (2005). Fgf signaling instructs position-dependent growth rate during zebrafish fin regeneration. Development *132*, 5173-5183.

Leerberg, D.M., R.E., H., and B.W., D. (2018). Fibroblast growth factor receptors function redundantly during zebrafish embryonic development. bioRxiv.

Li, X.Y., Yang, Q.F., Yu, H.Y., Wu, L.H., Zhao, Y.H., Zhang, C., Yue, X.T., Liu, Z., Wu, H., Haffty, B.G.*, et al.* (2014). LIF promotes tumorigenesis and metastasis of breast cancer through the AKT-mTOR pathway. Oncotarget *5*, 788-801.

doi:10.6342/NTU201903081

Lindner, V., and Reidy, M.A. (1991). Proliferation of Smooth-Muscle Cells after Vascular Injury Is Inhibited by an Antibody against Basic Fibroblast Growth-Factor. Proc. Natl. Acad. Sci. USA *88*, 3739-3743.

Liu, P., and Zhong, T.P. (2017). MAPK/ERK signalling is required for zebrafish cardiac regeneration. Biotechnol. Lett. *39*, 1069-1077.

Livak, K.J., and Schmittgen, T.D. (2001). Analysis of relative gene expression data using real-time quantitative PCR and the 2(-Delta Delta C(T)) Method. Methods *25*, 402-408.

Makarenkova, H.P., Hoffman, M.P., Beenken, A., Eliseenkova, A.V., Meech, R., Tsau, C., Patel, V.N., Lang, R.A., and Mohammadi, M. (2009). Differential interactions of FGFs with heparan sulfate control gradient formation and branching morphogenesis. Sci. Signal. *2*.

Matsui, Y., Zsebo, K., and Hogan, B.L. (1992). Derivation of pluripotential embryonic stem cells from murine primordial germ cells in culture. Cell *70*, 841-847.

Mellgren, E.M., and Johnson, S.L. (2005). *kitb*, a second zebrafish ortholog of mouse Kit. Dev. Genes Evol. *215*, 470-477.

Meyen, D., Tarbashevich, K., Banisch, T.U., Wittwer, C., Reichman-Fried, M., Maugis, B., Grimaldi, C., Messerschmidt, E.M., and Raz, E. (2015). Dynamic filopodia are required for chemokine-dependent intracellular polarization during guided cell migration in vivo. Elife *4*.

Mishima, Y., Giraldez, A.J., Takeda, Y., Fujiwara, T., Sakamoto, H., Schier, A.F., and Inoue, K. (2006). Differential regulation of germline mRNAs in soma and germ cells by zebrafish miR-430. Curr. Biol. *16*, 2135-2142.

Mizoguchi, T., Verkade, H., Heath, J.K., Kuroiwa, A., and Kikuchi, Y. (2008). Sdf1/Cxcr4 signaling controls the dorsal migration of endodermal cells during zebrafish gastrulation. Development *135*, 2521-2529.

Molyneaux, K.A., Zinszner, H., Kunwar, P.S., Schaible, K., Stebler, J., Sunshine, M.J., O'Brien, W., Raz, E., Littman, D., Wylie, C.*, et al.* (2003). The chemokine SDF1/CXCL12 and its receptor CXCR4 regulate mouse germ cell migration and survival. Development *130*, 4279-4286.

Nasevicius, A., and Ekker, S.C. (2000). Effective targeted gene 'knockdown' in zebrafish. Nat. Genet. *26*, 216-220.

doi:10.6342/NTU201903081

Ori, A., Wilkinson, M.C., and Fernig, D.G. (2011). A Systems Biology Approach for the Investigation of the Heparin/Heparan Sulfate Interactome. J. Biol. Chem. *286*, 19892-19904.

Ori, A., Wilkinson, M.C., and Fernig, D.G. (2011). A Systems Biology Approach for the Investigation of the Heparin/Heparan Sulfate Interactome. J. Biol. Chem. *286*, 19892-19904.

Ornitz, D.M., and Itoh, N. (2001). Fibroblast growth factors. Genome Biol. *2*.

Ornitz, D.M., Xu, J.S., Colvin, J.S., McEwen, D.G., MacArthur, C.A., Coulier, F., Gao, G.X., and Goldfarb, M. (1996). Receptor specificity of the fibroblast growth factor family. J. Biol. Chem. *271*, 15292-15297.

Ota, S., Tonou-Fujimori, N., and Yamasu, K. (2009). The roles of the FGF signal in zebrafish embryos analyzed using constitutive activation and dominant-negative suppression of different FGF receptors. Mech. Dev. *126*, 1-17.

Paksa, A., Bandemer, J., Hoeckendorf, B., Razin, N., Tarbashevich, K., Minina, S., Meyen, D., Biundo, A., Leidel, S.A., Peyrieras, N.*, et al.* (2016). Repulsive cues combined with physical barriers and cell-cell adhesion determine progenitor cell positioning during organogenesis. Nat. Commun. *7*, 11288.

Pares, G., and Ricardo, S. (2016). FGF control of E-cadherin targeting in the Drosophila midgut impacts on primordial germ cell motility. J. Cell Sci. *129*, 354-366.

Parichy, D.M., Rawls, J.F., Pratt, S.J., Whitfield, T.T., and Johnson, S.L. (1999). Zebrafish sparse corresponds to an orthologue of c-kit and is required for the morphogenesis of a subpopulation of melanocytes, but is not essential for hematopoiesis or primordial germ cell development. Development *126*, 3425-3436.

Peter, M., Ameer-Beg, S.M., Hughes, M.K., Keppler, M.D., Prag, S., Marsh, M., Vojnovic, B., and Ng, T. (2005). Multiphoton-FLIM quantification of the EGFP-mRFP1 FRET pair for localization of membrane receptor-kinase interactions. Biophys. J. *88*, 1224-1237.

Peters, K.G., Marie, J., Wilson, E., Ives, H.E., Escobedo, J., Del Rosario, M., Mirda, D., and Williams, L.T. (1992). Point mutation of an FGF receptor abolishes phosphatidylinositol turnover and Ca2+ flux but not mitogenesis. Nature *358*, 678-681.

doi:10.6342/NTU201903081

Petit, I., Szyper-Kravitz, M., Nagler, A., Lahav, M., Peled, A., Habler, L., Ponomaryov, T., Taichman, R.S., Arenzana-Seisdedos, F., Fujii, N.*, et al.* (2002). G-CSF induces stem cell mobilization by decreasing bone marrow SDF-1 and up-regulating CXCR4. Nat Immunol *3*, 687-694.

Petryszak, R., Keays, M., Tang, Y.A., Fonseca, N.A., Barrera, E., Burdett, T., Fullgrabe, A., Fuentes, A.M., Jupp, S., Koskinen, S.*, et al.* (2016). Expression Atlas update--an integrated database of gene and protein expression in humans, animals and plants. Nucleic Acids Res. *44*, D746-752.

Pfeiffer, J., Tarbashevich, K., Bandemer, J., Palm, T., and Raz, E. (2018). Rapid progression through the cell cycle ensures efficient migration of primordial germ cells - The role of Hsp90. Dev. Biol. *436*, 84-93.

Plotnikov, A.N., Hubbard, S.R., Schlessinger, J., and Mohammadi, M. (2000). Crystal structures of two FGF-FGFR complexes reveal the determinants of ligand-receptor specificity. Cell *101*, 413-424.

R Core Team (2019). A language and environment for statistical computing (Vienna, Austria: R Foundation for Statistical Computing).

Raffioni, S., Thomas, D., Foehr, E.D., Thompson, L.M., and Bradshaw, R.A. (1999). Comparison of the intracellular signaling responses by three chimeric fibroblast growth factor receptors in PC12 cells. Proc. Natl. Acad. Sci. USA *96*, 7178-7183.

Rapraeger, A.C., Krufka, A., and Olwin, B.B. (1991). Requirement of Heparan-Sulfate for Bfgf-Mediated Fibroblast Growth and Myoblast Differentiation. Science *252*, 1705-1708.

Raz, E. (2003). Primordial germ-cell development: The zebrafish perspective. Nat. Rev. Genet. *4*, 690-700.

Reichman-Fried, M., Minina, S., and Raz, E. (2004). Autonomous modes of behavior in primordial germ cell migration. Dev. Cell *6*, 589-596.

Resnick, J.L., Bixler, L.S., Cheng, L., and Donovan, P.J. (1992). Long-term proliferation of mouse primordial germ cells in culture. Nature *359*, 550-551.

Resnick, J.L., Ortiz, M., Keller, J.R., and Donovan, P.J. (1998). Role of fibroblast growth factors and their receptors in mouse primordial germ cell growth. Biol. Reprod. *59*, 1224-1229.

doi:10.6342/NTU201903081

Richardson, B.E., and Lehmann, R. (2010). Mechanisms guiding primordial germ cell migration: strategies from different organisms. Nat. Rev. Mol. Cell Bio. *11*, 37-49.

Rohner, N., Bercsenyi, M., Orban, L., Kolanczyk, M.E., Linke, D., Brand, M., Nusslein-Volhard, C., and Harris, M.P. (2009). Duplication of fgfr1 permits Fgf signaling to serve as a target for selection during domestication. Curr. Biol. *19*, 1642-1647.

Runyan, C., Schaible, K., Molyneaux, K., Wang, Z.Q., Levin, L., and Wylie, C. (2006). Steel factor controls midline cell death of primordial germ cells and is essential for their normal proliferation and migration. Development *133*, 4861-4869.

Samsa, L.A., Fleming, N., Magness, S., Qian, L., and Liu, J. (2016). Isolation and Characterization of Single Cells from Zebrafish Embryos. J. Vis. Exp.

Sang, X., Curran, M.S., and Wood, A.W. (2008). Paracrine insulin-like growth factor signaling influences primordial germ cell migration: in vivo evidence from the zebrafish model. Endocrinology *149*, 5035-5042.

Sarrazin, S., Lamanna, W.C., and Esko, J.D. (2011). Heparan sulfate proteoglycans. Cold Spring Harb. Perspect. Biol. *3*.

Schlessinger, J., Plotnikov, A.N., Ibrahimi, O.A., Eliseenkova, A.V., Yeh, B.K., Yayon, A., Linhardt, R.J., and Mohammadi, M. (2000). Crystal structure of a ternary FGF-FGFR-heparin complex reveals a dual role for heparin in FGFR binding and dimerization. Mol. Cell. *6*, 743-750.

Schlueter, P.J., Sang, X., Duan, C., and Wood, A.W. (2007). Insulin-like growth factor receptor 1b is required for zebrafish primordial germ cell migration and survival. Dev. Biol. *305*, 377-387.

Schweigerer, L., Neufeld, G., Friedman, J., Abraham, J.A., Fiddes, J.C., and Gospodarowicz, D. (1987). Capillary endothelial-cells express basic fibroblast growth-factor, a mitogen that promotes their own growth. Nature *325*, 257-259.

Seifert, J.R., and Lehmann, R. (2012). Drosophila primordial germ cell migration requires epithelial remodeling of the endoderm. Development *139*, 2101-2106.

Sekine, K., Ohuchi, H., Fujiwara, M., Yamasaki, M., Yoshizawa, T., Sato, T., Yagishita, N., Matsui, D., Koga, Y., Itoh, N.*, et al.* (1999). Fgf10 is essential for limb and lung formation. Nat. Genet. *21*, 138-141.

doi:10.6342/NTU201903081

Seydoux, G., and Strome, S. (1999). Launching the germline in Caenorhabditis elegans: regulation of gene expression in early germ cells. Development *126*, 3275-3283.

Shamblott, M.J., Axelman, J., Wang, S., Bugg, E.M., Littlefield, J.W., Donovan, P.J., Blumenthal, P.D., Huggins, G.R., and Gearhart, J.D. (1998). Derivation of pluripotent stem cells from cultured human primordial germ cells. Proc. Natl. Acad. Sci. USA *95*, 13726-13731.

Staton, A.A., Knaut, H., and Giraldez, A.J. (2011). miRNA regulation of Sdf1 chemokine signaling provides genetic robustness to germ cell migration. Nat. Genet. *43*, 204-211.

Staton, A.A., Knaut, H., and Giraldez, A.J. (2013). Reply to: "On the robustness of germ cell migration and microRNA-mediated regulation of chemokine signaling". Nat. Genet. *45*, 1266-1267.

Stebler, J., Spieler, D., Slanchev, K., Molyneaux, K.A., Richter, U., Cojocaru, V., Tarabykin, V., Wylie, C., Kessel, M., and Raz, E. (2004). Primordial germ cell migration in the chick and mouse embryo: the role of the chemokine SDF-1/CXCL12. Dev. Biol. *272*, 351-361.

Streit, A., Berliner, A.J., Papanayotou, C., Sirulnik, A., and Stern, C.D. (2000). Initiation of neural induction by FGF signalling before gastrulation. Nature *406*, 74-78.

Strome, S., and Lehmann, R. (2007). Germ versus soma decisions: Lessons from flies and worms. Science *316*, 392-393.

Strome, S., and Updike, D. (2015). Specifying and protecting germ cell fate. Nat Rev Mol. Cell. Bio. *16*, 406-416.

Sugiyama, T., Kohara, H., Noda, M., and Nagasawa, T. (2006). Maintenance of the hematopoietic stem cell pool by CXCL12-CXCR4 chemokine signaling in bone marrow stromal cell niches. Immunity *25*, 977-988.

Sun, X., Mariani, F.V., and Martin, G.R. (2002). Functions of FGF signalling from the apical ectodermal ridge in limb development. Nature *418*, 501-508.

Sutherland, D., Samakovlis, C., and Krasnow, M.A. (1996). Branchless encodes a Drosophila FGF homolog that controls tracheal cell migration and the pattern of branching. Cell *87*, 1091-1101.

doi:10.6342/NTU201903081

Tada, H., Mochii, M., Orii, H., and Watanabe, K. (2012). Ectopic formation of primordial germ cells by transplantation of the germ plasm: direct evidence for germ cell determinant in *Xenopus*. Dev. Biol. *371*, 86-93.

Takada, T., Katagiri, T., Ifuku, M., Morimura, N., Kobayashi, M., Hasegawa, K., Ogamo, A., and Kamijo, R. (2003). Sulfated polysaccharides enhance the biological activities of bone morphogenetic proteins. J. Biol. Chem. *278*, 43229-43235.

Takeuchi, T., Tanigawa, Y., Minamide, R., Ikenishi, K., and Komiya, T. (2010). Analysis of SDF-1/CXCR4 signaling in primordial germ cell migration and survival or differentiation in *Xenopus laevis*. Mech. Dev. *127*, 146-158.

Takeuchi, Y., Molyneaux, K., Runyan, C., Schaible, K., and Wylie, C. (2005). The roles of FGF signaling in germ cell migration in the mouse. Development *132*, 5399-5409.

Tarbashevich, K., Reichman-Fried, M., Grimaldi, C., and Raz, E. (2015). Chemokine-dependent pH elevation at the cell front sustains polarity in directionally migrating zebrafish germ cells. Curr. Biol. *25*, 1096-1103.

Theusch, E.V., Brown, K.J., and Pelegri, F. (2006). Separate pathways of RNA recruitment lead to the compartmentalization of the zebrafish germ plasm. Dev. Biol. *292*, 129-141.

Thisse, C., and Thisse, B. (2008). High-resolution in situ hybridization to whole-mount zebrafish embryos. Nat. Protoc. *3*, 59-69.

Thomsen, E.R., Mich, J.K., Yao, Z., Hodge, R.D., Doyle, A.M., Jang, S., Shehata, S.I., Nelson, A.M., Shapovalova, N.V., Levi, B.P.*, et al.* (2016). Fixed single-cell transcriptomic characterization of human radial glial diversity. Nat. Methods *13*, 87-93.

Tzung, K.W., Goto, R., Saju, J.M., Sreenivasan, R., Saito, T., Arai, K., Yamaha, E., Hossain, M.S., Calvert, M.E.K., and Orban, L. (2015). Early depletion of primordial germ cells in zebrafish promotes testis formation. Stem Cell Reports *4*, 61-73.

Uchimura, K., Morimoto-Tomita, M., Bistrup, A., Li, J., Lyon, M., Gallagher, J., Werb, Z., and Rosen, S.D. (2006). HSulf-2, an extracellular endosulfatase, is secreted by MCF-7 breast carcinoma cells and selectively mobilizes heparin-bound VEGF, FGF-1, and SDF-1. Faseb. J. *20*, A1364-A1364.

Ueno, H., Gunn, M., Dell, K., Tseng, A., Jr., and Williams, L. (1992). A truncated form of fibroblast growth factor receptor 1 inhibits signal transduction by multiple types of fibroblast growth factor receptor. J. Biol. Chem. *267*, 1470-1476.

doi:10.6342/NTU201903081

Urness, L.D., Bleyl, S.B., Wright, T.J., Moon, A.M., and Mansour, S.L. (2011). Redundant and dosage sensitive requirements for Fgf3 and Fgf10 in cardiovascular development. Dev. Biol. *356*, 383-397.

van de Lavoir, M.C., Diamond, J.H., Leighton, P.A., Mather-Love, C., Heyer, B.S., Bradshaw, R., Kerchner, A., Hooi, L.T., Gessaro, T.M., Swanberg, S.E.*, et al.* (2006). Germline transmission of genetically modified primordial germ cells. Nature *441*, 766-769.

Vanhauwaert, S., Van Peer, G., Rihani, A., Janssens, E., Rondou, P., Lefever, S., De Paepe, A., Coucke, P.J., Speleman, F., Vandesompele, J.*, et al.* (2014). Expressed repeat elements improve RT-qPCR normalization across a wide range of zebrafish gene expression studies. PLoS One *9*, e109091.

Walicke, P., Cowan, W.M., Ueno, N., Baird, A., and Guillemin, R. (1986). Fibroblast Growth-Factor Promotes Survival of Dissociated Hippocampal-Neurons and Enhances Neurite Extension. Proc. Natl. Acad. Sci. USA *83*, 3012-3016.

Wang, F., Kan, M., Yan, G., Xu, J., and McKeehan, W.L. (1995). Alternately spliced NH2-terminal immunoglobulin-like Loop I in the ectodomain of the fibroblast growth factor (FGF) receptor 1 lowers affinity for both heparin and FGF-1. J. Biol. Chem. *270*, 10231-10235.

Wang, M., Zhang, C., Huang, C., Cheng, S., He, N., Wang, Y., Ahmed, M.F., Zhao, R., Jin, J., Zuo, Q.*, et al.* (2018). Regulation of fibroblast growth factor 8 (FGF8) in chicken embryonic stem cells differentiation into spermatogonial stem cells. J. Cell. Biochem. *119*, 2396-2407.

Wei, K.H., and Liu, I.H. (2014). Heparan sulfate glycosaminoglycans modulate migration and survival in zebrafish primordial germ cells. Theriogenology *81*, 1275-1285.

Weidinger, G., Stebler, J., Slanchev, K., Dumstrei, K., Wise, C., Lovell-Badge, R., Thisse, C., Thisse, B., and Raz, E. (2003). *dead end*, a novel vertebrate germ plasm component, is required for zebrafish primordial germ cell migration and survival. Curr. Biol. *13*, 1429-1434.

Weidinger, G., Wolke, U., Koprunner, M., Klinger, M., and Raz, E. (1999). Identification of tissues and patterning events required for distinct steps in early migration of zebrafish primordial germ cells. Development *126*, 5295-5307.

doi:10.6342/NTU201903081

Weinstein, M., Xu, X., Ohyama, K., and Deng, C.X. (1998). FGFR-3 and FGFR-4 function cooperatively to direct alveogenesis in the murine lung. Development *125*, 3615-3623.

Westerfield, M. (2007). The zebrafish book. A guide for the laboratory use of zebrafish (Danio rerio), 4 edn (University of Oregon Press, Eugene).

Whyte, J., Glover, J.D., Woodcock, M., Brzeszczynska, J., Taylor, L., Sherman, A., Kaiser, P., and McGrew, M.J. (2015). FGF, Insulin, and SMAD signaling cooperate for avian primordial germ cell self-renewal. Stem Cell Rep. *5*, 1171-1182.

Williams, A.F., and Barclay, A.N. (1988). The immunoglobulin superfamily--domains for cell surface recognition. Annu. Rev. Immunol. *6*, 381-405.

Williamson, A., and Lehmann, R. (1996). Germ cell development in Drosophila. Annu. Rev. Cell Dev. Biol. *12*, 365-391.

Wolke, U., Weidinger, G., Koprunner, M., and Raz, E. (2002). Multiple levels of posttranscriptional control lead to germ line-specific gene expression in the zebrafish. Curr. Biol. *12*, 289-294.

Wong, T.T., and Collodi, P. (2013). Effects of specific and prolonged expression of zebrafish growth factors, Fgf2 and Lif in primordial germ cells in vivo. Biochem. Biophys. Res. Commun. *430*, 347-351.

Xu, H., Kardash, E., Chen, S.H., Raz, E., and Lin, F. (2012). G beta gamma signaling controls the polarization of zebrafish primordial germ cells by regulating Rac activity. Development *139*, 57-62.

Yayon, A., Klagsbrun, M., Esko, J.D., Leder, P., and Ornitz, D.M. (1991). Cell surface, heparin-like molecules are required for binding of basic fibroblast growth factor to its high affinity receptor. Cell *64*, 841-848.

Ye, D., Zhu, L., Zhang, Q., Xiong, F., Wang, H., Wang, X., He, M., Zhu, Z., and Sun, Y. (2019). Abundance of Early Embryonic Primordial Germ Cells Promotes Zebrafish Female Differentiation as Revealed by Lifetime Labeling of Germline. Mar. Biotechnol. (NY) *21*, 217-228.

Ye, J., Coulouris, G., Zaretskaya, I., Cutcutache, I., Rozen, S., and Madden, T.L. (2012). Primer-BLAST: a tool to design target-specific primers for polymerase chain reaction. BMC Bioinformatics *13*, 134.

doi:10.6342/NTU201903081

Yeh, B.K., Igarashi, M., Eliseenkova, A.V., Plotnikov, A.N., Sher, I., Ron, D., Aaronson, S.A., and Mohammadi, M. (2003). Structural basis by which alternative splicing confers specificity in fibroblast growth factor receptors. Proc. Natl. Acad. Sci. USA *100*, 2266-2271.

Yoon, C., Kawakami, K., and Hopkins, N. (1997). Zebrafish vasa homologue RNA is localized to the cleavage planes of 2- and 4-cell-stage embryos and is expressed in the primordial germ cells. Development *124*, 3157-3165.

doi:10.6342/NTU201903081

8. Q&A

1. 無法重複先前實驗室使用 *hpse-nos* mRNA 降低 PGC 數量的實驗，是否使用了與先前不同的質體，或是施打劑量的人為差異所致？

在計畫初始我使用的是前人留下來的質體，因為無法重複實驗結果，定序後發現 *hpse* 上有影響胺基酸序列的 SNP，故重新從斑馬魚 cDNA 中取得 *hpse* 序列重做實驗，亦無法得到相同結果。由於顯微注射的劑量的確因人而已，因此聽從老師們的建議，做了一次劑量依賴性實驗，當劑量達到每個胚給予 400 amol *hpse-nos* mRNA 時，一日齡的胚已出現顯著的外觀異常，但 PGC 專一性的基因表現仍無下降之趨勢 (Figure 11)，因此目前在我手中無法重現學姐的實驗結果。

2. HS 作為訊息分子與受器的「輔助因子」，是否適合以 coreceptor 稱之？

HS 輔助訊息分子的接收，係直接以其分子結構參與蛋白質的栓合，所以大多來自權威人士撰寫的文獻回顧以 co-receptor 稱之 (Bernfield et al., 1999; Sarrazin et al., 2011)，亦有少數文獻以 cofactor 稱之 (Ornitz and Itoh, 2015)。

3. 使用 40 個 PCR cycle 偵測基因表現，且沒有負控制組，容易產生 false positive。

事後我重新使用了起始為 5000、8000、9000 顆受精後 6、8、10 小時細胞重複試驗，其 RNA 回溶於 14 μL 的水中並取 11 μL 進行 RT 反應，最終取 1 μL 進行 PCR 試驗 ，因此每個反應來自起始為 200、310 及 350 顆細胞。最初直接進行 30 及 35 個 cycle 的 PCR，但體細胞組別及六小時組別的 actb1 表現難以偵測，因此改使用 nested PCR，以不同組引子進行 15 加上 25 個 cycle 的 PCR。同時，也將剩餘的 RNA 混合在一起進行同樣操作，但少加了 RT 的酵素作為負控制組，在膠圖上並沒有條帶產生，表示所看到的基因表現並非來自 gDNA 或是污染所致。

doi:10.6342/NTU201903081

4. 偵測 *fgfr* 的表現無法證實 PGC 能接受 Fgf，建議結論止於 PGC 表現了 *fgfr* 的 RNA。

已修正結果 (4.1) 及討論 (5.1) 的敘述，陳述 PGC 表現了 *fgfr* RNA，以及競爭 Fgfr 能夠產生表現型，不過度解讀 Fgf 透過 Fgfr 影響 PGC 生理。

5. 為何使用 dnR3，而非 PGC 最多的 dnR4。

如結果所述，dn-Fgfr 的競爭不具專一性 (Ueno et al., 1992)，且目前學界認為 Fgfr 之間對於下游的調控並無不同 (Gattineni et al., 2014; Lavine et al., 2005; Weinstein et al., 1998)，因此選擇 dn-Fgfr 以其效力為主，不以內源孰多孰寡區分。過去偵測 dn-Fgfr 能力為透過不同 dn-Fgfr 去拯救過量表現不同種類 Fgf 的魚胚，而 dnR3 拯救的 Fgf 種類最為全面 (Ota et al., 2009)。但抑制外源的 Fgf 與內源的 Fgfr 的確不能完全等同視之，或許能將不同種類的 dn-Fgfr 混合施打，便能達到更好的效果。

6. 不同 mRNA 施打的劑量如何抉擇？

決定單一劑量前，我都會先廣泛地施打不同的劑量作為測試，以不造成體組織異常的安全劑量作為最終決定之劑量。已將施打不同劑量之一日齡魚胚圖置於 Figure 9。

7. 即使使用了 *nanos3* 3'UTR，基因仍然會再體細胞中表現？如何知道看到的是對於 PGC 專一的機制？

Nanos3 3'UTR 的機制是透過 miRNA 抑制其於體細胞轉譯及水解 (Giraldez et al., 2006; Koprunner et al., 2001; Mishima et al., 2006)。的確，根據綠色螢光的數據，體細胞中仍然會有蛋白質的轉譯，但約為 PGC 的一成以下 (Figure 4)，因此每個基因都需要重新判定適合劑量，已確認在體細胞中多少濃度是能夠被忍受的。

doi:10.6342/NTU201903081

8. 異位 PGC 的數量和外顯率並不高，如何推銷這個實驗成果？

由於使用 *nanos3* 3'UTR 的緣故，劑量的使用上較為保守，因此看到的可能是部分抑制的結果，而透過統計的確可以看到顯著的差異 (Figure 12)。之後也提高了施打劑量，成功引導出更多異位 PGC (Figure 12)，但同時體組織出現異常的比例也增加 (Figure 9F)。未來若欲改善，可於 4 或 8 細胞時期注射 mRNA 在一顆細胞以降低體細胞受到的干擾。

另外，即使 Fgf signaling 只對於少數 PGC 遷移有重要性，此發現仍有價值。首先，因為 PGC 具有全能性，異位的 PGC 可能形成生殖細胞瘤；此外抵達性腺的 PGC 數目降低雖不影響生育，但可能影響物種的性別比，所以在演化上有其必要性 (Dai et al., 2015; Tzung et al., 2015; Ye et al., 2019)。

9. 觀察 6 小時的 PGC 分佈，是如何確保胚盤是正朝上的？

ISH 染色後，我使用 BBBA 作為 clearing reagent，並且放至塑膠材質的 petri dish 上觀察，魚胚會黏在盤底上無法自由滾動，並且可以以毛筆翻轉方向。受精後 6 小時 epiboly 進行於剛好一半的位置，因此我是先找到胚盤邊緣的切線，並將一邊的切線翻轉剛好至視野消失的位置。的確，在視野下胚盤可能並不完全的水平，以數學模型計算，若胚盤與水平相差 15 度，那麼一個在胚盤邊緣處的 PGC 相對距離會有 3.4 % 的誤差，相對於 PGC 於胚盤分布的散度此誤差是可接受的。

10. 觀察 6 小時的 PGC 分佈，如何挑選 PGC 計算？

我首先會調整照片對比，使得藍色訊號變得清楚，接下來計算所有觀察到的藍點，包括一些比一般 PGC 微小的點，因為並不清楚 *ca15b* 在細胞內的分佈是否均勻，且不希望因為選擇大小之故產生偏頗。

doi:10.6342/NTU201903081

11. 本研究最有價值之處為何？

過去研究 PGC 對於訊息因子 (如 FGF) 的需求，大多於體外試驗。體內試驗也有之，但便無法得知是微環境的改變還是因子的直接作用。因此我的研究以斑馬魚作為模式動物，專一的抑制 PGC 的 Fgf 訊息傳遞，確認 Fgf 為直接亦或間接的影響。而先前認為體細胞需要 FGF signaling 穩定 PGC 遷移的路徑 (Barton et al., 2016)，在我的研究中顯示 PGC 本身也需要 FGF 訊息完成遷移。

doi:10.6342/NTU201903081